Once the gradients on the internal nodes of the computational graph are obtained, we can obtain the gradients on the parameter nodes. Because the parameters are shared across many time steps, we must take some care when denoting calculus operations involving these variables. The equations we wish to implement use the `bprop` method of section 6.5.6, that computes the contribution of a single edge in the computational graph to the gradient. However, the $\nabla_{\boldsymbol{W}} f$ operator used in calculus takes into account the contribution of $\boldsymbol{W}$ to the value of f due to *all* edges in the computational graph. To resolve this ambiguity, we introduce dummy variables $\boldsymbol{W}^{(t)}$ that are defined to be copies of $\boldsymbol{W}$ but with each $\boldsymbol{W}^{(t)}$ used only at time step t. We may then use $\nabla_{\boldsymbol{W}^{(t)}}$ to denote the contribution of the weights at time step t to the gradient.

Using this notation, the gradient on the remaining parameters is given by:

$$\nabla_{\boldsymbol{c}} L = \sum_t \left(\frac{\partial \boldsymbol{o}^{(t)}}{\partial \boldsymbol{c}} \right)^\top \nabla_{\boldsymbol{o}^{(t)}} L = \sum_t \nabla_{\boldsymbol{o}^{(t)}} L \tag{10.22}$$

$$\nabla_{\boldsymbol{b}} L = \sum_t \left(\frac{\partial \boldsymbol{h}^{(t)}}{\partial \boldsymbol{b}^{(t)}} \right)^\top \nabla_{\boldsymbol{h}^{(t)}} L = \sum_t \operatorname{diag}\left(1 - \left(\boldsymbol{h}^{(t)}\right)^2\right) \nabla_{\boldsymbol{h}^{(t)}} L \tag{10.23}$$

$$\nabla_{\boldsymbol{V}} L = \sum_t \sum_i \left(\frac{\partial L}{\partial o_i^{(t)}} \right) \nabla_{\boldsymbol{V}} o_i^{(t)} = \sum_t \left(\nabla_{\boldsymbol{o}^{(t)}} L\right) \boldsymbol{h}^{(t)\top} \tag{10.24}$$

$$\nabla_{\boldsymbol{W}} L = \sum_t \sum_i \left(\frac{\partial L}{\partial h_i^{(t)}} \right) \nabla_{\boldsymbol{W}^{(t)}} h_i^{(t)} \tag{10.25}$$

$$= \sum_t \operatorname{diag}\left(1 - \left(\boldsymbol{h}^{(t)}\right)^2\right) \left(\nabla_{\boldsymbol{h}^{(t)}} L\right) \boldsymbol{h}^{(t-1)\top} \tag{10.26}$$

$$\nabla_{\boldsymbol{U}} L = \sum_t \sum_i \left(\frac{\partial L}{\partial h_i^{(t)}} \right) \nabla_{\boldsymbol{U}^{(t)}} h_i^{(t)} \tag{10.27}$$

$$= \sum_t \operatorname{diag}\left(1 - \left(\boldsymbol{h}^{(t)}\right)^2\right) \left(\nabla_{\boldsymbol{h}^{(t)}} L\right) \boldsymbol{x}^{(t)\top} \tag{10.28}$$

We do not need to compute the gradient with respect to $\boldsymbol{x}^{(t)}$ for training because it does not have any parameters as ancestors in the computational graph defining the loss.

10.2.3 Recurrent Networks as Directed Graphical Models

In the example recurrent network we have developed so far, the losses $L^{(t)}$ were cross-entropies between training targets $\boldsymbol{y}^{(t)}$ and outputs $\boldsymbol{o}^{(t)}$. As with a feedforward network, it is in principle possible to use almost any loss with a recurrent network. The loss should be chosen based on the task. As with a feedforward network, we usually wish to interpret the output of the RNN as a probability distribution, and we usually use the cross-entropy associated with that distribution to define the loss. Mean squared error is the cross-entropy loss associated with an output distribution that is a unit Gaussian, for example, just as with a feedforward network.

When we use a predictive log-likelihood training objective, such as equation 10.12, we train the RNN to estimate the conditional distribution of the next sequence element $\boldsymbol{y}^{(t)}$ given the past inputs. This may mean that we maximize the log-likelihood

$$\log p(\boldsymbol{y}^{(t)} \mid \boldsymbol{x}^{(1)}, \dots, \boldsymbol{x}^{(t)}), \tag{10.29}$$

or, if the model includes connections from the output at one time step to the next time step,

$$\log p(\boldsymbol{y}^{(t)} \mid \boldsymbol{x}^{(1)}, \dots, \boldsymbol{x}^{(t)}, \boldsymbol{y}^{(1)}, \dots, \boldsymbol{y}^{(t-1)}). \tag{10.30}$$

Decomposing the joint probability over the sequence of $\boldsymbol{y}$ values as a series of one-step probabilistic predictions is one way to capture the full joint distribution across the whole sequence. When we do not feed past $\boldsymbol{y}$ values as inputs that condition the next step prediction, the directed graphical model contains no edges from any $\boldsymbol{y}^{(i)}$ in the past to the current $\boldsymbol{y}^{(t)}$. In this case, the outputs $\boldsymbol{y}$ are conditionally independent given the sequence of $\boldsymbol{x}$ values. When we do feed the actual $\boldsymbol{y}$ values (not their prediction, but the actual observed or generated values) back into the network, the directed graphical model contains edges from all $\boldsymbol{y}^{(i)}$ values in the past to the current $y^{(t)}$ value.

As a simple example, let us consider the case where the RNN models only a sequence of scalar random variables $\mathbb{Y} = \{\mathrm{y}^{(1)}, \dots, \mathrm{y}^{(\tau)}\}$, with no additional inputs x. The input at time step t is simply the output at time step $t-1$. The RNN then defines a directed graphical model over the y variables. We parametrize the joint distribution of these observations using the chain rule (equation 3.6) for conditional probabilities:

$$P(\mathbb{Y}) = P(\mathbf{y}^{(1)}, \dots, \mathbf{y}^{(\tau)}) = \prod_{t=1}^{\tau} P(\mathbf{y}^{(t)} \mid \mathbf{y}^{(t-1)}, \mathbf{y}^{(t-2)}, \dots, \mathbf{y}^{(1)}) \tag{10.31}$$

where the right-hand side of the bar is empty for $t = 1$, of course. Hence the negative log-likelihood of a set of values $\{y^{(1)}, \dots, y^{(\tau)}\}$ according to such a model

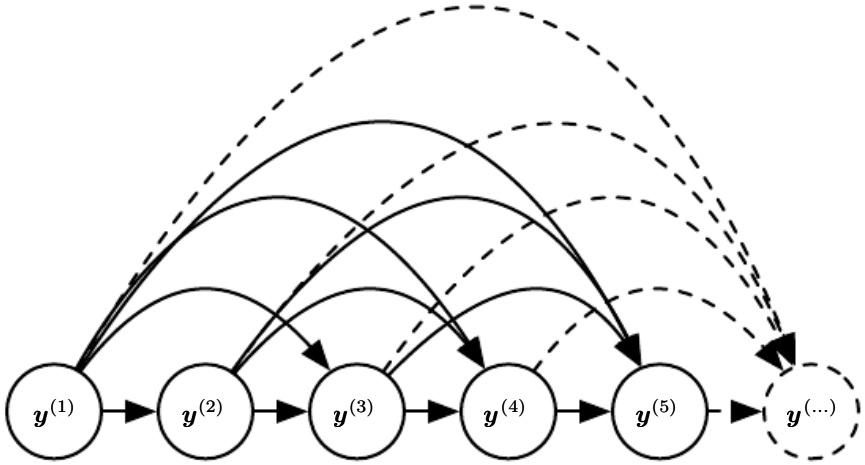

Figure 10.7: Fully connected graphical model for a sequence $y^{(1)}, y^{(2)}, \dots, y^{(t)}, \dots$: every past observation $y^{(i)}$ may influence the conditional distribution of some $y^{(t)}$ (for $t > i$), given the previous values. Parametrizing the graphical model directly according to this graph (as in equation 10.6) might be very inefficient, with an ever growing number of inputs and parameters for each element of the sequence. RNNs obtain the same full connectivity but efficient parametrization, as illustrated in figure 10.8.

is

$$L = \sum_t L^{(t)} \tag{10.32}$$

where

$$L^{(t)} = -\log P(\mathrm{y}^{(t)} = y^{(t)} \mid y^{(t-1)}, y^{(t-2)}, \dots, y^{(1)}). \tag{10.33}$$

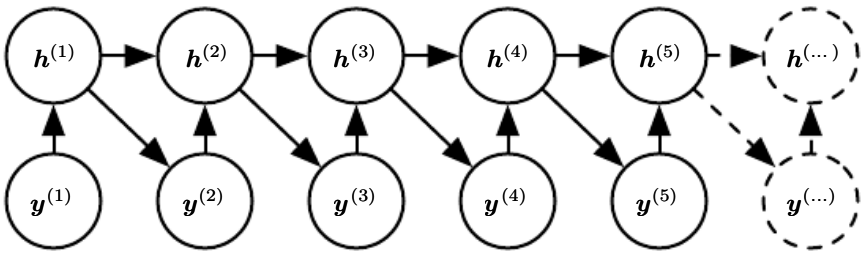

Figure 10.8: Introducing the state variable in the graphical model of the RNN, even though it is a deterministic function of its inputs, helps to see how we can obtain a very efficient parametrization, based on equation 10.5. Every stage in the sequence (for $\boldsymbol{h}^{(t)}$ and $\boldsymbol{y}^{(t)}$) involves the same structure (the same number of inputs for each node) and can share the same parameters with the other stages.

The edges in a graphical model indicate which variables depend directly on other variables. Many graphical models aim to achieve statistical and computational efficiency by omitting edges that do not correspond to strong interactions. For

example, it is common to make the Markov assumption that the graphical model should only contain edges from $\{\mathrm{y}^{(t-k)}, \ldots, \mathrm{y}^{(t-1)}\}$ to $\mathrm{y}^{(t)}$, rather than containing edges from the entire past history. However, in some cases, we believe that all past inputs should have an influence on the next element of the sequence. RNNs are useful when we believe that the distribution over $\mathrm{y}^{(t)}$ may depend on a value of $\mathrm{y}^{(i)}$ from the distant past in a way that is not captured by the effect of $\mathrm{y}^{(i)}$ on $\mathrm{y}^{(t-1)}$.

One way to interpret an RNN as a graphical model is to view the RNN as defining a graphical model whose structure is the complete graph, able to represent direct dependencies between any pair of y values. The graphical model over the y values with the complete graph structure is shown in figure 10.7. The complete graph interpretation of the RNN is based on ignoring the hidden units $\boldsymbol{h}^{(t)}$ by marginalizing them out of the model.

It is more interesting to consider the graphical model structure of RNNs that results from regarding the hidden units $\boldsymbol{h}^{(t)}$ as random variables.[1] Including the hidden units in the graphical model reveals that the RNN provides a very efficient parametrization of the joint distribution over the observations. Suppose that we represented an arbitrary joint distribution over discrete values with a tabular representation—an array containing a separate entry for each possible assignment of values, with the value of that entry giving the probability of that assignment occurring. If y can take on k different values, the tabular representation would have $O(k^{\tau})$ parameters. By comparison, due to parameter sharing, the number of parameters in the RNN is $O(1)$ as a function of sequence length. The number of parameters in the RNN may be adjusted to control model capacity but is not forced to scale with sequence length. Equation 10.5 shows that the RNN parametrizes long-term relationships between variables efficiently, using recurrent applications of the same function f and same parameters $\boldsymbol{\theta}$ at each time step. Figure 10.8 illustrates the graphical model interpretation. Incorporating the $\boldsymbol{h}^{(t)}$ nodes in the graphical model decouples the past and the future, acting as an intermediate quantity between them. A variable $y^{(i)}$ in the distant past may influence a variable $y^{(t)}$ via its effect on $\boldsymbol{h}$. The structure of this graph shows that the model can be efficiently parametrized by using the same conditional probability distributions at each time step, and that when the variables are all observed, the probability of the joint assignment of all variables can be evaluated efficiently.

Even with the efficient parametrization of the graphical model, some operations remain computationally challenging. For example, it is difficult to predict missing

[1] The conditional distribution over these variables given their parents is deterministic. This is perfectly legitimate, though it is somewhat rare to design a graphical model with such deterministic hidden units.

values in the middle of the sequence.

The price recurrent networks pay for their reduced number of parameters is that *optimizing* the parameters may be difficult.

The parameter sharing used in recurrent networks relies on the assumption that the same parameters can be used for different time steps. Equivalently, the assumption is that the conditional probability distribution over the variables at time $t+1$ given the variables at time t is **stationary**, meaning that the relationship between the previous time step and the next time step does not depend on t. In principle, it would be possible to use t as an extra input at each time step and let the learner discover any time-dependence while sharing as much as it can between different time steps. This would already be much better than using a different conditional probability distribution for each t, but the network would then have to extrapolate when faced with new values of t.

To complete our view of an RNN as a graphical model, we must describe how to draw samples from the model. The main operation that we need to perform is simply to sample from the conditional distribution at each time step. However, there is one additional complication. The RNN must have some mechanism for determining the length of the sequence. This can be achieved in various ways.

In the case when the output is a symbol taken from a vocabulary, one can add a special symbol corresponding to the end of a sequence (Schmidhuber, 2012). When that symbol is generated, the sampling process stops. In the training set, we insert this symbol as an extra member of the sequence, immediately after $\boldsymbol{x}^{(\tau)}$ in each training example.

Another option is to introduce an extra Bernoulli output to the model that represents the decision to either continue generation or halt generation at each time step. This approach is more general than the approach of adding an extra symbol to the vocabulary, because it may be applied to any RNN, rather than only RNNs that output a sequence of symbols. For example, it may be applied to an RNN that emits a sequence of real numbers. The new output unit is usually a sigmoid unit trained with the cross-entropy loss. In this approach the sigmoid is trained to maximize the log-probability of the correct prediction as to whether the sequence ends or continues at each time step.

Another way to determine the sequence length τ is to add an extra output to the model that predicts the integer τ itself. The model can sample a value of τ and then sample τ steps worth of data. This approach requires adding an extra input to the recurrent update at each time step so that the recurrent update is aware of whether it is near the end of the generated sequence. This extra input can either consist of the value of τ or can consist of $\tau - t$, the number of remaining

time steps. Without this extra input, the RNN might generate sequences that end abruptly, such as a sentence that ends before it is complete. This approach is based on the decomposition

$$P(\boldsymbol{x}^{(1)}, \ldots, \boldsymbol{x}^{(\tau)}) = P(\tau) P(\boldsymbol{x}^{(1)}, \ldots, \boldsymbol{x}^{(\tau)} \mid \tau). \tag{10.34}$$

The strategy of predicting τ directly is used for example by Goodfellow *et al.* (2014d).

10.2.4 Modeling Sequences Conditioned on Context with RNNs

In the previous section we described how an RNN could correspond to a directed graphical model over a sequence of random variables $y^{(t)}$ with no inputs $\boldsymbol{x}$. Of course, our development of RNNs as in equation 10.8 included a sequence of inputs $\boldsymbol{x}^{(1)}, \boldsymbol{x}^{(2)}, \ldots, \boldsymbol{x}^{(\tau)}$. In general, RNNs allow the extension of the graphical model view to represent not only a joint distribution over the y variables but also a conditional distribution over y given $\boldsymbol{x}$. As discussed in the context of feedforward networks in section 6.2.1.1, any model representing a variable $P(\boldsymbol{y}; \boldsymbol{\theta})$ can be reinterpreted as a model representing a conditional distribution $P(\boldsymbol{y} | \boldsymbol{\omega})$ with $\boldsymbol{\omega} = \boldsymbol{\theta}$. We can extend such a model to represent a distribution $P(\boldsymbol{y} \mid \boldsymbol{x})$ by using the same $P(\boldsymbol{y} \mid \boldsymbol{\omega})$ as before, but making $\boldsymbol{\omega}$ a function of $\boldsymbol{x}$. In the case of an RNN, this can be achieved in different ways. We review here the most common and obvious choices.

Previously, we have discussed RNNs that take a sequence of vectors $\boldsymbol{x}^{(t)}$ for $t = 1, \ldots, \tau$ as input. Another option is to take only a single vector $\boldsymbol{x}$ as input. When $\boldsymbol{x}$ is a fixed-size vector, we can simply make it an extra input of the RNN that generates the $\mathbf{y}$ sequence. Some common ways of providing an extra input to an RNN are:

1. as an extra input at each time step, or
2. as the initial state $\boldsymbol{h}^{(0)}$, or
3. both.

The first and most common approach is illustrated in figure 10.9. The interaction between the input $\boldsymbol{x}$ and each hidden unit vector $\boldsymbol{h}^{(t)}$ is parametrized by a newly introduced weight matrix $\boldsymbol{R}$ that was absent from the model of only the sequence of y values. The same product $\boldsymbol{x}^{\top}\boldsymbol{R}$ is added as additional input to the hidden units at every time step. We can think of the choice of $\boldsymbol{x}$ as determining the value

of $\boldsymbol{x}^\top \boldsymbol{R}$ that is effectively a new bias parameter used for each of the hidden units. The weights remain independent of the input. We can think of this model as taking the parameters $\boldsymbol{\theta}$ of the non-conditional model and turning them into $\boldsymbol{\omega}$, where the bias parameters within $\boldsymbol{\omega}$ are now a function of the input.

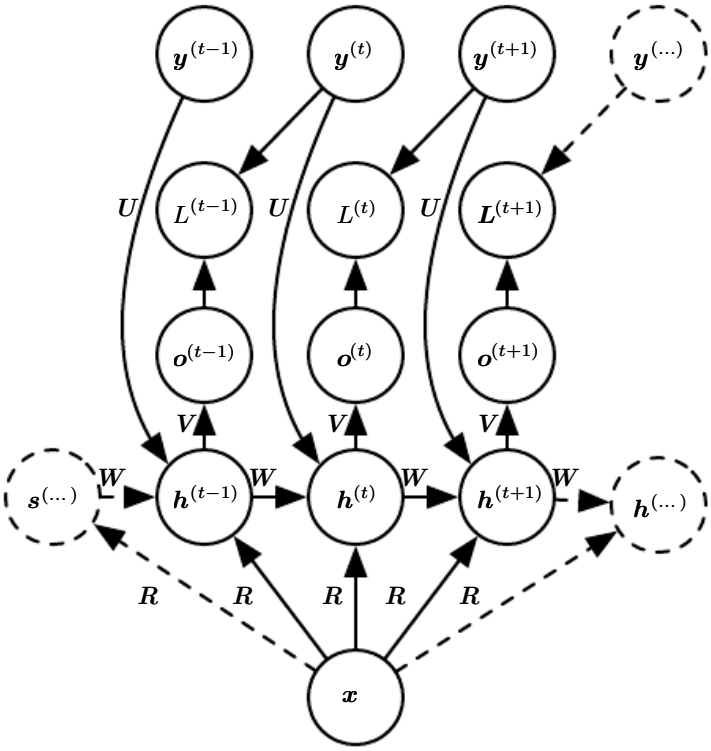

Figure 10.9: An RNN that maps a fixed-length vector $\boldsymbol{x}$ into a distribution over sequences $\mathbf{Y}$. This RNN is appropriate for tasks such as image captioning, where a single image is used as input to a model that then produces a sequence of words describing the image. Each element $\boldsymbol{y}^{(t)}$ of the observed output sequence serves both as input (for the current time step) and, during training, as target (for the previous time step).

Rather than receiving only a single vector $\boldsymbol{x}$ as input, the RNN may receive a sequence of vectors $\boldsymbol{x}^{(t)}$ as input. The RNN described in equation 10.8 corresponds to a conditional distribution $P(\boldsymbol{y}^{(1)}, \dots, \boldsymbol{y}^{(\tau)} \mid \boldsymbol{x}^{(1)}, \dots, \boldsymbol{x}^{(\tau)})$ that makes a conditional independence assumption that this distribution factorizes as

$$\prod_t P(\boldsymbol{y}^{(t)} \mid \boldsymbol{x}^{(1)}, \dots, \boldsymbol{x}^{(t)}). \tag{10.35}$$

To remove the conditional independence assumption, we can add connections from the output at time t to the hidden unit at time $t+1$, as shown in figure 10.10. The model can then represent arbitrary probability distributions over the $\boldsymbol{y}$ sequence. This kind of model representing a distribution over a sequence given another

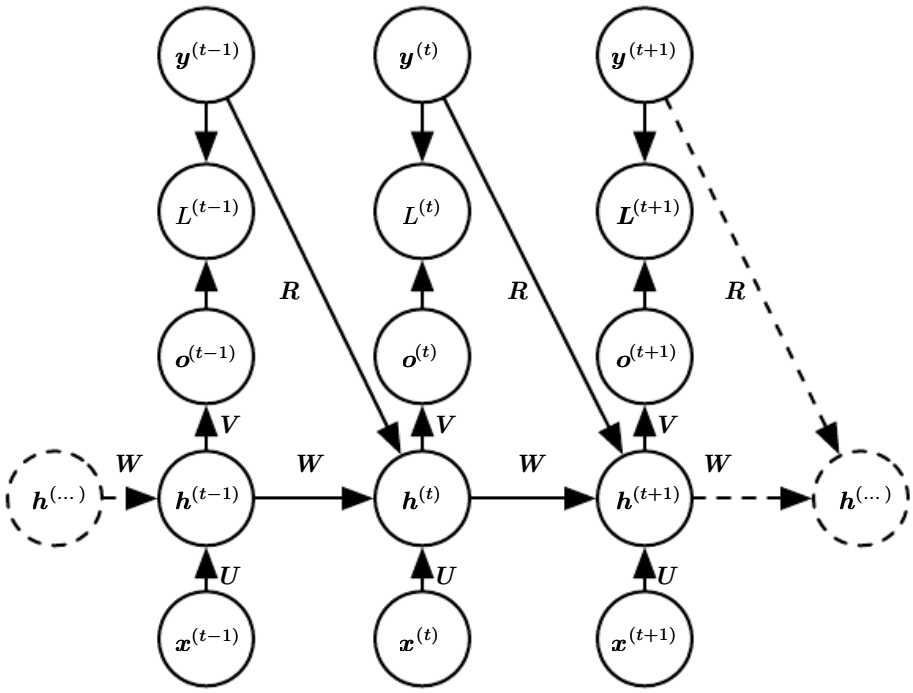

Figure 10.10: A conditional recurrent neural network mapping a variable-length sequence of $\boldsymbol{x}$ values into a distribution over sequences of $\boldsymbol{y}$ values of the same length. Compared to figure 10.3, this RNN contains connections from the previous output to the current state. These connections allow this RNN to model an arbitrary distribution over sequences of $\boldsymbol{y}$ given sequences of $\boldsymbol{x}$ of the same length. The RNN of figure 10.3 is only able to represent distributions in which the $\boldsymbol{y}$ values are conditionally independent from each other given the $\boldsymbol{x}$ values.

sequence still has one restriction, which is that the length of both sequences must be the same. We describe how to remove this restriction in section 10.4.

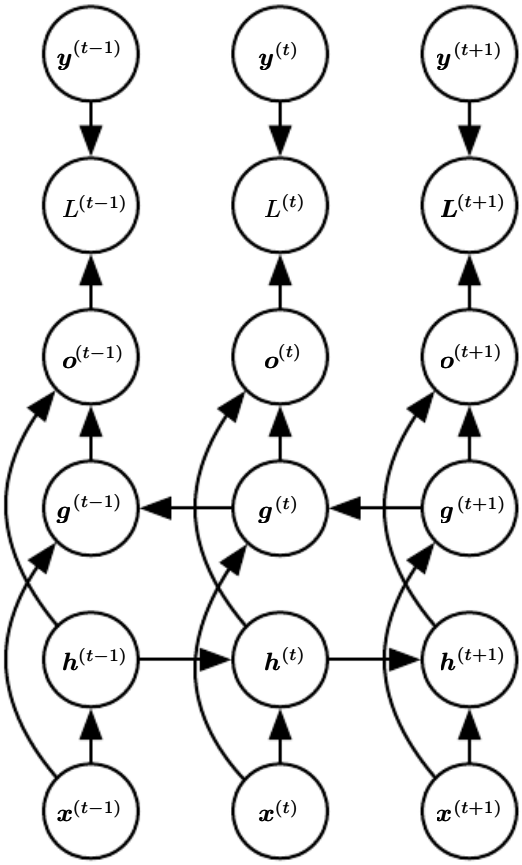

Figure 10.11: Computation of a typical bidirectional recurrent neural network, meant to learn to map input sequences $\boldsymbol{x}$ to target sequences $\boldsymbol{y}$, with loss $L^{(t)}$ at each step t. The $\boldsymbol{h}$ recurrence propagates information forward in time (towards the right) while the $\boldsymbol{g}$ recurrence propagates information backward in time (towards the left). Thus at each point t, the output units $\boldsymbol{o}^{(t)}$ can benefit from a relevant summary of the past in its $\boldsymbol{h}^{(t)}$ input and from a relevant summary of the future in its $\boldsymbol{g}^{(t)}$ input.

10.3 Bidirectional RNNs

All of the recurrent networks we have considered up to now have a "causal" structure, meaning that the state at time t only captures information from the past, $\boldsymbol{x}^{(1)}, \ldots, \boldsymbol{x}^{(t-1)}$, and the present input $\boldsymbol{x}^{(t)}$. Some of the models we have discussed also allow information from past $\boldsymbol{y}$ values to affect the current state when the $\boldsymbol{y}$ values are available.

However, in many applications we want to output a prediction of $\boldsymbol{y}^{(t)}$ which may

depend on *the whole input sequence*. For example, in speech recognition, the correct interpretation of the current sound as a phoneme may depend on the next few phonemes because of co-articulation and potentially may even depend on the next few words because of the linguistic dependencies between nearby words: if there are two interpretations of the current word that are both acoustically plausible, we may have to look far into the future (and the past) to disambiguate them. This is also true of handwriting recognition and many other sequence-to-sequence learning tasks, described in the next section.

Bidirectional recurrent neural networks (or bidirectional RNNs) were invented to address that need (Schuster and Paliwal, 1997). They have been extremely successful (Graves, 2012) in applications where that need arises, such as handwriting recognition (Graves *et al.*, 2008; Graves and Schmidhuber, 2009), speech recognition (Graves and Schmidhuber, 2005; Graves *et al.*, 2013) and bioinformatics (Baldi *et al.*, 1999).

As the name suggests, bidirectional RNNs combine an RNN that moves forward through time beginning from the start of the sequence with another RNN that moves backward through time beginning from the end of the sequence. Figure 10.11 illustrates the typical bidirectional RNN, with $\boldsymbol{h}^{(t)}$ standing for the state of the sub-RNN that moves forward through time and $\boldsymbol{g}^{(t)}$ standing for the state of the sub-RNN that moves backward through time. This allows the output units $\boldsymbol{o}^{(t)}$ to compute a representation that depends on *both the past and the future* but is most sensitive to the input values around time t, without having to specify a fixed-size window around t (as one would have to do with a feedforward network, a convolutional network, or a regular RNN with a fixed-size look-ahead buffer).

This idea can be naturally extended to 2-dimensional input, such as images, by having *four* RNNs, each one going in one of the four directions: up, down, left, right. At each point (i, j) of a 2-D grid, an output $O_{i,j}$ could then compute a representation that would capture mostly local information but could also depend on long-range inputs, if the RNN is able to learn to carry that information. Compared to a convolutional network, RNNs applied to images are typically more expensive but allow for long-range lateral interactions between features in the same feature map (Visin *et al.*, 2015; Kalchbrenner *et al.*, 2015). Indeed, the forward propagation equations for such RNNs may be written in a form that shows they use a convolution that computes the bottom-up input to each layer, prior to the recurrent propagation across the feature map that incorporates the lateral interactions.

10.4 Encoder-Decoder Sequence-to-Sequence Architectures

We have seen in figure 10.5 how an RNN can map an input sequence to a fixed-size vector. We have seen in figure 10.9 how an RNN can map a fixed-size vector to a sequence. We have seen in figures 10.3, 10.4, 10.10 and 10.11 how an RNN can map an input sequence to an output sequence of the same length.

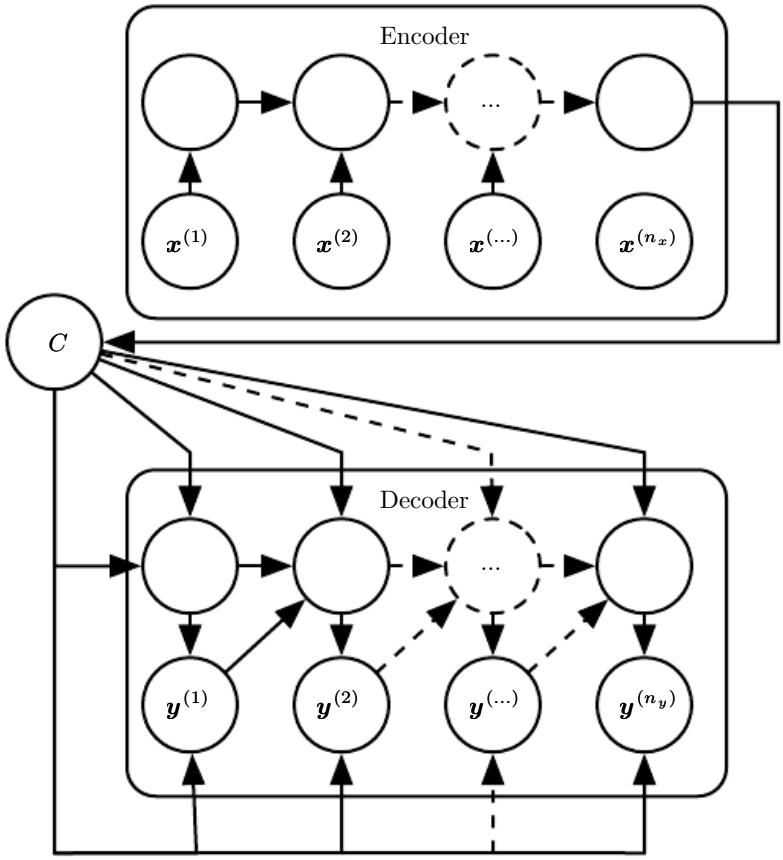

Figure 10.12: Example of an encoder-decoder or sequence-to-sequence RNN architecture, for learning to generate an output sequence $(\mathbf{y}^{(1)}, \ldots, \mathbf{y}^{(n_y)})$ given an input sequence $(\mathbf{x}^{(1)}, \mathbf{x}^{(2)}, \ldots, \mathbf{x}^{(n_x)})$. It is composed of an encoder RNN that reads the input sequence and a decoder RNN that generates the output sequence (or computes the probability of a given output sequence). The final hidden state of the encoder RNN is used to compute a generally fixed-size context variable C which represents a semantic summary of the input sequence and is given as input to the decoder RNN.

Here we discuss how an RNN can be trained to map an input sequence to an output sequence which is not necessarily of the same length. This comes up in many applications, such as speech recognition, machine translation or question

answering, where the input and output sequences in the training set are generally not of the same length (although their lengths might be related).

We often call the input to the RNN the "context." We want to produce a representation of this context, C. The context C might be a vector or sequence of vectors that summarize the input sequence $\boldsymbol{X} = (\boldsymbol{x}^{(1)}, \ldots, \boldsymbol{x}^{(n_x)})$.

The simplest RNN architecture for mapping a variable-length sequence to another variable-length sequence was first proposed by Cho *et al.* (2014a) and shortly after by Sutskever *et al.* (2014), who independently developed that architecture and were the first to obtain state-of-the-art translation using this approach. The former system is based on scoring proposals generated by another machine translation system, while the latter uses a standalone recurrent network to generate the translations. These authors respectively called this architecture, illustrated in figure 10.12, the encoder-decoder or sequence-to-sequence architecture. The idea is very simple: (1) an **encoder** or **reader** or **input** RNN processes the input sequence. The encoder emits the context C, usually as a simple function of its final hidden state. (2) a **decoder** or **writer** or **output** RNN is conditioned on that fixed-length vector (just like in figure 10.9) to generate the output sequence $\boldsymbol{Y} = (\boldsymbol{y}^{(1)}, \ldots, \boldsymbol{y}^{(n_y)})$. The innovation of this kind of architecture over those presented in earlier sections of this chapter is that the lengths n_x and n_y can vary from each other, while previous architectures constrained $n_x = n_y = \tau$. In a sequence-to-sequence architecture, the two RNNs are trained jointly to maximize the average of $\log P(\boldsymbol{y}^{(1)}, \ldots, \boldsymbol{y}^{(n_y)} \mid \boldsymbol{x}^{(1)}, \ldots, \boldsymbol{x}^{(n_x)})$ over all the pairs of $\boldsymbol{x}$ and $\boldsymbol{y}$ sequences in the training set. The last state $\boldsymbol{h}_{n_x}$ of the encoder RNN is typically used as a representation C of the input sequence that is provided as input to the decoder RNN.

If the context C is a vector, then the decoder RNN is simply a vector-to-sequence RNN as described in section 10.2.4. As we have seen, there are at least two ways for a vector-to-sequence RNN to receive input. The input can be provided as the initial state of the RNN, or the input can be connected to the hidden units at each time step. These two ways can also be combined.

There is no constraint that the encoder must have the same size of hidden layer as the decoder.

One clear limitation of this architecture is when the context C output by the encoder RNN has a dimension that is too small to properly summarize a long sequence. This phenomenon was observed by Bahdanau *et al.* (2015) in the context of machine translation. They proposed to make C a variable-length sequence rather than a fixed-size vector. Additionally, they introduced an **attention mechanism** that learns to associate elements of the sequence C to elements of the output

sequence. See section 12.4.5.1 for more details.

10.5 Deep Recurrent Networks

The computation in most RNNs can be decomposed into three blocks of parameters and associated transformations:

1. from the input to the hidden state,
2. from the previous hidden state to the next hidden state, and
3. from the hidden state to the output.

With the RNN architecture of figure 10.3, each of these three blocks is associated with a single weight matrix. In other words, when the network is unfolded, each of these corresponds to a shallow transformation. By a shallow transformation, we mean a transformation that would be represented by a single layer within a deep MLP. Typically this is a transformation represented by a learned affine transformation followed by a fixed nonlinearity.

Would it be advantageous to introduce depth in each of these operations? Experimental evidence (Graves *et al.*, 2013; Pascanu *et al.*, 2014a) strongly suggests so. The experimental evidence is in agreement with the idea that we need enough depth in order to perform the required mappings. See also Schmidhuber (1992), El Hihi and Bengio (1996), or Jaeger (2007a) for earlier work on deep RNNs.

Graves *et al.* (2013) were the first to show a significant benefit of decomposing the state of an RNN into multiple layers as in figure 10.13 (left). We can think of the lower layers in the hierarchy depicted in figure 10.13a as playing a role in transforming the raw input into a representation that is more appropriate, at the higher levels of the hidden state. Pascanu *et al.* (2014a) go a step further and propose to have a separate MLP (possibly deep) for each of the three blocks enumerated above, as illustrated in figure 10.13b. Considerations of representational capacity suggest to allocate enough capacity in each of these three steps, but doing so by adding depth may hurt learning by making optimization difficult. In general, it is easier to optimize shallower architectures, and adding the extra depth of figure 10.13b makes the shortest path from a variable in time step t to a variable in time step $t+1$ become longer. For example, if an MLP with a single hidden layer is used for the state-to-state transition, we have doubled the length of the shortest path between variables in any two different time steps, compared with the ordinary RNN of figure 10.3. However, as argued by Pascanu *et al.* (2014a), this

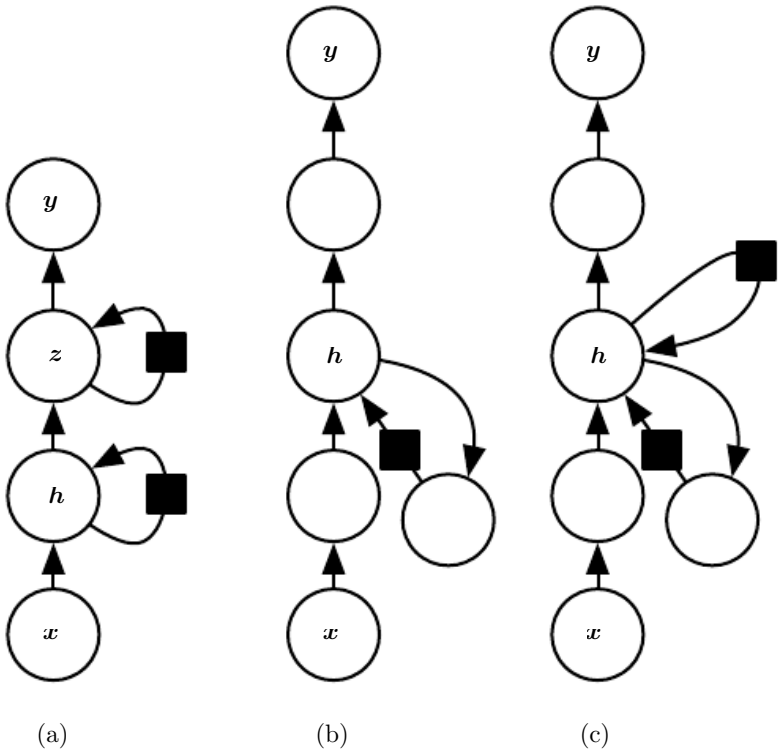

Figure 10.13: A recurrent neural network can be made deep in many ways (Pascanu *et al.*, 2014a). *(a)*The hidden recurrent state can be broken down into groups organized hierarchically. *(b)*Deeper computation (e.g., an MLP) can be introduced in the input-to-hidden, hidden-to-hidden and hidden-to-output parts. This may lengthen the shortest path linking different time steps. *(c)*The path-lengthening effect can be mitigated by introducing skip connections.

can be mitigated by introducing skip connections in the hidden-to-hidden path, as illustrated in figure 10.13c.

10.6 Recursive Neural Networks

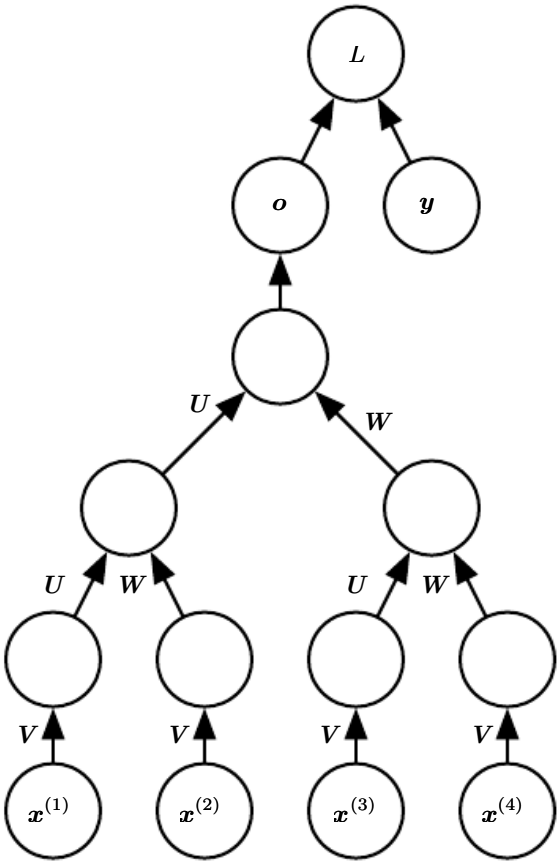

Figure 10.14: A recursive network has a computational graph that generalizes that of the recurrent network from a chain to a tree. A variable-size sequence $\boldsymbol{x}^{(1)}, \boldsymbol{x}^{(2)}, \ldots, \boldsymbol{x}^{(t)}$ can be mapped to a fixed-size representation (the output $\boldsymbol{o}$), with a fixed set of parameters (the weight matrices $\boldsymbol{U}$, $\boldsymbol{V}$, $\boldsymbol{W}$). The figure illustrates a supervised learning case in which some target $\boldsymbol{y}$ is provided which is associated with the whole sequence.

Recursive neural networks[2] represent yet another generalization of recurrent networks, with a different kind of computational graph, which is structured as a deep tree, rather than the chain-like structure of RNNs. The typical computational graph for a recursive network is illustrated in figure 10.14. Recursive neural

[2] We suggest to not abbreviate "recursive neural network" as "RNN" to avoid confusion with "recurrent neural network."

networks were introduced by Pollack (1990) and their potential use for learning to reason was described by Bottou (2011). Recursive networks have been successfully applied to processing *data structures* as input to neural nets (Frasconi *et al.*, 1997, 1998), in natural language processing (Socher *et al.*, 2011a,c, 2013a) as well as in computer vision (Socher *et al.*, 2011b).

One clear advantage of recursive nets over recurrent nets is that for a sequence of the same length τ, the depth (measured as the number of compositions of nonlinear operations) can be drastically reduced from τ to $O(\log \tau)$, which might help deal with long-term dependencies. An open question is how to best structure the tree. One option is to have a tree structure which does not depend on the data, such as a balanced binary tree. In some application domains, external methods can suggest the appropriate tree structure. For example, when processing natural language sentences, the tree structure for the recursive network can be fixed to the structure of the parse tree of the sentence provided by a natural language parser (Socher *et al.*, 2011a, 2013a). Ideally, one would like the learner itself to discover and infer the tree structure that is appropriate for any given input, as suggested by Bottou (2011).

Many variants of the recursive net idea are possible. For example, Frasconi *et al.* (1997) and Frasconi *et al.* (1998) associate the data with a tree structure, and associate the inputs and targets with individual nodes of the tree. The computation performed by each node does not have to be the traditional artificial neuron computation (affine transformation of all inputs followed by a monotone nonlinearity). For example, Socher *et al.* (2013a) propose using tensor operations and bilinear forms, which have previously been found useful to model relationships between concepts (Weston *et al.*, 2010; Bordes *et al.*, 2012) when the concepts are represented by continuous vectors (embeddings).

10.7 The Challenge of Long-Term Dependencies

The mathematical challenge of learning long-term dependencies in recurrent networks was introduced in section 8.2.5. The basic problem is that gradients propagated over many stages tend to either vanish (most of the time) or explode (rarely, but with much damage to the optimization). Even if we assume that the parameters are such that the recurrent network is stable (can store memories, with gradients not exploding), the difficulty with long-term dependencies arises from the exponentially smaller weights given to long-term interactions (involving the multiplication of many Jacobians) compared to short-term ones. Many other sources provide a deeper treatment (Hochreiter, 1991; Doya, 1993; Bengio *et al.*,

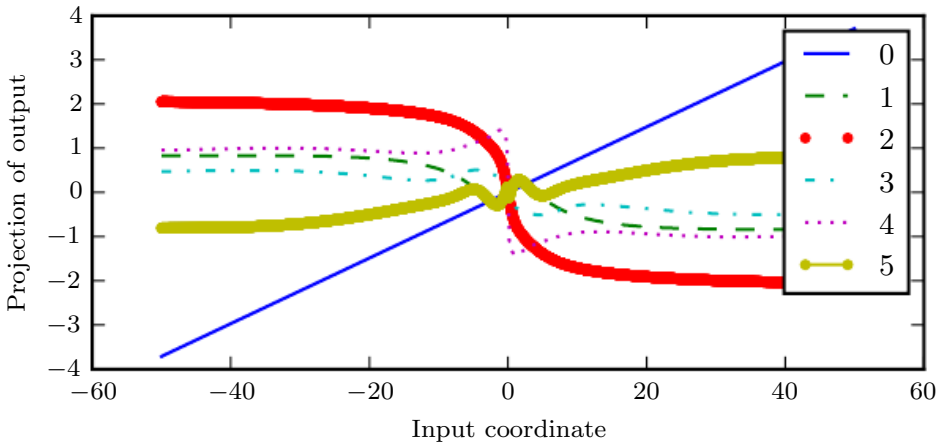

Figure 10.15: When composing many nonlinear functions (like the linear-tanh layer shown here), the result is highly nonlinear, typically with most of the values associated with a tiny derivative, some values with a large derivative, and many alternations between increasing and decreasing. In this plot, we plot a linear projection of a 100-dimensional hidden state down to a single dimension, plotted on the y-axis. The x-axis is the coordinate of the initial state along a random direction in the 100-dimensional space. We can thus view this plot as a linear cross-section of a high-dimensional function. The plots show the function after each time step, or equivalently, after each number of times the transition function has been composed.

1994; Pascanu *et al.*, 2013) . In this section, we describe the problem in more detail. The remaining sections describe approaches to overcoming the problem.

Recurrent networks involve the composition of the same function multiple times, once per time step. These compositions can result in extremely nonlinear behavior, as illustrated in figure 10.15.

In particular, the function composition employed by recurrent neural networks somewhat resembles matrix multiplication. We can think of the recurrence relation

$$\boldsymbol{h}^{(t)} = \boldsymbol{W}^{\top} \boldsymbol{h}^{(t-1)} \tag{10.36}$$

as a very simple recurrent neural network lacking a nonlinear activation function, and lacking inputs $\boldsymbol{x}$. As described in section 8.2.5, this recurrence relation essentially describes the power method. It may be simplified to

$$\boldsymbol{h}^{(t)} = \left(\boldsymbol{W}^{t}\right)^{\top} \boldsymbol{h}^{(0)}, \tag{10.37}$$

and if $\boldsymbol{W}$ admits an eigendecomposition of the form

$$\boldsymbol{W} = \boldsymbol{Q}\boldsymbol{\Lambda}\boldsymbol{Q}^{\top}, \tag{10.38}$$

with orthogonal $\boldsymbol{Q}$, the recurrence may be simplified further to

$$\boldsymbol{h}^{(t)} = \boldsymbol{Q}^\top \boldsymbol{\Lambda}^t \boldsymbol{Q} \boldsymbol{h}^{(0)}. \tag{10.39}$$

The eigenvalues are raised to the power of t causing eigenvalues with magnitude less than one to decay to zero and eigenvalues with magnitude greater than one to explode. Any component of $\boldsymbol{h}^{(0)}$ that is not aligned with the largest eigenvector will eventually be discarded.

This problem is particular to recurrent networks. In the scalar case, imagine multiplying a weight w by itself many times. The product w^t will either vanish or explode depending on the magnitude of w. However, if we make a non-recurrent network that has a different weight $w^{(t)}$ at each time step, the situation is different. If the initial state is given by 1, then the state at time t is given by $\prod_t w^{(t)}$. Suppose that the $w^{(t)}$ values are generated randomly, independently from one another, with zero mean and variance v. The variance of the product is $O(v^n)$. To obtain some desired variance v^* we may choose the individual weights with variance $v = \sqrt[n]{v^*}$. Very deep feedforward networks with carefully chosen scaling can thus avoid the vanishing and exploding gradient problem, as argued by Sussillo (2014).

The vanishing and exploding gradient problem for RNNs was independently discovered by separate researchers (Hochreiter, 1991; Bengio *et al.*, 1993, 1994). One may hope that the problem can be avoided simply by staying in a region of parameter space where the gradients do not vanish or explode. Unfortunately, in order to store memories in a way that is robust to small perturbations, the RNN must enter a region of parameter space where gradients vanish (Bengio *et al.*, 1993, 1994). Specifically, whenever the model is able to represent long term dependencies, the gradient of a long term interaction has exponentially smaller magnitude than the gradient of a short term interaction. It does not mean that it is impossible to learn, but that it might take a very long time to learn long-term dependencies, because the signal about these dependencies will tend to be hidden by the smallest fluctuations arising from short-term dependencies. In practice, the experiments in Bengio *et al.* (1994) show that as we increase the span of the dependencies that need to be captured, gradient-based optimization becomes increasingly difficult, with the probability of successful training of a traditional RNN via SGD rapidly reaching 0 for sequences of only length 10 or 20.

For a deeper treatment of recurrent networks as dynamical systems, see Doya (1993), Bengio *et al.* (1994) and Siegelmann and Sontag (1995), with a review in Pascanu *et al.* (2013). The remaining sections of this chapter discuss various approaches that have been proposed to reduce the difficulty of learning long-term dependencies (in some cases allowing an RNN to learn dependencies across

hundreds of steps), but the problem of learning long-term dependencies remains one of the main challenges in deep learning.

10.8 Echo State Networks

The recurrent weights mapping from $\boldsymbol{h}^{(t-1)}$ to $\boldsymbol{h}^{(t)}$ and the input weights mapping from $\boldsymbol{x}^{(t)}$ to $\boldsymbol{h}^{(t)}$ are some of the most difficult parameters to learn in a recurrent network. One proposed (Jaeger, 2003; Maass *et al.*, 2002; Jaeger and Haas, 2004; Jaeger, 2007b) approach to avoiding this difficulty is to set the recurrent weights such that the recurrent hidden units do a good job of capturing the history of past inputs, and *learn only the output weights*. This is the idea that was independently proposed for **echo state networks** or ESNs (Jaeger and Haas, 2004; Jaeger, 2007b) and **liquid state machines** (Maass *et al.*, 2002). The latter is similar, except that it uses spiking neurons (with binary outputs) instead of the continuous-valued hidden units used for ESNs. Both ESNs and liquid state machines are termed **reservoir computing** (Lukoševičius and Jaeger, 2009) to denote the fact that the hidden units form of reservoir of temporal features which may capture different aspects of the history of inputs.

One way to think about these reservoir computing recurrent networks is that they are similar to kernel machines: they map an arbitrary length sequence (the history of inputs up to time t) into a fixed-length vector (the recurrent state $\boldsymbol{h}^{(t)}$), on which a linear predictor (typically a linear regression) can be applied to solve the problem of interest. The training criterion may then be easily designed to be convex as a function of the output weights. For example, if the output consists of linear regression from the hidden units to the output targets, and the training criterion is mean squared error, then it is convex and may be solved reliably with simple learning algorithms (Jaeger, 2003).

The important question is therefore: how do we set the input and recurrent weights so that a rich set of histories can be represented in the recurrent neural network state? The answer proposed in the reservoir computing literature is to view the recurrent net as a dynamical system, and set the input and recurrent weights such that the dynamical system is near the edge of stability.

The original idea was to make the eigenvalues of the Jacobian of the state-to-state transition function be close to 1. As explained in section 8.2.5, an important characteristic of a recurrent network is the eigenvalue spectrum of the Jacobians $\boldsymbol{J}^{(t)} = \frac{\partial s^{(t)}}{\partial s^{(t-1)}}$. Of particular importance is the **spectral radius** of $\boldsymbol{J}^{(t)}$, defined to be the maximum of the absolute values of its eigenvalues.

To understand the effect of the spectral radius, consider the simple case of back-propagation with a Jacobian matrix $\boldsymbol{J}$ that does not change with t. This case happens, for example, when the network is purely linear. Suppose that $\boldsymbol{J}$ has an eigenvector $\boldsymbol{v}$ with corresponding eigenvalue λ. Consider what happens as we propagate a gradient vector backwards through time. If we begin with a gradient vector $\boldsymbol{g}$, then after one step of back-propagation, we will have $\boldsymbol{J}\boldsymbol{g}$, and after n steps we will have $\boldsymbol{J}^n\boldsymbol{g}$. Now consider what happens if we instead back-propagate a perturbed version of $\boldsymbol{g}$. If we begin with $\boldsymbol{g} + \delta\boldsymbol{v}$, then after one step, we will have $\boldsymbol{J}(\boldsymbol{g} + \delta\boldsymbol{v})$. After n steps, we will have $\boldsymbol{J}^n(\boldsymbol{g} + \delta\boldsymbol{v})$. From this we can see that back-propagation starting from $\boldsymbol{g}$ and back-propagation starting from $\boldsymbol{g} + \delta\boldsymbol{v}$ diverge by $\delta\boldsymbol{J}^n\boldsymbol{v}$ after n steps of back-propagation. If $\boldsymbol{v}$ is chosen to be a unit eigenvector of $\boldsymbol{J}$ with eigenvalue λ, then multiplication by the Jacobian simply scales the difference at each step. The two executions of back-propagation are separated by a distance of $\delta|\lambda|^n$. When $\boldsymbol{v}$ corresponds to the largest value of $|\lambda|$, this perturbation achieves the widest possible separation of an initial perturbation of size δ.

When $|\lambda| > 1$, the deviation size $\delta|\lambda|^n$ grows exponentially large. When $|\lambda| < 1$, the deviation size becomes exponentially small.

Of course, this example assumed that the Jacobian was the same at every time step, corresponding to a recurrent network with no nonlinearity. When a nonlinearity is present, the derivative of the nonlinearity will approach zero on many time steps, and help to prevent the explosion resulting from a large spectral radius. Indeed, the most recent work on echo state networks advocates using a spectral radius much larger than unity (Yildiz *et al.*, 2012; Jaeger, 2012).

Everything we have said about back-propagation via repeated matrix multiplication applies equally to forward propagation in a network with no nonlinearity, where the state $\boldsymbol{h}^{(t+1)} = \boldsymbol{h}^{(t)\top}\boldsymbol{W}$.

When a linear map $\boldsymbol{W}^\top$ always shrinks $\boldsymbol{h}$ as measured by the L^2 norm, then we say that the map is **contractive**. When the spectral radius is less than one, the mapping from $\boldsymbol{h}^{(t)}$ to $\boldsymbol{h}^{(t+1)}$ is contractive, so a small change becomes smaller after each time step. This necessarily makes the network forget information about the past when we use a finite level of precision (such as 32 bit integers) to store the state vector.

The Jacobian matrix tells us how a small change of $\boldsymbol{h}^{(t)}$ propagates one step forward, or equivalently, how the gradient on $\boldsymbol{h}^{(t+1)}$ propagates one step backward, during back-propagation. Note that neither $\boldsymbol{W}$ nor $\boldsymbol{J}$ need to be symmetric (although they are square and real), so they can have complex-valued eigenvalues and eigenvectors, with imaginary components corresponding to potentially oscillatory

behavior (if the same Jacobian was applied iteratively). Even though $\boldsymbol{h}^{(t)}$ or a small variation of $\boldsymbol{h}^{(t)}$ of interest in back-propagation are real-valued, they can be expressed in such a complex-valued basis. What matters is what happens to the magnitude (complex absolute value) of these possibly complex-valued basis coefficients, when we multiply the matrix by the vector. An eigenvalue with magnitude greater than one corresponds to magnification (exponential growth, if applied iteratively) or shrinking (exponential decay, if applied iteratively).

With a nonlinear map, the Jacobian is free to change at each step. The dynamics therefore become more complicated. However, it remains true that a small initial variation can turn into a large variation after several steps. One difference between the purely linear case and the nonlinear case is that the use of a squashing nonlinearity such as tanh can cause the recurrent dynamics to become bounded. Note that it is possible for back-propagation to retain unbounded dynamics even when forward propagation has bounded dynamics, for example, when a sequence of tanh units are all in the middle of their linear regime and are connected by weight matrices with spectral radius greater than 1. However, it is rare for all of the tanh units to simultaneously lie at their linear activation point.

The strategy of echo state networks is simply to fix the weights to have some spectral radius such as 3, where information is carried forward through time but does not explode due to the stabilizing effect of saturating nonlinearities like tanh.

More recently, it has been shown that the techniques used to set the weights in ESNs could be used to *initialize* the weights in a fully trainable recurrent network (with the hidden-to-hidden recurrent weights trained using back-propagation through time), helping to learn long-term dependencies (Sutskever, 2012; Sutskever *et al.*, 2013). In this setting, an initial spectral radius of 1.2 performs well, combined with the sparse initialization scheme described in section 8.4.

10.9 Leaky Units and Other Strategies for Multiple Time Scales

One way to deal with long-term dependencies is to design a model that operates at multiple time scales, so that some parts of the model operate at fine-grained time scales and can handle small details, while other parts operate at coarse time scales and transfer information from the distant past to the present more efficiently. Various strategies for building both fine and coarse time scales are possible. These include the addition of skip connections across time, "leaky units" that integrate signals with different time constants, and the removal of some of the connections

used to model fine-grained time scales.

10.9.1 Adding Skip Connections through Time

One way to obtain coarse time scales is to add direct connections from variables in the distant past to variables in the present. The idea of using such skip connections dates back to Lin *et al.* (1996) and follows from the idea of incorporating delays in feedforward neural networks (Lang and Hinton, 1988). In an ordinary recurrent network, a recurrent connection goes from a unit at time t to a unit at time $t+1$. It is possible to construct recurrent networks with longer delays (Bengio, 1991).

As we have seen in section 8.2.5, gradients may vanish or explode exponentially *with respect to the number of time steps*. Lin *et al.* (1996) introduced recurrent connections with a time-delay of d to mitigate this problem. Gradients now diminish exponentially as a function of $\frac{\tau}{d}$ rather than τ. Since there are both delayed and single step connections, gradients may still explode exponentially in τ. This allows the learning algorithm to capture longer dependencies although not all long-term dependencies may be represented well in this way.

10.9.2 Leaky Units and a Spectrum of Different Time Scales

Another way to obtain paths on which the product of derivatives is close to one is to have units with *linear* self-connections and a weight near one on these connections.

When we accumulate a running average $\mu^{(t)}$ of some value $v^{(t)}$ by applying the update $\mu^{(t)} \leftarrow \alpha\mu^{(t-1)} + (1-\alpha)v^{(t)}$ the α parameter is an example of a linear self-connection from $\mu^{(t-1)}$ to $\mu^{(t)}$. When α is near one, the running average remembers information about the past for a long time, and when α is near zero, information about the past is rapidly discarded. Hidden units with linear self-connections can behave similarly to such running averages. Such hidden units are called **leaky units**.

Skip connections through d time steps are a way of ensuring that a unit can always learn to be influenced by a value from d time steps earlier. The use of a linear self-connection with a weight near one is a different way of ensuring that the unit can access values from the past. The linear self-connection approach allows this effect to be adapted more smoothly and flexibly by adjusting the real-valued α rather than by adjusting the integer-valued skip length.

These ideas were proposed by Mozer (1992) and by El Hihi and Bengio (1996). Leaky units were also found to be useful in the context of echo state networks (Jaeger *et al.*, 2007).

There are two basic strategies for setting the time constants used by leaky units. One strategy is to manually fix them to values that remain constant, for example by sampling their values from some distribution once at initialization time. Another strategy is to make the time constants free parameters and learn them. Having such leaky units at different time scales appears to help with long-term dependencies (Mozer, 1992; Pascanu *et al.*, 2013).

10.9.3 Removing Connections

Another approach to handle long-term dependencies is the idea of organizing the state of the RNN at multiple time-scales (El Hihi and Bengio, 1996), with information flowing more easily through long distances at the slower time scales.

This idea differs from the skip connections through time discussed earlier because it involves actively *removing* length-one connections and replacing them with longer connections. Units modified in such a way are forced to operate on a long time scale. Skip connections through time *add* edges. Units receiving such new connections may learn to operate on a long time scale but may also choose to focus on their other short-term connections.

There are different ways in which a group of recurrent units can be forced to operate at different time scales. One option is to make the recurrent units leaky, but to have different groups of units associated with different fixed time scales. This was the proposal in Mozer (1992) and has been successfully used in Pascanu *et al.* (2013). Another option is to have explicit and discrete updates taking place at different times, with a different frequency for different groups of units. This is the approach of El Hihi and Bengio (1996) and Koutnik *et al.* (2014). It worked well on a number of benchmark datasets.

10.10 The Long Short-Term Memory and Other Gated RNNs

As of this writing, the most effective sequence models used in practical applications are called **gated RNNs**. These include the **long short-term memory** and networks based on the **gated recurrent unit**.

Like leaky units, gated RNNs are based on the idea of creating paths through time that have derivatives that neither vanish nor explode. Leaky units did this with connection weights that were either manually chosen constants or were parameters. Gated RNNs generalize this to connection weights that may change

at each time step.

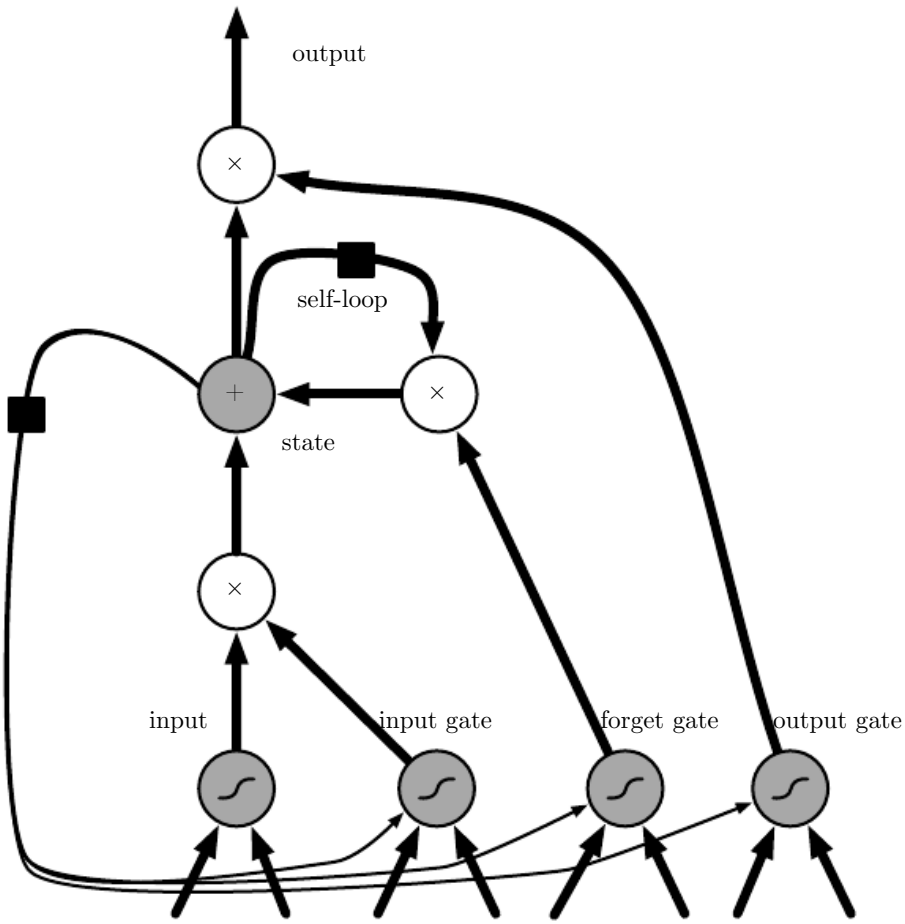

Figure 10.16: Block diagram of the LSTM recurrent network "cell." Cells are connected recurrently to each other, replacing the usual hidden units of ordinary recurrent networks. An input feature is computed with a regular artificial neuron unit. Its value can be accumulated into the state if the sigmoidal input gate allows it. The state unit has a linear self-loop whose weight is controlled by the forget gate. The output of the cell can be shut off by the output gate. All the gating units have a sigmoid nonlinearity, while the input unit can have any squashing nonlinearity. The state unit can also be used as an extra input to the gating units. The black square indicates a delay of a single time step.

Leaky units allow the network to *accumulate* information (such as evidence for a particular feature or category) over a long duration. However, once that information has been used, it might be useful for the neural network to *forget* the old state. For example, if a sequence is made of sub-sequences and we want a leaky unit to accumulate evidence inside each sub-subsequence, we need a mechanism to forget the old state by setting it to zero. Instead of manually deciding when to clear the state, we want the neural network to learn to decide when to do it. This

is what gated RNNs do.

10.10.1 LSTM

The clever idea of introducing self-loops to produce paths where the gradient can flow for long durations is a core contribution of the initial **long short-term memory (LSTM)** model (Hochreiter and Schmidhuber, 1997). A crucial addition has been to make the weight on this self-loop conditioned on the context, rather than fixed (Gers *et al.*, 2000). By making the weight of this self-loop gated (controlled by another hidden unit), the time scale of integration can be changed dynamically. In this case, we mean that even for an LSTM with fixed parameters, the time scale of integration can change based on the input sequence, because the time constants are output by the model itself. The LSTM has been found extremely successful in many applications, such as unconstrained handwriting recognition (Graves *et al.*, 2009), speech recognition (Graves *et al.*, 2013; Graves and Jaitly, 2014), handwriting generation (Graves, 2013), machine translation (Sutskever *et al.*, 2014), image captioning (Kiros *et al.*, 2014b; Vinyals *et al.*, 2014b; Xu *et al.*, 2015) and parsing (Vinyals *et al.*, 2014a).

The LSTM block diagram is illustrated in figure 10.16. The corresponding forward propagation equations are given below, in the case of a shallow recurrent network architecture. Deeper architectures have also been successfully used (Graves *et al.*, 2013; Pascanu *et al.*, 2014a). Instead of a unit that simply applies an element-wise nonlinearity to the affine transformation of inputs and recurrent units, LSTM recurrent networks have "LSTM cells" that have an internal recurrence (a self-loop), in addition to the outer recurrence of the RNN. Each cell has the same inputs and outputs as an ordinary recurrent network, but has more parameters and a system of gating units that controls the flow of information. The most important component is the state unit $s_i^{(t)}$ that has a linear self-loop similar to the leaky units described in the previous section. However, here, the self-loop weight (or the associated time constant) is controlled by a **forget gate** unit $f_i^{(t)}$ (for time step t and cell i), that sets this weight to a value between 0 and 1 via a sigmoid unit:

$$f_i^{(t)} = \sigma\left(b_i^f + \sum_j U_{i,j}^f x_j^{(t)} + \sum_j W_{i,j}^f h_j^{(t-1)}\right), \tag{10.40}$$

where $\boldsymbol{x}^{(t)}$ is the current input vector and $\boldsymbol{h}^{(t)}$ is the current hidden layer vector, containing the outputs of all the LSTM cells, and $\boldsymbol{b}^f$,$\boldsymbol{U}^f$, $\boldsymbol{W}^f$ are respectively biases, input weights and recurrent weights for the forget gates. The LSTM cell

internal state is thus updated as follows, but with a conditional self-loop weight $f_i^{(t)}$:

$$s_i^{(t)} = f_i^{(t)} s_i^{(t-1)} + g_i^{(t)} \sigma \left(b_i + \sum_j U_{i,j} x_j^{(t)} + \sum_j W_{i,j} h_j^{(t-1)} \right), \tag{10.41}$$

where $\boldsymbol{b}$, $\boldsymbol{U}$ and $\boldsymbol{W}$ respectively denote the biases, input weights and recurrent weights into the LSTM cell. The **external input gate** unit $g_i^{(t)}$ is computed similarly to the forget gate (with a sigmoid unit to obtain a gating value between 0 and 1), but with its own parameters:

$$g_i^{(t)} = \sigma \left(b_i^g + \sum_j U_{i,j}^g x_j^{(t)} + \sum_j W_{i,j}^g h_j^{(t-1)} \right). \tag{10.42}$$

The output $h_i^{(t)}$ of the LSTM cell can also be shut off, via the **output gate** $q_i^{(t)}$, which also uses a sigmoid unit for gating:

$$h_i^{(t)} = \tanh \left(s_i^{(t)} \right) q_i^{(t)} \tag{10.43}$$

$$q_i^{(t)} = \sigma \left(b_i^o + \sum_j U_{i,j}^o x_j^{(t)} + \sum_j W_{i,j}^o h_j^{(t-1)} \right) \tag{10.44}$$

which has parameters $\boldsymbol{b}^o$, $\boldsymbol{U}^o$, $\boldsymbol{W}^o$ for its biases, input weights and recurrent weights, respectively. Among the variants, one can choose to use the cell state $s_i^{(t)}$ as an extra input (with its weight) into the three gates of the i-th unit, as shown in figure 10.16. This would require three additional parameters.

LSTM networks have been shown to learn long-term dependencies more easily than the simple recurrent architectures, first on artificial data sets designed for testing the ability to learn long-term dependencies (Bengio *et al.*, 1994; Hochreiter and Schmidhuber, 1997; Hochreiter *et al.*, 2001), then on challenging sequence processing tasks where state-of-the-art performance was obtained (Graves, 2012; Graves *et al.*, 2013; Sutskever *et al.*, 2014). Variants and alternatives to the LSTM have been studied and used and are discussed next.

10.10.2 Other Gated RNNs

Which pieces of the LSTM architecture are actually necessary? What other successful architectures could be designed that allow the network to dynamically control the time scale and forgetting behavior of different units?

Some answers to these questions are given with the recent work on gated RNNs, whose units are also known as gated recurrent units or GRUs (Cho *et al.*, 2014b; Chung *et al.*, 2014, 2015a; Jozefowicz *et al.*, 2015; Chrupala *et al.*, 2015). The main difference with the LSTM is that a single gating unit simultaneously controls the forgetting factor and the decision to update the state unit. The update equations are the following:

$$h_i^{(t)} = u_i^{(t-1)} h_i^{(t-1)} + (1 - u_i^{(t-1)}) \sigma \left(b_i + \sum_j U_{i,j} x_j^{(t-1)} + \sum_j W_{i,j} r_j^{(t-1)} h_j^{(t-1)} \right), \tag{10.45}$$

where $\boldsymbol{u}$ stands for "update" gate and $\boldsymbol{r}$ for "reset" gate. Their value is defined as usual:

$$u_i^{(t)} = \sigma \left(b_i^u + \sum_j U_{i,j}^u x_j^{(t)} + \sum_j W_{i,j}^u h_j^{(t)} \right) \tag{10.46}$$

and

$$r_i^{(t)} = \sigma \left(b_i^r + \sum_j U_{i,j}^r x_j^{(t)} + \sum_j W_{i,j}^r h_j^{(t)} \right). \tag{10.47}$$

The reset and updates gates can individually "ignore" parts of the state vector. The update gates act like conditional leaky integrators that can linearly gate any dimension, thus choosing to copy it (at one extreme of the sigmoid) or completely ignore it (at the other extreme) by replacing it by the new "target state" value (towards which the leaky integrator wants to converge). The reset gates control which parts of the state get used to compute the next target state, introducing an additional nonlinear effect in the relationship between past state and future state.

Many more variants around this theme can be designed. For example the reset gate (or forget gate) output could be shared across multiple hidden units. Alternately, the product of a global gate (covering a whole group of units, such as an entire layer) and a local gate (per unit) could be used to combine global control and local control. However, several investigations over architectural variations of the LSTM and GRU found no variant that would clearly beat both of these across a wide range of tasks (Greff *et al.*, 2015; Jozefowicz *et al.*, 2015). Greff *et al.* (2015) found that a crucial ingredient is the forget gate, while Jozefowicz *et al.* (2015) found that adding a bias of 1 to the LSTM forget gate, a practice advocated by Gers *et al.* (2000), makes the LSTM as strong as the best of the explored architectural variants.

10.11 Optimization for Long-Term Dependencies

Section 8.2.5 and section 10.7 have described the vanishing and exploding gradient problems that occur when optimizing RNNs over many time steps.

An interesting idea proposed by Martens and Sutskever (2011) is that second derivatives may vanish at the same time that first derivatives vanish. Second-order optimization algorithms may roughly be understood as dividing the first derivative by the second derivative (in higher dimension, multiplying the gradient by the inverse Hessian). If the second derivative shrinks at a similar rate to the first derivative, then the ratio of first and second derivatives may remain relatively constant. Unfortunately, second-order methods have many drawbacks, including high computational cost, the need for a large minibatch, and a tendency to be attracted to saddle points. Martens and Sutskever (2011) found promising results using second-order methods. Later, Sutskever *et al.* (2013) found that simpler methods such as Nesterov momentum with careful initialization could achieve similar results. See Sutskever (2012) for more detail. Both of these approaches have largely been replaced by simply using SGD (even without momentum) applied to LSTMs. This is part of a continuing theme in machine learning that it is often much easier to design a model that is easy to optimize than it is to design a more powerful optimization algorithm.

10.11.1 Clipping Gradients

As discussed in section 8.2.4, strongly nonlinear functions such as those computed by a recurrent net over many time steps tend to have derivatives that can be either very large or very small in magnitude. This is illustrated in figure 8.3 and figure 10.17, in which we see that the objective function (as a function of the parameters) has a "landscape" in which one finds "cliffs": wide and rather flat regions separated by tiny regions where the objective function changes quickly, forming a kind of cliff.

The difficulty that arises is that when the parameter gradient is very large, a gradient descent parameter update could throw the parameters very far, into a region where the objective function is larger, undoing much of the work that had been done to reach the current solution. The gradient tells us the direction that corresponds to the steepest descent within an infinitesimal region surrounding the current parameters. Outside of this infinitesimal region, the cost function may begin to curve back upwards. The update must be chosen to be small enough to avoid traversing too much upward curvature. We typically use learning rates that

decay slowly enough that consecutive steps have approximately the same learning rate. A step size that is appropriate for a relatively linear part of the landscape is often inappropriate and causes uphill motion if we enter a more curved part of the landscape on the next step.

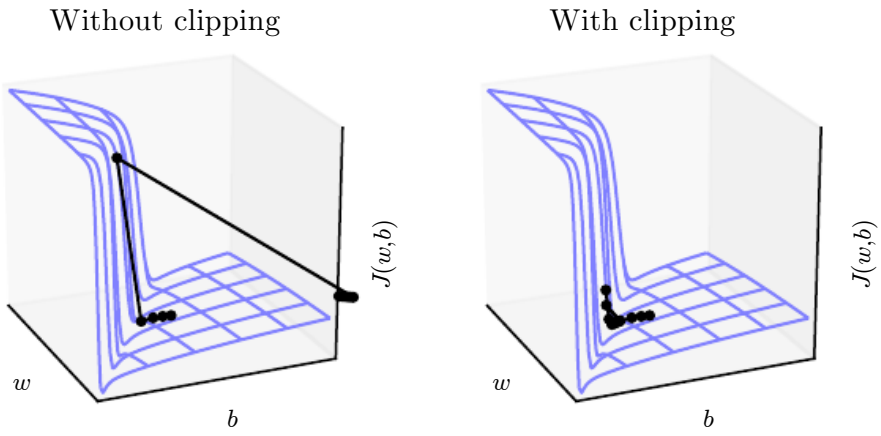

Figure 10.17: Example of the effect of gradient clipping in a recurrent network with two parameters $\boldsymbol{w}$ and $\boldsymbol{b}$. Gradient clipping can make gradient descent perform more reasonably in the vicinity of extremely steep cliffs. These steep cliffs commonly occur in recurrent networks near where a recurrent network behaves approximately linearly. The cliff is exponentially steep in the number of time steps because the weight matrix is multiplied by itself once for each time step. *(Left)*Gradient descent without gradient clipping overshoots the bottom of this small ravine, then receives a very large gradient from the cliff face. The large gradient catastrophically propels the parameters outside the axes of the plot. *(Right)*Gradient descent with gradient clipping has a more moderate reaction to the cliff. While it does ascend the cliff face, the step size is restricted so that it cannot be propelled away from steep region near the solution. Figure adapted with permission from Pascanu *et al.* (2013).

A simple type of solution has been in use by practitioners for many years: **clipping the gradient**. There are different instances of this idea (Mikolov, 2012; Pascanu *et al.*, 2013). One option is to clip the parameter gradient from a minibatch *element-wise* (Mikolov, 2012) just before the parameter update. Another is to *clip the norm* $||\boldsymbol{g}||$ *of the gradient* $\boldsymbol{g}$ (Pascanu *et al.*, 2013) just before the parameter update:

$$\text{if } ||\boldsymbol{g}|| > v \tag{10.48}$$

$$\boldsymbol{g} \leftarrow \frac{\boldsymbol{g}v}{||\boldsymbol{g}||} \tag{10.49}$$

where v is the norm threshold and $\boldsymbol{g}$ is used to update parameters. Because the gradient of all the parameters (including different groups of parameters, such as weights and biases) is renormalized jointly with a single scaling factor, the latter method has the advantage that it guarantees that each step is still in the gradient direction, but experiments suggest that both forms work similarly. Although the parameter update has the same direction as the true gradient, with gradient norm clipping, the parameter update vector norm is now bounded. This bounded gradient avoids performing a detrimental step when the gradient explodes. In fact, even simply taking a *random step* when the gradient magnitude is above a threshold tends to work almost as well. If the explosion is so severe that the gradient is numerically `Inf` or `Nan` (considered infinite or not-a-number), then a random step of size v can be taken and will typically move away from the numerically unstable configuration. Clipping the gradient norm per-minibatch will not change the direction of the gradient for an individual minibatch. However, taking the average of the norm-clipped gradient from many minibatches is not equivalent to clipping the norm of the true gradient (the gradient formed from using all examples). Examples that have large gradient norm, as well as examples that appear in the same minibatch as such examples, will have their contribution to the final direction diminished. This stands in contrast to traditional minibatch gradient descent, where the true gradient direction is equal to the average over all minibatch gradients. Put another way, traditional stochastic gradient descent uses an unbiased estimate of the gradient, while gradient descent with norm clipping introduces a heuristic bias that we know empirically to be useful. With element-wise clipping, the direction of the update is not aligned with the true gradient or the minibatch gradient, but it is still a descent direction. It has also been proposed (Graves, 2013) to clip the back-propagated gradient (with respect to hidden units) but no comparison has been published between these variants; we conjecture that all these methods behave similarly.

10.11.2 Regularizing to Encourage Information Flow

Gradient clipping helps to deal with exploding gradients, but it does not help with vanishing gradients. To address vanishing gradients and better capture long-term dependencies, we discussed the idea of creating paths in the computational graph of the unfolded recurrent architecture along which the product of gradients associated with arcs is near 1. One approach to achieve this is with LSTMs and other self-loops and gating mechanisms, described above in section 10.10. Another idea is to regularize or constrain the parameters so as to encourage "information flow." In particular, we would like the gradient vector $\nabla_{\boldsymbol{h}^{(t)}} L$ being back-propagated to

maintain its magnitude, even if the loss function only penalizes the output at the end of the sequence. Formally, we want

$$(\nabla_{\boldsymbol{h}^{(t)}} L) \frac{\partial \boldsymbol{h}^{(t)}}{\partial \boldsymbol{h}^{(t-1)}} \tag{10.50}$$

to be as large as

$$\nabla_{\boldsymbol{h}^{(t)}} L. \tag{10.51}$$

With this objective, Pascanu *et al.* (2013) propose the following regularizer:

$$\Omega = \sum_t \left(\frac{\left| \left| (\nabla_{\boldsymbol{h}^{(t)}} L) \frac{\partial \boldsymbol{h}^{(t)}}{\partial \boldsymbol{h}^{(t-1)}} \right| \right|}{||\nabla_{\boldsymbol{h}^{(t)}} L||} - 1 \right)^2 . \tag{10.52}$$

Computing the gradient of this regularizer may appear difficult, but Pascanu *et al.* (2013) propose an approximation in which we consider the back-propagated vectors $\nabla_{\boldsymbol{h}^{(t)}} L$ as if they were constants (for the purpose of this regularizer, so that there is no need to back-propagate through them). The experiments with this regularizer suggest that, if combined with the norm clipping heuristic (which handles gradient explosion), the regularizer can considerably increase the span of the dependencies that an RNN can learn. Because it keeps the RNN dynamics on the edge of explosive gradients, the gradient clipping is particularly important. Without gradient clipping, gradient explosion prevents learning from succeeding.

A key weakness of this approach is that it is not as effective as the LSTM for tasks where data is abundant, such as language modeling.

10.12 Explicit Memory

Intelligence requires knowledge and acquiring knowledge can be done via learning, which has motivated the development of large-scale deep architectures. However, there are different kinds of knowledge. Some knowledge can be implicit, subconscious, and difficult to verbalize—such as how to walk, or how a dog looks different from a cat. Other knowledge can be explicit, declarative, and relatively straightforward to put into words—every day commonsense knowledge, like "a cat is a kind of animal," or very specific facts that you need to know to accomplish your current goals, like "the meeting with the sales team is at 3:00 PM in room 141."

Neural networks excel at storing implicit knowledge. However, they struggle to memorize facts. Stochastic gradient descent requires many presentations of the

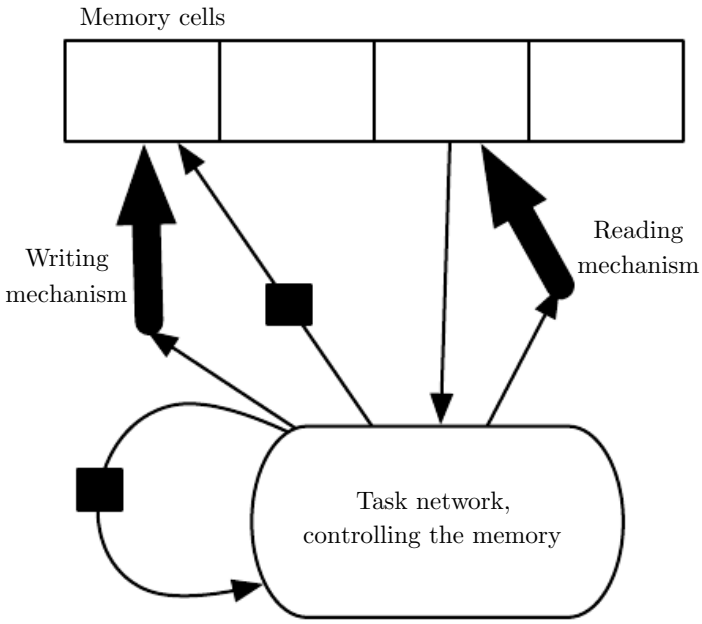

Figure 10.18: A schematic of an example of a network with an explicit memory, capturing some of the key design elements of the neural Turing machine. In this diagram we distinguish the "representation" part of the model (the "task network," here a recurrent net in the bottom) from the "memory" part of the model (the set of cells), which can store facts. The task network learns to "control" the memory, deciding where to read from and where to write to within the memory (through the reading and writing mechanisms, indicated by bold arrows pointing at the reading and writing addresses).

same input before it can be stored in a neural network parameters, and even then, that input will not be stored especially precisely. Graves *et al.* (2014b) hypothesized that this is because neural networks lack the equivalent of the **working memory** system that allows human beings to explicitly hold and manipulate pieces of information that are relevant to achieving some goal. Such explicit memory components would allow our systems not only to rapidly and "intentionally" store and retrieve specific facts but also to sequentially reason with them. The need for neural networks that can process information in a sequence of steps, changing the way the input is fed into the network at each step, has long been recognized as important for the ability to reason rather than to make automatic, intuitive responses to the input (Hinton, 1990).

To resolve this difficulty, Weston *et al.* (2014) introduced **memory networks** that include a set of memory cells that can be accessed via an addressing mechanism. Memory networks originally required a supervision signal instructing them how to use their memory cells. Graves *et al.* (2014b) introduced the **neural Turing machine**, which is able to learn to read from and write arbitrary content to memory cells without explicit supervision about which actions to undertake, and allowed end-to-end training without this supervision signal, via the use of a content-based soft attention mechanism (see Bahdanau *et al.* (2015) and section 12.4.5.1). This soft addressing mechanism has become standard with other related architectures emulating algorithmic mechanisms in a way that still allows gradient-based optimization (Sukhbaatar *et al.*, 2015; Joulin and Mikolov, 2015; Kumar *et al.*, 2015; Vinyals *et al.*, 2015a; Grefenstette *et al.*, 2015).

Each memory cell can be thought of as an extension of the memory cells in LSTMs and GRUs. The difference is that the network outputs an internal state that chooses which cell to read from or write to, just as memory accesses in a digital computer read from or write to a specific address.

It is difficult to optimize functions that produce exact, integer addresses. To alleviate this problem, NTMs actually read to or write from many memory cells simultaneously. To read, they take a weighted average of many cells. To write, they modify multiple cells by different amounts. The coefficients for these operations are chosen to be focused on a small number of cells, for example, by producing them via a softmax function. Using these weights with non-zero derivatives allows the functions controlling access to the memory to be optimized using gradient descent. The gradient on these coefficients indicates whether each of them should be increased or decreased, but the gradient will typically be large only for those memory addresses receiving a large coefficient.

These memory cells are typically augmented to contain a vector, rather than

the single scalar stored by an LSTM or GRU memory cell. There are two reasons to increase the size of the memory cell. One reason is that we have increased the cost of accessing a memory cell. We pay the computational cost of producing a coefficient for many cells, but we expect these coefficients to cluster around a small number of cells. By reading a vector value, rather than a scalar value, we can offset some of this cost. Another reason to use vector-valued memory cells is that they allow for **content-based addressing**, where the weight used to read to or write from a cell is a function of that cell. Vector-valued cells allow us to retrieve a complete vector-valued memory if we are able to produce a pattern that matches some but not all of its elements. This is analogous to the way that people can recall the lyrics of a song based on a few words. We can think of a content-based read instruction as saying, "Retrieve the lyrics of the song that has the chorus 'We all live in a yellow submarine.'" Content-based addressing is more useful when we make the objects to be retrieved large—if every letter of the song was stored in a separate memory cell, we would not be able to find them this way. By comparison, **location-based addressing** is not allowed to refer to the content of the memory. We can think of a location-based read instruction as saying "Retrieve the lyrics of the song in slot 347." Location-based addressing can often be a perfectly sensible mechanism even when the memory cells are small.

If the content of a memory cell is copied (not forgotten) at most time steps, then the information it contains can be propagated forward in time and the gradients propagated backward in time without either vanishing or exploding.

The explicit memory approach is illustrated in figure 10.18, where we see that a "task neural network" is coupled with a memory. Although that task neural network could be feedforward or recurrent, the overall system is a recurrent network. The task network can choose to read from or write to specific memory addresses. Explicit memory seems to allow models to learn tasks that ordinary RNNs or LSTM RNNs cannot learn. One reason for this advantage may be because information and gradients can be propagated (forward in time or backwards in time, respectively) for very long durations.

As an alternative to back-propagation through weighted averages of memory cells, we can interpret the memory addressing coefficients as probabilities and stochastically read just one cell (Zaremba and Sutskever, 2015). Optimizing models that make discrete decisions requires specialized optimization algorithms, described in section 20.9.1. So far, training these stochastic architectures that make discrete decisions remains harder than training deterministic algorithms that make soft decisions.

Whether it is soft (allowing back-propagation) or stochastic and hard, the

mechanism for choosing an address is in its form identical to the **attention mechanism** which had been previously introduced in the context of machine translation (Bahdanau *et al.*, 2015) and discussed in section 12.4.5.1. The idea of attention mechanisms for neural networks was introduced even earlier, in the context of handwriting generation (Graves, 2013), with an attention mechanism that was constrained to move only forward in time through the sequence. In the case of machine translation and memory networks, at each step, the focus of attention can move to a completely different place, compared to the previous step.

Recurrent neural networks provide a way to extend deep learning to sequential data. They are the last major tool in our deep learning toolbox. Our discussion now moves to how to choose and use these tools and how to apply them to real-world tasks.

Chapter 11

Practical Methodology

Successfully applying deep learning techniques requires more than just a good knowledge of what algorithms exist and the principles that explain how they work. A good machine learning practitioner also needs to know how to choose an algorithm for a particular application and how to monitor and respond to feedback obtained from experiments in order to improve a machine learning system. During day to day development of machine learning systems, practitioners need to decide whether to gather more data, increase or decrease model capacity, add or remove regularizing features, improve the optimization of a model, improve approximate inference in a model, or debug the software implementation of the model. All of these operations are at the very least time-consuming to try out, so it is important to be able to determine the right course of action rather than blindly guessing.

Most of this book is about different machine learning models, training algorithms, and objective functions. This may give the impression that the most important ingredient to being a machine learning expert is knowing a wide variety of machine learning techniques and being good at different kinds of math. In practice, one can usually do much better with a correct application of a commonplace algorithm than by sloppily applying an obscure algorithm. Correct application of an algorithm depends on mastering some fairly simple methodology. Many of the recommendations in this chapter are adapted from Ng (2015).

We recommend the following practical design process:

- Determine your goals—what error metric to use, and your target value for this error metric. These goals and error metrics should be driven by the problem that the application is intended to solve.
- Establish a working end-to-end pipeline as soon as possible, including the

estimation of the appropriate performance metrics.

- Instrument the system well to determine bottlenecks in performance. Diagnose which components are performing worse than expected and whether it is due to overfitting, underfitting, or a defect in the data or software.

- Repeatedly make incremental changes such as gathering new data, adjusting hyperparameters, or changing algorithms, based on specific findings from your instrumentation.

As a running example, we will use Street View address number transcription system (Goodfellow *et al.*, 2014d). The purpose of this application is to add buildings to Google Maps. Street View cars photograph the buildings and record the GPS coordinates associated with each photograph. A convolutional network recognizes the address number in each photograph, allowing the Google Maps database to add that address in the correct location. The story of how this commercial application was developed gives an example of how to follow the design methodology we advocate.

We now describe each of the steps in this process.

11.1 Performance Metrics

Determining your goals, in terms of which error metric to use, is a necessary first step because your error metric will guide all of your future actions. You should also have an idea of what level of performance you desire.

Keep in mind that for most applications, it is impossible to achieve absolute zero error. The Bayes error defines the minimum error rate that you can hope to achieve, even if you have infinite training data and can recover the true probability distribution. This is because your input features may not contain complete information about the output variable, or because the system might be intrinsically stochastic. You will also be limited by having a finite amount of training data.

The amount of training data can be limited for a variety of reasons. When your goal is to build the best possible real-world product or service, you can typically collect more data but must determine the value of reducing error further and weigh this against the cost of collecting more data. Data collection can require time, money, or human suffering (for example, if your data collection process involves performing invasive medical tests). When your goal is to answer a scientific question about which algorithm performs better on a fixed benchmark, the benchmark

specification usually determines the training set and you are not allowed to collect more data.

How can one determine a reasonable level of performance to expect? Typically, in the academic setting, we have some estimate of the error rate that is attainable based on previously published benchmark results. In the real-word setting, we have some idea of the error rate that is necessary for an application to be safe, cost-effective, or appealing to consumers. Once you have determined your realistic desired error rate, your design decisions will be guided by reaching this error rate.

Another important consideration besides the target value of the performance metric is the choice of which metric to use. Several different performance metrics may be used to measure the effectiveness of a complete application that includes machine learning components. These performance metrics are usually different from the cost function used to train the model. As described in section 5.1.2, it is common to measure the accuracy, or equivalently, the error rate, of a system.

However, many applications require more advanced metrics.

Sometimes it is much more costly to make one kind of a mistake than another. For example, an e-mail spam detection system can make two kinds of mistakes: incorrectly classifying a legitimate message as spam, and incorrectly allowing a spam message to appear in the inbox. It is much worse to block a legitimate message than to allow a questionable message to pass through. Rather than measuring the error rate of a spam classifier, we may wish to measure some form of total cost, where the cost of blocking legitimate messages is higher than the cost of allowing spam messages.

Sometimes we wish to train a binary classifier that is intended to detect some rare event. For example, we might design a medical test for a rare disease. Suppose that only one in every million people has this disease. We can easily achieve 99.9999% accuracy on the detection task, by simply hard-coding the classifier to always report that the disease is absent. Clearly, accuracy is a poor way to characterize the performance of such a system. One way to solve this problem is to instead measure **precision** and **recall**. Precision is the fraction of detections reported by the model that were correct, while recall is the fraction of true events that were detected. A detector that says no one has the disease would achieve perfect precision, but zero recall. A detector that says everyone has the disease would achieve perfect recall, but precision equal to the percentage of people who have the disease (0.0001% in our example of a disease that only one people in a million have). When using precision and recall, it is common to plot a **PR curve**, with precision on the y-axis and recall on the x-axis. The classifier generates a score that is higher if the event to be detected occurred. For example, a feedforward

network designed to detect a disease outputs $\hat{y} = P(y = 1 \mid \boldsymbol{x})$, estimating the probability that a person whose medical results are described by features $\boldsymbol{x}$ has the disease. We choose to report a detection whenever this score exceeds some threshold. By varying the threshold, we can trade precision for recall. In many cases, we wish to summarize the performance of the classifier with a single number rather than a curve. To do so, we can convert precision p and recall r into an **F-score** given by

$$F = \frac{2pr}{p + r}. \tag{11.1}$$

Another option is to report the total area lying beneath the PR curve.

In some applications, it is possible for the machine learning system to refuse to make a decision. This is useful when the machine learning algorithm can estimate how confident it should be about a decision, especially if a wrong decision can be harmful and if a human operator is able to occasionally take over. The Street View transcription system provides an example of this situation. The task is to transcribe the address number from a photograph in order to associate the location where the photo was taken with the correct address in a map. Because the value of the map degrades considerably if the map is inaccurate, it is important to add an address only if the transcription is correct. If the machine learning system thinks that it is less likely than a human being to obtain the correct transcription, then the best course of action is to allow a human to transcribe the photo instead. Of course, the machine learning system is only useful if it is able to dramatically reduce the amount of photos that the human operators must process. A natural performance metric to use in this situation is **coverage**. Coverage is the fraction of examples for which the machine learning system is able to produce a response. It is possible to trade coverage for accuracy. One can always obtain 100% accuracy by refusing to process any example, but this reduces the coverage to 0%. For the Street View task, the goal for the project was to reach human-level transcription accuracy while maintaining 95% coverage. Human-level performance on this task is 98% accuracy.

Many other metrics are possible. We can for example, measure click-through rates, collect user satisfaction surveys, and so on. Many specialized application areas have application-specific criteria as well.

What is important is to determine which performance metric to improve ahead of time, then concentrate on improving this metric. Without clearly defined goals, it can be difficult to tell whether changes to a machine learning system make progress or not.

11.2 Default Baseline Models

After choosing performance metrics and goals, the next step in any practical application is to establish a reasonable end-to-end system as soon as possible. In this section, we provide recommendations for which algorithms to use as the first baseline approach in various situations. Keep in mind that deep learning research progresses quickly, so better default algorithms are likely to become available soon after this writing.

Depending on the complexity of your problem, you may even want to begin without using deep learning. If your problem has a chance of being solved by just choosing a few linear weights correctly, you may want to begin with a simple statistical model like logistic regression.

If you know that your problem falls into an "AI-complete" category like object recognition, speech recognition, machine translation, and so on, then you are likely to do well by beginning with an appropriate deep learning model.

First, choose the general category of model based on the structure of your data. If you want to perform supervised learning with fixed-size vectors as input, use a feedforward network with fully connected layers. If the input has known topological structure (for example, if the input is an image), use a convolutional network. In these cases, you should begin by using some kind of piecewise linear unit (ReLUs or their generalizations like Leaky ReLUs, PreLus and maxout). If your input or output is a sequence, use a gated recurrent net (LSTM or GRU).

A reasonable choice of optimization algorithm is SGD with momentum with a decaying learning rate (popular decay schemes that perform better or worse on different problems include decaying linearly until reaching a fixed minimum learning rate, decaying exponentially, or decreasing the learning rate by a factor of 2-10 each time validation error plateaus). Another very reasonable alternative is Adam. Batch normalization can have a dramatic effect on optimization performance, especially for convolutional networks and networks with sigmoidal nonlinearities. While it is reasonable to omit batch normalization from the very first baseline, it should be introduced quickly if optimization appears to be problematic.

Unless your training set contains tens of millions of examples or more, you should include some mild forms of regularization from the start. Early stopping should be used almost universally. Dropout is an excellent regularizer that is easy to implement and compatible with many models and training algorithms. Batch normalization also sometimes reduces generalization error and allows dropout to be omitted, due to the noise in the estimate of the statistics used to normalize each variable.

If your task is similar to another task that has been studied extensively, you will probably do well by first copying the model and algorithm that is already known to perform best on the previously studied task. You may even want to copy a trained model from that task. For example, it is common to use the features from a convolutional network trained on ImageNet to solve other computer vision tasks (Girshick *et al.*, 2015).

A common question is whether to begin by using unsupervised learning, described further in part III. This is somewhat domain specific. Some domains, such as natural language processing, are known to benefit tremendously from unsupervised learning techniques such as learning unsupervised word embeddings. In other domains, such as computer vision, current unsupervised learning techniques do not bring a benefit, except in the semi-supervised setting, when the number of labeled examples is very small (Kingma *et al.*, 2014; Rasmus *et al.*, 2015). If your application is in a context where unsupervised learning is known to be important, then include it in your first end-to-end baseline. Otherwise, only use unsupervised learning in your first attempt if the task you want to solve is unsupervised. You can always try adding unsupervised learning later if you observe that your initial baseline overfits.

11.3 Determining Whether to Gather More Data

After the first end-to-end system is established, it is time to measure the performance of the algorithm and determine how to improve it. Many machine learning novices are tempted to make improvements by trying out many different algorithms. However, it is often much better to gather more data than to improve the learning algorithm.

How does one decide whether to gather more data? First, determine whether the performance on the training set is acceptable. If performance on the training set is poor, the learning algorithm is not using the training data that is already available, so there is no reason to gather more data. Instead, try increasing the size of the model by adding more layers or adding more hidden units to each layer. Also, try improving the learning algorithm, for example by tuning the learning rate hyperparameter. If large models and carefully tuned optimization algorithms do not work well, then the problem might be the *quality* of the training data. The data may be too noisy or may not include the right inputs needed to predict the desired outputs. This suggests starting over, collecting cleaner data or collecting a richer set of features.

If the performance on the training set is acceptable, then measure the per-

formance on a test set. If the performance on the test set is also acceptable, then there is nothing left to be done. If test set performance is much worse than training set performance, then gathering more data is one of the most effective solutions. The key considerations are the cost and feasibility of gathering more data, the cost and feasibility of reducing the test error by other means, and the amount of data that is expected to be necessary to improve test set performance significantly. At large internet companies with millions or billions of users, it is feasible to gather large datasets, and the expense of doing so can be considerably less than the other alternatives, so the answer is almost always to gather more training data. For example, the development of large labeled datasets was one of the most important factors in solving object recognition. In other contexts, such as medical applications, it may be costly or infeasible to gather more data. A simple alternative to gathering more data is to reduce the size of the model or improve regularization, by adjusting hyperparameters such as weight decay coefficients, or by adding regularization strategies such as dropout. If you find that the gap between train and test performance is still unacceptable even after tuning the regularization hyperparameters, then gathering more data is advisable.

When deciding whether to gather more data, it is also necessary to decide how much to gather. It is helpful to plot curves showing the relationship between training set size and generalization error, like in figure 5.4. By extrapolating such curves, one can predict how much additional training data would be needed to achieve a certain level of performance. Usually, adding a small fraction of the total number of examples will not have a noticeable impact on generalization error. It is therefore recommended to experiment with training set sizes on a logarithmic scale, for example doubling the number of examples between consecutive experiments.

If gathering much more data is not feasible, the only other way to improve generalization error is to improve the learning algorithm itself. This becomes the domain of research and not the domain of advice for applied practitioners.

11.4 Selecting Hyperparameters

Most deep learning algorithms come with many hyperparameters that control many aspects of the algorithm's behavior. Some of these hyperparameters affect the time and memory cost of running the algorithm. Some of these hyperparameters affect the quality of the model recovered by the training process and its ability to infer correct results when deployed on new inputs.

There are two basic approaches to choosing these hyperparameters: choosing them manually and choosing them automatically. Choosing the hyperparameters

manually requires understanding what the hyperparameters do and how machine learning models achieve good generalization. Automatic hyperparameter selection algorithms greatly reduce the need to understand these ideas, but they are often much more computationally costly.

11.4.1 Manual Hyperparameter Tuning

To set hyperparameters manually, one must understand the relationship between hyperparameters, training error, generalization error and computational resources (memory and runtime). This means establishing a solid foundation on the fundamental ideas concerning the effective capacity of a learning algorithm from chapter 5.

The goal of manual hyperparameter search is usually to find the lowest generalization error subject to some runtime and memory budget. We do not discuss how to determine the runtime and memory impact of various hyperparameters here because this is highly platform-dependent.

The primary goal of manual hyperparameter search is to adjust the effective capacity of the model to match the complexity of the task. Effective capacity is constrained by three factors: the representational capacity of the model, the ability of the learning algorithm to successfully minimize the cost function used to train the model, and the degree to which the cost function and training procedure regularize the model. A model with more layers and more hidden units per layer has higher representational capacity—it is capable of representing more complicated functions. It can not necessarily actually learn all of these functions though, if the training algorithm cannot discover that certain functions do a good job of minimizing the training cost, or if regularization terms such as weight decay forbid some of these functions.

The generalization error typically follows a U-shaped curve when plotted as a function of one of the hyperparameters, as in figure 5.3. At one extreme, the hyperparameter value corresponds to low capacity, and generalization error is high because training error is high. This is the underfitting regime. At the other extreme, the hyperparameter value corresponds to high capacity, and the generalization error is high because the gap between training and test error is high. Somewhere in the middle lies the optimal model capacity, which achieves the lowest possible generalization error, by adding a medium generalization gap to a medium amount of training error.

For some hyperparameters, overfitting occurs when the value of the hyperparameter is large. The number of hidden units in a layer is one such example,

because increasing the number of hidden units increases the capacity of the model. For some hyperparameters, overfitting occurs when the value of the hyperparameter is small. For example, the smallest allowable weight decay coefficient of zero corresponds to the greatest effective capacity of the learning algorithm.

Not every hyperparameter will be able to explore the entire U-shaped curve. Many hyperparameters are discrete, such as the number of units in a layer or the number of linear pieces in a maxout unit, so it is only possible to visit a few points along the curve. Some hyperparameters are binary. Usually these hyperparameters are switches that specify whether or not to use some optional component of the learning algorithm, such as a preprocessing step that normalizes the input features by subtracting their mean and dividing by their standard deviation. These hyperparameters can only explore two points on the curve. Other hyperparameters have some minimum or maximum value that prevents them from exploring some part of the curve. For example, the minimum weight decay coefficient is zero. This means that if the model is underfitting when weight decay is zero, we can not enter the overfitting region by modifying the weight decay coefficient. In other words, some hyperparameters can only subtract capacity.

The learning rate is perhaps the most important hyperparameter. If you have time to tune only one hyperparameter, tune the learning rate. It controls the effective capacity of the model in a more complicated way than other hyperparameters—the effective capacity of the model is highest when the learning rate is *correct* for the optimization problem, not when the learning rate is especially large or especially small. The learning rate has a U-shaped curve for *training* error, illustrated in figure 11.1. When the learning rate is too large, gradient descent can inadvertently increase rather than decrease the training error. In the idealized quadratic case, this occurs if the learning rate is at least twice as large as its optimal value (LeCun *et al.*, 1998a). When the learning rate is too small, training is not only slower, but may become permanently stuck with a high training error. This effect is poorly understood (it would not happen for a convex loss function).

Tuning the parameters other than the learning rate requires monitoring both training and test error to diagnose whether your model is overfitting or underfitting, then adjusting its capacity appropriately.

If your error on the training set is higher than your target error rate, you have no choice but to increase capacity. If you are not using regularization and you are confident that your optimization algorithm is performing correctly, then you must add more layers to your network or add more hidden units. Unfortunately, this increases the computational costs associated with the model.

If your error on the test set is higher than than your target error rate, you can

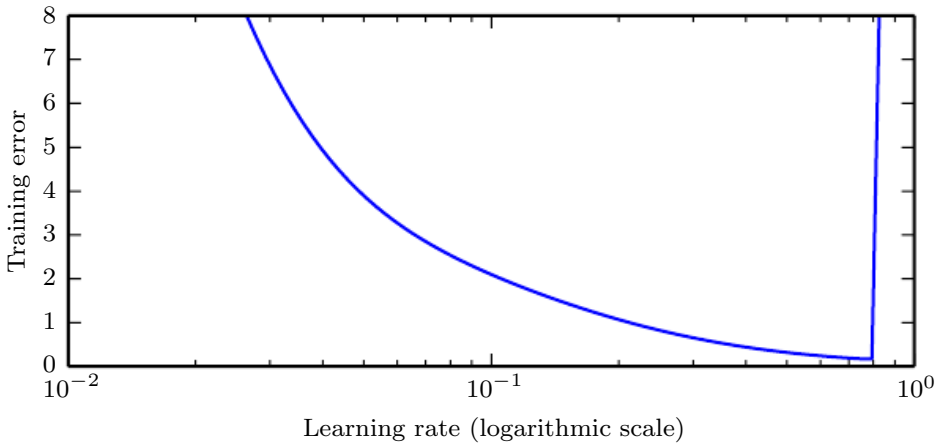

Figure 11.1: Typical relationship between the learning rate and the training error. Notice the sharp rise in error when the learning is above an optimal value. This is for a fixed training time, as a smaller learning rate may sometimes only slow down training by a factor proportional to the learning rate reduction. Generalization error can follow this curve or be complicated by regularization effects arising out of having a too large or too small learning rates, since poor optimization can, to some degree, reduce or prevent overfitting, and even points with equivalent training error can have different generalization error.

now take two kinds of actions. The test error is the sum of the training error and the gap between training and test error. The optimal test error is found by trading off these quantities. Neural networks typically perform best when the training error is very low (and thus, when capacity is high) and the test error is primarily driven by the gap between train and test error. Your goal is to reduce this gap without increasing training error faster than the gap decreases. To reduce the gap, change regularization hyperparameters to reduce effective model capacity, such as by adding dropout or weight decay. Usually the best performance comes from a large model that is regularized well, for example by using dropout.

Most hyperparameters can be set by reasoning about whether they increase or decrease model capacity. Some examples are included in Table 11.1.

While manually tuning hyperparameters, do not lose sight of your end goal: good performance on the test set. Adding regularization is only one way to achieve this goal. As long as you have low training error, you can always reduce generalization error by collecting more training data. The brute force way to practically guarantee success is to continually increase model capacity and training set size until the task is solved. This approach does of course increase the computational cost of training and inference, so it is only feasible given appropriate resources. In

Hyperparameter	Increases capacity when...	Reason	Caveats
Number of hidden units	increased	Increasing the number of hidden units increases the representational capacity of the model.	Increasing the number of hidden units increases both the time and memory cost of essentially every operation on the model.
Learning rate	tuned optimally	An improper learning rate, whether too high or too low, results in a model with low effective capacity due to optimization failure	
Convolution kernel width	increased	Increasing the kernel width increases the number of parameters in the model	A wider kernel results in a narrower output dimension, reducing model capacity unless you use implicit zero padding to reduce this effect. Wider kernels require more memory for parameter storage and increase runtime, but a narrower output reduces memory cost.
Implicit zero padding	increased	Adding implicit zeros before convolution keeps the representation size large	Increased time and memory cost of most operations.
Weight decay coefficient	decreased	Decreasing the weight decay coefficient frees the model parameters to become larger	
Dropout rate	decreased	Dropping units less often gives the units more opportunities to "conspire" with each other to fit the training set	

Table 11.1: The effect of various hyperparameters on model capacity.

principle, this approach could fail due to optimization difficulties, but for many problems optimization does not seem to be a significant barrier, provided that the model is chosen appropriately.

11.4.2 Automatic Hyperparameter Optimization Algorithms

The ideal learning algorithm just takes a dataset and outputs a function, without requiring hand-tuning of hyperparameters. The popularity of several learning algorithms such as logistic regression and SVMs stems in part from their ability to perform well with only one or two tuned hyperparameters. Neural networks can sometimes perform well with only a small number of tuned hyperparameters, but often benefit significantly from tuning of forty or more hyperparameters. Manual hyperparameter tuning can work very well when the user has a good starting point, such as one determined by others having worked on the same type of application and architecture, or when the user has months or years of experience in exploring hyperparameter values for neural networks applied to similar tasks. However, for many applications, these starting points are not available. In these cases, automated algorithms can find useful values of the hyperparameters.

If we think about the way in which the user of a learning algorithm searches for good values of the hyperparameters, we realize that an optimization is taking place: we are trying to find a value of the hyperparameters that optimizes an objective function, such as validation error, sometimes under constraints (such as a budget for training time, memory or recognition time). It is therefore possible, in principle, to develop **hyperparameter optimization** algorithms that wrap a learning algorithm and choose its hyperparameters, thus hiding the hyperparameters of the learning algorithm from the user. Unfortunately, hyperparameter optimization algorithms often have their own hyperparameters, such as the range of values that should be explored for each of the learning algorithm's hyperparameters. However, these secondary hyperparameters are usually easier to choose, in the sense that acceptable performance may be achieved on a wide range of tasks using the same secondary hyperparameters for all tasks.

11.4.3 Grid Search

When there are three or fewer hyperparameters, the common practice is to perform **grid search**. For each hyperparameter, the user selects a small finite set of values to explore. The grid search algorithm then trains a model for every joint specification of hyperparameter values in the Cartesian product of the set of values for each individual hyperparameter. The experiment that yields the best validation

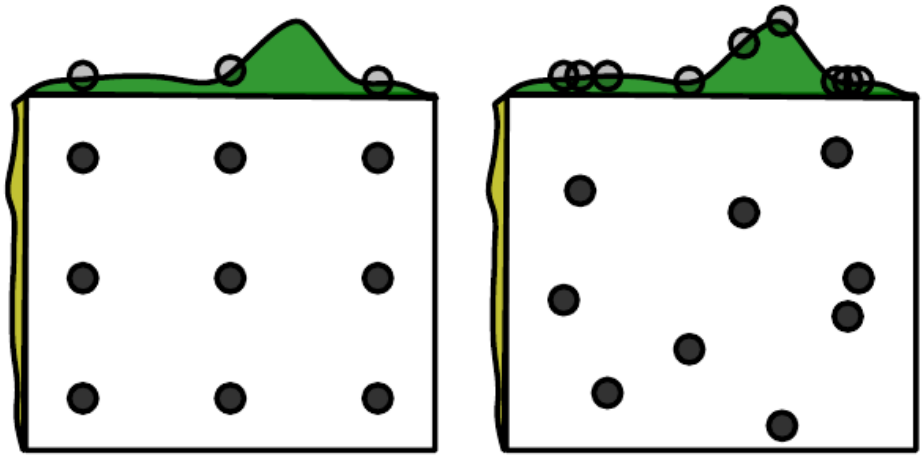

Figure 11.2: Comparison of grid search and random search. For illustration purposes we display two hyperparameters but we are typically interested in having many more. *(Left)*To perform grid search, we provide a set of values for each hyperparameter. The search algorithm runs training for every joint hyperparameter setting in the cross product of these sets. *(Right)*To perform random search, we provide a probability distribution over joint hyperparameter configurations. Usually most of these hyperparameters are independent from each other. Common choices for the distribution over a single hyperparameter include uniform and log-uniform (to sample from a log-uniform distribution, take the exp of a sample from a uniform distribution). The search algorithm then randomly samples joint hyperparameter configurations and runs training with each of them. Both grid search and random search evaluate the validation set error and return the best configuration. The figure illustrates the typical case where only some hyperparameters have a significant influence on the result. In this illustration, only the hyperparameter on the horizontal axis has a significant effect. Grid search wastes an amount of computation that is exponential in the number of non-influential hyperparameters, while random search tests a unique value of every influential hyperparameter on nearly every trial. Figure reproduced with permission from Bergstra and Bengio (2012).

set error is then chosen as having found the best hyperparameters. See the left of figure 11.2 for an illustration of a grid of hyperparameter values.

How should the lists of values to search over be chosen? In the case of numerical (ordered) hyperparameters, the smallest and largest element of each list is chosen conservatively, based on prior experience with similar experiments, to make sure that the optimal value is very likely to be in the selected range. Typically, a grid search involves picking values approximately on a *logarithmic scale*, e.g., a learning rate taken within the set $\{.1, .01, 10^{-3}, 10^{-4}, 10^{-5}\}$, or a number of hidden units taken with the set $\{50, 100, 200, 500, 1000, 2000\}$.

Grid search usually performs best when it is performed repeatedly. For example, suppose that we ran a grid search over a hyperparameter α using values of $\{-1, 0, 1\}$. If the best value found is 1, then we underestimated the range in which the best α lies and we should shift the grid and run another search with α in, for example, $\{1, 2, 3\}$. If we find that the best value of α is 0, then we may wish to refine our estimate by zooming in and running a grid search over $\{-.1, 0, .1\}$.

The obvious problem with grid search is that its computational cost grows exponentially with the number of hyperparameters. If there are m hyperparameters, each taking at most n values, then the number of training and evaluation trials required grows as $O(n^m)$. The trials may be run in parallel and exploit loose parallelism (with almost no need for communication between different machines carrying out the search) Unfortunately, due to the exponential cost of grid search, even parallelization may not provide a satisfactory size of search.

11.4.4 Random Search

Fortunately, there is an alternative to grid search that is as simple to program, more convenient to use, and converges much faster to good values of the hyperparameters: random search (Bergstra and Bengio, 2012).

A random search proceeds as follows. First we define a marginal distribution for each hyperparameter, e.g., a Bernoulli or multinoulli for binary or discrete hyperparameters, or a uniform distribution on a log-scale for positive real-valued hyperparameters. For example,

$$\texttt{log\_learning\_rate} \sim u(-1, -5) \tag{11.2}$$

$$\texttt{learning\_rate} = 10^{\texttt{log\_learning\_rate}}. \tag{11.3}$$

where $u(a, b)$ indicates a sample of the uniform distribution in the interval (a, b). Similarly the `log_number_of_hidden_units` may be sampled from $u(\log(50), \log(2000))$.

Unlike in the case of a grid search, one *should not discretize* or bin the values of the hyperparameters. This allows one to explore a larger set of values, and does not incur additional computational cost. In fact, as illustrated in figure 11.2, a random search can be exponentially more efficient than a grid search, when there are several hyperparameters that do not strongly affect the performance measure. This is studied at length in Bergstra and Bengio (2012), who found that random search reduces the validation set error much faster than grid search, in terms of the number of trials run by each method.

As with grid search, one may often want to run repeated versions of random search, to refine the search based on the results of the first run.

The main reason why random search finds good solutions faster than grid search is that there are no wasted experimental runs, unlike in the case of grid search, when two values of a hyperparameter (given values of the other hyperparameters) would give the same result. In the case of grid search, the other hyperparameters would have the same values for these two runs, whereas with random search, they would usually have different values. Hence if the change between these two values does not marginally make much difference in terms of validation set error, grid search will unnecessarily repeat two equivalent experiments while random search will still give two independent explorations of the other hyperparameters.

11.4.5 Model-Based Hyperparameter Optimization

The search for good hyperparameters can be cast as an optimization problem. The decision variables are the hyperparameters. The cost to be optimized is the validation set error that results from training using these hyperparameters. In simplified settings where it is feasible to compute the gradient of some differentiable error measure on the validation set with respect to the hyperparameters, we can simply follow this gradient (Bengio *et al.*, 1999; Bengio, 2000; Maclaurin *et al.*, 2015). Unfortunately, in most practical settings, this gradient is unavailable, either due to its high computation and memory cost, or due to hyperparameters having intrinsically non-differentiable interactions with the validation set error, as in the case of discrete-valued hyperparameters.

To compensate for this lack of a gradient, we can build a model of the validation set error, then propose new hyperparameter guesses by performing optimization within this model. Most model-based algorithms for hyperparameter search use a Bayesian regression model to estimate both the expected value of the validation set error for each hyperparameter and the uncertainty around this expectation. Optimization thus involves a tradeoff between exploration (proposing hyperparameters

for which there is high uncertainty, which may lead to a large improvement but may also perform poorly) and exploitation (proposing hyperparameters which the model is confident will perform as well as any hyperparameters it has seen so far—usually hyperparameters that are very similar to ones it has seen before). Contemporary approaches to hyperparameter optimization include Spearmint (Snoek *et al.*, 2012), TPE (Bergstra *et al.*, 2011) and SMAC (Hutter *et al.*, 2011).

Currently, we cannot unambiguously recommend Bayesian hyperparameter optimization as an established tool for achieving better deep learning results or for obtaining those results with less effort. Bayesian hyperparameter optimization sometimes performs comparably to human experts, sometimes better, but fails catastrophically on other problems. It may be worth trying to see if it works on a particular problem but is not yet sufficiently mature or reliable. That being said, hyperparameter optimization is an important field of research that, while often driven primarily by the needs of deep learning, holds the potential to benefit not only the entire field of machine learning but the discipline of engineering in general.

One drawback common to most hyperparameter optimization algorithms with more sophistication than random search is that they require for a training experiment to run to completion before they are able to extract any information from the experiment. This is much less efficient, in the sense of how much information can be gleaned early in an experiment, than manual search by a human practitioner, since one can usually tell early on if some set of hyperparameters is completely pathological. Swersky *et al.* (2014) have introduced an early version of an algorithm that maintains a set of multiple experiments. At various time points, the hyperparameter optimization algorithm can choose to begin a new experiment, to "freeze" a running experiment that is not promising, or to "thaw" and resume an experiment that was earlier frozen but now appears promising given more information.

11.5 Debugging Strategies

When a machine learning system performs poorly, it is usually difficult to tell whether the poor performance is intrinsic to the algorithm itself or whether there is a bug in the implementation of the algorithm. Machine learning systems are difficult to debug for a variety of reasons.

In most cases, we do not know a priori what the intended behavior of the algorithm is. In fact, the entire point of using machine learning is that it will discover useful behavior that we were not able to specify ourselves. If we train a

neural network on a *new* classification task and it achieves 5% test error, we have no straightforward way of knowing if this is the expected behavior or sub-optimal behavior.

A further difficulty is that most machine learning models have multiple parts that are each adaptive. If one part is broken, the other parts can adapt and still achieve roughly acceptable performance. For example, suppose that we are training a neural net with several layers parametrized by weights $\boldsymbol{W}$ and biases $\boldsymbol{b}$. Suppose further that we have manually implemented the gradient descent rule for each parameter separately, and we made an error in the update for the biases:

$$\boldsymbol{b} \leftarrow \boldsymbol{b} - \alpha \tag{11.4}$$

where α is the learning rate. This erroneous update does not use the gradient at all. It causes the biases to constantly become negative throughout learning, which is clearly not a correct implementation of any reasonable learning algorithm. The bug may not be apparent just from examining the output of the model though. Depending on the distribution of the input, the weights may be able to adapt to compensate for the negative biases.

Most debugging strategies for neural nets are designed to get around one or both of these two difficulties. Either we design a case that is so simple that the correct behavior actually can be predicted, or we design a test that exercises one part of the neural net implementation in isolation.

Some important debugging tests include:

Visualize the model in action : When training a model to detect objects in images, view some images with the detections proposed by the model displayed superimposed on the image. When training a generative model of speech, listen to some of the speech samples it produces. This may seem obvious, but it is easy to fall into the practice of only looking at quantitative performance measurements like accuracy or log-likelihood. Directly observing the machine learning model performing its task will help to determine whether the quantitative performance numbers it achieves seem reasonable. Evaluation bugs can be some of the most devastating bugs because they can mislead you into believing your system is performing well when it is not.

Visualize the worst mistakes : Most models are able to output some sort of confidence measure for the task they perform. For example, classifiers based on a softmax output layer assign a probability to each class. The probability assigned to the most likely class thus gives an estimate of the confidence the model has in its classification decision. Typically, maximum likelihood training results in these values being overestimates rather than accurate probabilities of correct prediction,

but they are somewhat useful in the sense that examples that are actually less likely to be correctly labeled receive smaller probabilities under the model. By viewing the training set examples that are the hardest to model correctly, one can often discover problems with the way the data has been preprocessed or labeled. For example, the Street View transcription system originally had a problem where the address number detection system would crop the image too tightly and omit some of the digits. The transcription network then assigned very low probability to the correct answer on these images. Sorting the images to identify the most confident mistakes showed that there was a systematic problem with the cropping. Modifying the detection system to crop much wider images resulted in much better performance of the overall system, even though the transcription network needed to be able to process greater variation in the position and scale of the address numbers.

Reasoning about software using train and test error: It is often difficult to determine whether the underlying software is correctly implemented. Some clues can be obtained from the train and test error. If training error is low but test error is high, then it is likely that that the training procedure works correctly, and the model is overfitting for fundamental algorithmic reasons. An alternative possibility is that the test error is measured incorrectly due to a problem with saving the model after training then reloading it for test set evaluation, or if the test data was prepared differently from the training data. If both train and test error are high, then it is difficult to determine whether there is a software defect or whether the model is underfitting due to fundamental algorithmic reasons. This scenario requires further tests, described next.

Fit a tiny dataset: If you have high error on the training set, determine whether it is due to genuine underfitting or due to a software defect. Usually even small models can be guaranteed to be able fit a sufficiently small dataset. For example, a classification dataset with only one example can be fit just by setting the biases of the output layer correctly. Usually if you cannot train a classifier to correctly label a single example, an autoencoder to successfully reproduce a single example with high fidelity, or a generative model to consistently emit samples resembling a single example, there is a software defect preventing successful optimization on the training set. This test can be extended to a small dataset with few examples.

Compare back-propagated derivatives to numerical derivatives: If you are using a software framework that requires you to implement your own gradient computations, or if you are adding a new operation to a differentiation library and must define its `bprop` method, then a common source of error is implementing this gradient expression incorrectly. One way to verify that these derivatives are correct

is to compare the derivatives computed by your implementation of automatic differentiation to the derivatives computed by a **finite differences**. Because

$$f'(x) = \lim_{\epsilon \to 0} \frac{f(x+\epsilon) - f(x)}{\epsilon}, \tag{11.5}$$

we can approximate the derivative by using a small, finite ϵ:

$$f'(x) \approx \frac{f(x+\epsilon) - f(x)}{\epsilon}. \tag{11.6}$$

We can improve the accuracy of the approximation by using the **centered difference**:

$$f'(x) \approx \frac{f(x+\frac{1}{2}\epsilon) - f(x-\frac{1}{2}\epsilon)}{\epsilon}. \tag{11.7}$$

The perturbation size ϵ must chosen to be large enough to ensure that the perturbation is not rounded down too much by finite-precision numerical computations.

Usually, we will want to test the gradient or Jacobian of a vector-valued function $g : \mathbb{R}^m \to \mathbb{R}^n$. Unfortunately, finite differencing only allows us to take a single derivative at a time. We can either run finite differencing mn times to evaluate all of the partial derivatives of g, or we can apply the test to a new function that uses random projections at both the input and output of g. For example, we can apply our test of the implementation of the derivatives to $f(x)$ where $f(x) = \boldsymbol{u}^T g(\boldsymbol{v}x)$, where $\boldsymbol{u}$ and $\boldsymbol{v}$ are randomly chosen vectors. Computing $f'(x)$ correctly requires being able to back-propagate through g correctly, yet is efficient to do with finite differences because f has only a single input and a single output. It is usually a good idea to repeat this test for more than one value of $\boldsymbol{u}$ and $\boldsymbol{v}$ to reduce the chance that the test overlooks mistakes that are orthogonal to the random projection.

If one has access to numerical computation on complex numbers, then there is a very efficient way to numerically estimate the gradient by using complex numbers as input to the function (Squire and Trapp, 1998). The method is based on the observation that

$$f(x+i\epsilon) = f(x) + i\epsilon f'(x) + O(\epsilon^2) \tag{11.8}$$

$$\text{real}(f(x+i\epsilon)) = f(x) + O(\epsilon^2), \quad \text{imag}(\frac{f(x+i\epsilon)}{\epsilon}) = f'(x) + O(\epsilon^2), \tag{11.9}$$

where $i = \sqrt{-1}$. Unlike in the real-valued case above, there is no cancellation effect due to taking the difference between the value of f at different points. This allows the use of tiny values of ϵ like $\epsilon = 10^{-150}$, which make the $O(\epsilon^2)$ error insignificant for all practical purposes.

Monitor histograms of activations and gradient: It is often useful to visualize statistics of neural network activations and gradients, collected over a large amount of training iterations (maybe one epoch). The pre-activation value of hidden units can tell us if the units saturate, or how often they do. For example, for rectifiers, how often are they off? Are there units that are always off? For tanh units, the average of the absolute value of the pre-activations tells us how saturated the unit is. In a deep network where the propagated gradients quickly grow or quickly vanish, optimization may be hampered. Finally, it is useful to compare the magnitude of parameter gradients to the magnitude of the parameters themselves. As suggested by Bottou (2015), we would like the magnitude of parameter updates over a minibatch to represent something like 1% of the magnitude of the parameter, not 50% or 0.001% (which would make the parameters move too slowly). It may be that some groups of parameters are moving at a good pace while others are stalled. When the data is sparse (like in natural language), some parameters may be very rarely updated, and this should be kept in mind when monitoring their evolution.

Finally, many deep learning algorithms provide some sort of guarantee about the results produced at each step. For example, in part III, we will see some approximate inference algorithms that work by using algebraic solutions to optimization problems. Typically these can be debugged by testing each of their guarantees. Some guarantees that some optimization algorithms offer include that the objective function will never increase after one step of the algorithm, that the gradient with respect to some subset of variables will be zero after each step of the algorithm, and that the gradient with respect to all variables will be zero at convergence. Usually due to rounding error, these conditions will not hold exactly in a digital computer, so the debugging test should include some tolerance parameter.

11.6 Example: Multi-Digit Number Recognition

To provide an end-to-end description of how to apply our design methodology in practice, we present a brief account of the Street View transcription system, from the point of view of designing the deep learning components. Obviously, many other components of the complete system, such as the Street View cars, the database infrastructure, and so on, were of paramount importance.

From the point of view of the machine learning task, the process began with data collection. The cars collected the raw data and human operators provided labels. The transcription task was preceded by a significant amount of dataset curation, including using other machine learning techniques to *detect* the house

numbers prior to transcribing them.

The transcription project began with a choice of performance metrics and desired values for these metrics. An important general principle is to tailor the choice of metric to the business goals for the project. Because maps are only useful if they have high accuracy, it was important to set a high accuracy requirement for this project. Specifically, the goal was to obtain human-level, 98% accuracy. This level of accuracy may not always be feasible to obtain. In order to reach this level of accuracy, the Street View transcription system sacrifices coverage. Coverage thus became the main performance metric optimized during the project, with accuracy held at 98%. As the convolutional network improved, it became possible to reduce the confidence threshold below which the network refuses to transcribe the input, eventually exceeding the goal of 95% coverage.

After choosing quantitative goals, the next step in our recommended methodology is to rapidly establish a sensible baseline system. For vision tasks, this means a convolutional network with rectified linear units. The transcription project began with such a model. At the time, it was not common for a convolutional network to output a sequence of predictions. In order to begin with the simplest possible baseline, the first implementation of the output layer of the model consisted of n different softmax units to predict a sequence of n characters. These softmax units were trained exactly the same as if the task were classification, with each softmax unit trained independently.

Our recommended methodology is to iteratively refine the baseline and test whether each change makes an improvement. The first change to the Street View transcription system was motivated by a theoretical understanding of the coverage metric and the structure of the data. Specifically, the network refuses to classify an input $\boldsymbol{x}$ whenever the probability of the output sequence $p(\boldsymbol{y} \mid \boldsymbol{x}) < t$ for some threshold t. Initially, the definition of $p(\boldsymbol{y} \mid \boldsymbol{x})$ was ad-hoc, based on simply multiplying all of the softmax outputs together. This motivated the development of a specialized output layer and cost function that actually computed a principled log-likelihood. This approach allowed the example rejection mechanism to function much more effectively.

At this point, coverage was still below 90%, yet there were no obvious theoretical problems with the approach. Our methodology therefore suggests to instrument the train and test set performance in order to determine whether the problem is underfitting or overfitting. In this case, train and test set error were nearly identical. Indeed, the main reason this project proceeded so smoothly was the availability of a dataset with tens of millions of labeled examples. Because train and test set error were so similar, this suggested that the problem was either due

to underfitting or due to a problem with the training data. One of the debugging strategies we recommend is to visualize the model's worst errors. In this case, that meant visualizing the incorrect training set transcriptions that the model gave the highest confidence. These proved to mostly consist of examples where the input image had been cropped too tightly, with some of the digits of the address being removed by the cropping operation. For example, a photo of an address "1849" might be cropped too tightly, with only the "849" remaining visible. This problem could have been resolved by spending weeks improving the accuracy of the address number detection system responsible for determining the cropping regions. Instead, the team took a much more practical decision, to simply expand the width of the crop region to be systematically wider than the address number detection system predicted. This single change added ten percentage points to the transcription system's coverage.

Finally, the last few percentage points of performance came from adjusting hyperparameters. This mostly consisted of making the model larger while maintaining some restrictions on its computational cost. Because train and test error remained roughly equal, it was always clear that any performance deficits were due to underfitting, as well as due to a few remaining problems with the dataset itself.

Overall, the transcription project was a great success, and allowed hundreds of millions of addresses to be transcribed both faster and at lower cost than would have been possible via human effort.

We hope that the design principles described in this chapter will lead to many other similar successes.

Chapter 12

Applications

In this chapter, we describe how to use deep learning to solve applications in computer vision, speech recognition, natural language processing, and other application areas of commercial interest. We begin by discussing the large scale neural network implementations required for most serious AI applications. Next, we review several specific application areas that deep learning has been used to solve. While one goal of deep learning is to design algorithms that are capable of solving a broad variety of tasks, so far some degree of specialization is needed. For example, vision tasks require processing a large number of input features (pixels) per example. Language tasks require modeling a large number of possible values (words in the vocabulary) per input feature.

12.1 Large-Scale Deep Learning

Deep learning is based on the philosophy of connectionism: while an individual biological neuron or an individual feature in a machine learning model is not intelligent, a large population of these neurons or features acting together can exhibit intelligent behavior. It truly is important to emphasize the fact that the number of neurons must be *large*. One of the key factors responsible for the improvement in neural network's accuracy and the improvement of the complexity of tasks they can solve between the 1980s and today is the dramatic increase in the size of the networks we use. As we saw in section 1.2.3, network sizes have grown exponentially for the past three decades, yet artificial neural networks are only as large as the nervous systems of insects.

Because the size of neural networks is of paramount importance, deep learning

requires high performance hardware and software infrastructure.

12.1.1 Fast CPU Implementations

Traditionally, neural networks were trained using the CPU of a single machine. Today, this approach is generally considered insufficient. We now mostly use GPU computing or the CPUs of many machines networked together. Before moving to these expensive setups, researchers worked hard to demonstrate that CPUs could not manage the high computational workload required by neural networks.

A description of how to implement efficient numerical CPU code is beyond the scope of this book, but we emphasize here that careful implementation for specific CPU families can yield large improvements. For example, in 2011, the best CPUs available could run neural network workloads faster when using fixed-point arithmetic rather than floating-point arithmetic. By creating a carefully tuned fixed-point implementation, Vanhoucke *et al.* (2011) obtained a threefold speedup over a strong floating-point system. Each new model of CPU has different performance characteristics, so sometimes floating-point implementations can be faster too. The important principle is that careful specialization of numerical computation routines can yield a large payoff. Other strategies, besides choosing whether to use fixed or floating point, include optimizing data structures to avoid cache misses and using vector instructions. Many machine learning researchers neglect these implementation details, but when the performance of an implementation restricts the size of the model, the accuracy of the model suffers.

12.1.2 GPU Implementations

Most modern neural network implementations are based on graphics processing units. Graphics processing units (GPUs) are specialized hardware components that were originally developed for graphics applications. The consumer market for video gaming systems spurred development of graphics processing hardware. The performance characteristics needed for good video gaming systems turn out to be beneficial for neural networks as well.

Video game rendering requires performing many operations in parallel quickly. Models of characters and environments are specified in terms of lists of 3-D coordinates of vertices. Graphics cards must perform matrix multiplication and division on many vertices in parallel to convert these 3-D coordinates into 2-D on-screen coordinates. The graphics card must then perform many computations at each pixel in parallel to determine the color of each pixel. In both cases, the

computations are fairly simple and do not involve much branching compared to the computational workload that a CPU usually encounters. For example, each vertex in the same rigid object will be multiplied by the same matrix; there is no need to evaluate an if statement per-vertex to determine which matrix to multiply by. The computations are also entirely independent of each other, and thus may be parallelized easily. The computations also involve processing massive buffers of memory, containing bitmaps describing the texture (color pattern) of each object to be rendered. Together, this results in graphics cards having been designed to have a high degree of parallelism and high memory bandwidth, at the cost of having a lower clock speed and less branching capability relative to traditional CPUs.

Neural network algorithms require the same performance characteristics as the real-time graphics algorithms described above. Neural networks usually involve large and numerous buffers of parameters, activation values, and gradient values, each of which must be completely updated during every step of training. These buffers are large enough to fall outside the cache of a traditional desktop computer so the memory bandwidth of the system often becomes the rate limiting factor. GPUs offer a compelling advantage over CPUs due to their high memory bandwidth. Neural network training algorithms typically do not involve much branching or sophisticated control, so they are appropriate for GPU hardware. Since neural networks can be divided into multiple individual "neurons" that can be processed independently from the other neurons in the same layer, neural networks easily benefit from the parallelism of GPU computing.

GPU hardware was originally so specialized that it could only be used for graphics tasks. Over time, GPU hardware became more flexible, allowing custom subroutines to be used to transform the coordinates of vertices or assign colors to pixels. In principle, there was no requirement that these pixel values actually be based on a rendering task. These GPUs could be used for scientific computing by writing the output of a computation to a buffer of pixel values. Steinkrau *et al.* (2005) implemented a two-layer fully connected neural network on a GPU and reported a threefold speedup over their CPU-based baseline. Shortly thereafter, Chellapilla *et al.* (2006) demonstrated that the same technique could be used to accelerate supervised convolutional networks.

The popularity of graphics cards for neural network training exploded after the advent of **general purpose GPUs**. These GP-GPUs could execute arbitrary code, not just rendering subroutines. NVIDIA's CUDA programming language provided a way to write this arbitrary code in a C-like language. With their relatively convenient programming model, massive parallelism, and high memory

bandwidth, GP-GPUs now offer an ideal platform for neural network programming. This platform was rapidly adopted by deep learning researchers soon after it became available (Raina *et al.*, 2009; Ciresan *et al.*, 2010).

Writing efficient code for GP-GPUs remains a difficult task best left to specialists. The techniques required to obtain good performance on GPU are very different from those used on CPU. For example, good CPU-based code is usually designed to read information from the cache as much as possible. On GPU, most writable memory locations are not cached, so it can actually be faster to compute the same value twice, rather than compute it once and read it back from memory. GPU code is also inherently multi-threaded and the different threads must be coordinated with each other carefully. For example, memory operations are faster if they can be **coalesced**. Coalesced reads or writes occur when several threads can each read or write a value that they need simultaneously, as part of a single memory transaction. Different models of GPUs are able to coalesce different kinds of read or write patterns. Typically, memory operations are easier to coalesce if among n threads, thread i accesses byte $i + j$ of memory, and j is a multiple of some power of 2. The exact specifications differ between models of GPU. Another common consideration for GPUs is making sure that each thread in a group executes the same instruction simultaneously. This means that branching can be difficult on GPU. Threads are divided into small groups called **warps**. Each thread in a warp executes the same instruction during each cycle, so if different threads within the same warp need to execute different code paths, these different code paths must be traversed sequentially rather than in parallel.

Due to the difficulty of writing high performance GPU code, researchers should structure their workflow to avoid needing to write new GPU code in order to test new models or algorithms. Typically, one can do this by building a software library of high performance operations like convolution and matrix multiplication, then specifying models in terms of calls to this library of operations. For example, the machine learning library Pylearn2 (Goodfellow *et al.*, 2013c) specifies all of its machine learning algorithms in terms of calls to Theano (Bergstra *et al.*, 2010; Bastien *et al.*, 2012) and cuda-convnet (Krizhevsky, 2010), which provide these high-performance operations. This factored approach can also ease support for multiple kinds of hardware. For example, the same Theano program can run on either CPU or GPU, without needing to change any of the calls to Theano itself. Other libraries like TensorFlow (Abadi *et al.*, 2015) and Torch (Collobert *et al.*, 2011b) provide similar features.

12.1.3 Large-Scale Distributed Implementations

In many cases, the computational resources available on a single machine are insufficient. We therefore want to distribute the workload of training and inference across many machines.

Distributing inference is simple, because each input example we want to process can be run by a separate machine. This is known as **data parallelism**.

It is also possible to get **model parallelism**, where multiple machines work together on a single datapoint, with each machine running a different part of the model. This is feasible for both inference and training.

Data parallelism during training is somewhat harder. We can increase the size of the minibatch used for a single SGD step, but usually we get less than linear returns in terms of optimization performance. It would be better to allow multiple machines to compute multiple gradient descent steps in parallel. Unfortunately, the standard definition of gradient descent is as a completely sequential algorithm: the gradient at step t is a function of the parameters produced by step $t - 1$.

This can be solved using **asynchronous stochastic gradient descent** (Bengio *et al.*, 2001; Recht *et al.*, 2011). In this approach, several processor cores share the memory representing the parameters. Each core reads parameters without a lock, then computes a gradient, then increments the parameters without a lock. This reduces the average amount of improvement that each gradient descent step yields, because some of the cores overwrite each other's progress, but the increased rate of production of steps causes the learning process to be faster overall. Dean *et al.* (2012) pioneered the multi-machine implementation of this lock-free approach to gradient descent, where the parameters are managed by a **parameter server** rather than stored in shared memory. Distributed asynchronous gradient descent remains the primary strategy for training large deep networks and is used by most major deep learning groups in industry (Chilimbi *et al.*, 2014; Wu *et al.*, 2015). Academic deep learning researchers typically cannot afford the same scale of distributed learning systems but some research has focused on how to build distributed networks with relatively low-cost hardware available in the university setting (Coates *et al.*, 2013).

12.1.4 Model Compression

In many commercial applications, it is much more important that the time and memory cost of running inference in a machine learning model be low than that the time and memory cost of training be low. For applications that do not require

personalization, it is possible to train a model once, then deploy it to be used by billions of users. In many cases, the end user is more resource-constrained than the developer. For example, one might train a speech recognition network with a powerful computer cluster, then deploy it on mobile phones.

A key strategy for reducing the cost of inference is **model compression** (Buciluǎ *et al.*, 2006). The basic idea of model compression is to replace the original, expensive model with a smaller model that requires less memory and runtime to store and evaluate.

Model compression is applicable when the size of the original model is driven primarily by a need to prevent overfitting. In most cases, the model with the lowest generalization error is an ensemble of several independently trained models. Evaluating all n ensemble members is expensive. Sometimes, even a single model generalizes better if it is large (for example, if it is regularized with dropout).

These large models learn some function $f(\boldsymbol{x})$, but do so using many more parameters than are necessary for the task. Their size is necessary only due to the limited number of training examples. As soon as we have fit this function $f(\boldsymbol{x})$, we can generate a training set containing infinitely many examples, simply by applying f to randomly sampled points $\boldsymbol{x}$. We then train the new, smaller, model to match $f(\boldsymbol{x})$ on these points. In order to most efficiently use the capacity of the new, small model, it is best to sample the new $\boldsymbol{x}$ points from a distribution resembling the actual test inputs that will be supplied to the model later. This can be done by corrupting training examples or by drawing points from a generative model trained on the original training set.

Alternatively, one can train the smaller model only on the original training points, but train it to copy other features of the model, such as its posterior distribution over the incorrect classes (Hinton *et al.*, 2014, 2015).

12.1.5 Dynamic Structure

One strategy for accelerating data processing systems in general is to build systems that have **dynamic structure** in the graph describing the computation needed to process an input. Data processing systems can dynamically determine which subset of many neural networks should be run on a given input. Individual neural networks can also exhibit dynamic structure internally by determining which subset of features (hidden units) to compute given information from the input. This form of dynamic structure inside neural networks is sometimes called **conditional computation** (Bengio, 2013; Bengio *et al.*, 2013b). Since many components of the architecture may be relevant only for a small amount of possible inputs, the

system can run faster by computing these features only when they are needed.

Dynamic structure of computations is a basic computer science principle applied generally throughout the software engineering discipline. The simplest versions of dynamic structure applied to neural networks are based on determining which subset of some group of neural networks (or other machine learning models) should be applied to a particular input.

A venerable strategy for accelerating inference in a classifier is to use a **cascade** of classifiers. The cascade strategy may be applied when the goal is to detect the presence of a rare object (or event). To know for sure that the object is present, we must use a sophisticated classifier with high capacity, that is expensive to run. However, because the object is rare, we can usually use much less computation to reject inputs as not containing the object. In these situations, we can train a sequence of classifiers. The first classifiers in the sequence have low capacity, and are trained to have high recall. In other words, they are trained to make sure we do not wrongly reject an input when the object is present. The final classifier is trained to have high precision. At test time, we run inference by running the classifiers in a sequence, abandoning any example as soon as any one element in the cascade rejects it. Overall, this allows us to verify the presence of objects with high confidence, using a high capacity model, but does not force us to pay the cost of full inference for every example. There are two different ways that the cascade can achieve high capacity. One way is to make the later members of the cascade individually have high capacity. In this case, the system as a whole obviously has high capacity, because some of its individual members do. It is also possible to make a cascade in which every individual model has low capacity but the system as a whole has high capacity due to the combination of many small models. Viola and Jones (2001) used a cascade of boosted decision trees to implement a fast and robust face detector suitable for use in handheld digital cameras. Their classifier localizes a face using essentially a sliding window approach in which many windows are examined and rejected if they do not contain faces. Another version of cascades uses the earlier models to implement a sort of hard attention mechanism: the early members of the cascade localize an object and later members of the cascade perform further processing given the location of the object. For example, Google transcribes address numbers from Street View imagery using a two-step cascade that first locates the address number with one machine learning model and then transcribes it with another (Goodfellow *et al.*, 2014d).

Decision trees themselves are an example of dynamic structure, because each node in the tree determines which of its subtrees should be evaluated for each input. A simple way to accomplish the union of deep learning and dynamic structure

is to train a decision tree in which each node uses a neural network to make the splitting decision (Guo and Gelfand, 1992), though this has typically not been done with the primary goal of accelerating inference computations.

In the same spirit, one can use a neural network, called the **gater** to select which one out of several **expert networks** will be used to compute the output, given the current input. The first version of this idea is called the **mixture of experts** (Nowlan, 1990; Jacobs *et al.*, 1991), in which the gater outputs a set of probabilities or weights (obtained via a softmax nonlinearity), one per expert, and the final output is obtained by the weighted combination of the output of the experts. In that case, the use of the gater does not offer a reduction in computational cost, but if a single expert is chosen by the gater for each example, we obtain the **hard mixture of experts** (Collobert *et al.*, 2001, 2002), which can considerably accelerate training and inference time. This strategy works well when the number of gating decisions is small because it is not combinatorial. But when we want to select different subsets of units or parameters, it is not possible to use a "soft switch" because it requires enumerating (and computing outputs for) all the gater configurations. To deal with this problem, several approaches have been explored to train combinatorial gaters. Bengio *et al.* (2013b) experiment with several estimators of the gradient on the gating probabilities, while Bacon *et al.* (2015) and Bengio *et al.* (2015a) use reinforcement learning techniques (policy gradient) to learn a form of conditional dropout on blocks of hidden units and get an actual reduction in computational cost without impacting negatively on the quality of the approximation.

Another kind of dynamic structure is a switch, where a hidden unit can receive input from different units depending on the context. This dynamic routing approach can be interpreted as an attention mechanism (Olshausen *et al.*, 1993). So far, the use of a hard switch has not proven effective on large-scale applications. Contemporary approaches instead use a weighted average over many possible inputs, and thus do not achieve all of the possible computational benefits of dynamic structure. Contemporary attention mechanisms are described in section 12.4.5.1.

One major obstacle to using dynamically structured systems is the decreased degree of parallelism that results from the system following different code branches for different inputs. This means that few operations in the network can be described as matrix multiplication or batch convolution on a minibatch of examples. We can write more specialized sub-routines that convolve each example with different kernels or multiply each row of a design matrix by a different set of columns of weights. Unfortunately, these more specialized subroutines are difficult to implement efficiently. CPU implementations will be slow due to the lack of cache

coherence and GPU implementations will be slow due to the lack of coalesced memory transactions and the need to serialize warps when members of a warp take different branches. In some cases, these issues can be mitigated by partitioning the examples into groups that all take the same branch, and processing these groups of examples simultaneously. This can be an acceptable strategy for minimizing the time required to process a fixed amount of examples in an offline setting. In a real-time setting where examples must be processed continuously, partitioning the workload can result in load-balancing issues. For example, if we assign one machine to process the first step in a cascade and another machine to process the last step in a cascade, then the first will tend to be overloaded and the last will tend to be underloaded. Similar issues arise if each machine is assigned to implement different nodes of a neural decision tree.

12.1.6 Specialized Hardware Implementations of Deep Networks

Since the early days of neural networks research, hardware designers have worked on specialized hardware implementations that could speed up training and/or inference of neural network algorithms. See early and more recent reviews of specialized hardware for deep networks (Lindsey and Lindblad, 1994; Beiu *et al.*, 2003; Misra and Saha, 2010).

Different forms of specialized hardware (Graf and Jackel, 1989; Mead and Ismail, 2012; Kim *et al.*, 2009; Pham *et al.*, 2012; Chen *et al.*, 2014a,b) have been developed over the last decades, either with ASICs (application-specific integrated circuit), either with digital (based on binary representations of numbers), analog (Graf and Jackel, 1989; Mead and Ismail, 2012) (based on physical implementations of continuous values as voltages or currents) or hybrid implementations (combining digital and analog components). In recent years more flexible FPGA (field programmable gated array) implementations (where the particulars of the circuit can be written on the chip after it has been built) have been developed.

Though software implementations on general-purpose processing units (CPUs and GPUs) typically use 32 or 64 bits of precision to represent floating point numbers, it has long been known that it was possible to use less precision, at least at inference time (Holt and Baker, 1991; Holi and Hwang, 1993; Presley and Haggard, 1994; Simard and Graf, 1994; Wawrzynek *et al.*, 1996; Savich *et al.*, 2007). This has become a more pressing issue in recent years as deep learning has gained in popularity in industrial products, and as the great impact of faster hardware was demonstrated with GPUs. Another factor that motivates current research on specialized hardware for deep networks is that the rate of progress of a single CPU or GPU core has slowed down, and most recent improvements in

computing speed have come from parallelization across cores (either in CPUs or GPUs). This is very different from the situation of the 1990s (the previous neural network era) where the hardware implementations of neural networks (which might take two years from inception to availability of a chip) could not keep up with the rapid progress and low prices of general-purpose CPUs. Building specialized hardware is thus a way to push the envelope further, at a time when new hardware designs are being developed for low-power devices such as phones, aiming for general-public applications of deep learning (e.g., with speech, computer vision or natural language).

Recent work on low-precision implementations of backprop-based neural nets (Vanhoucke *et al.*, 2011; Courbariaux *et al.*, 2015; Gupta *et al.*, 2015) suggests that between 8 and 16 bits of precision can suffice for using or training deep neural networks with back-propagation. What is clear is that more precision is required during training than at inference time, and that some forms of dynamic fixed point representation of numbers can be used to reduce how many bits are required per number. Traditional fixed point numbers are restricted to a fixed range (which corresponds to a given exponent in a floating point representation). Dynamic fixed point representations share that range among a set of numbers (such as all the weights in one layer). Using fixed point rather than floating point representations and using less bits per number reduces the hardware surface area, power requirements and computing time needed for performing multiplications, and multiplications are the most demanding of the operations needed to use or train a modern deep network with backprop.

12.2 Computer Vision

Computer vision has traditionally been one of the most active research areas for deep learning applications, because vision is a task that is effortless for humans and many animals but challenging for computers (Ballard *et al.*, 1983). Many of the most popular standard benchmark tasks for deep learning algorithms are forms of object recognition or optical character recognition.

Computer vision is a very broad field encompassing a wide variety of ways of processing images, and an amazing diversity of applications. Applications of computer vision range from reproducing human visual abilities, such as recognizing faces, to creating entirely new categories of visual abilities. As an example of the latter category, one recent computer vision application is to recognize sound waves from the vibrations they induce in objects visible in a video (Davis *et al.*, 2014). Most deep learning research on computer vision has not focused on such

exotic applications that expand the realm of what is possible with imagery but rather a small core of AI goals aimed at replicating human abilities. Most deep learning for computer vision is used for object recognition or detection of some form, whether this means reporting which object is present in an image, annotating an image with bounding boxes around each object, transcribing a sequence of symbols from an image, or labeling each pixel in an image with the identity of the object it belongs to. Because generative modeling has been a guiding principle of deep learning research, there is also a large body of work on image synthesis using deep models. While image synthesis *ex nihilo* is usually not considered a computer vision endeavor, models capable of image synthesis are usually useful for image restoration, a computer vision task involving repairing defects in images or removing objects from images.

12.2.1 Preprocessing

Many application areas require sophisticated preprocessing because the original input comes in a form that is difficult for many deep learning architectures to represent. Computer vision usually requires relatively little of this kind of preprocessing. The images should be standardized so that their pixels all lie in the same, reasonable range, like [0,1] or [-1, 1]. Mixing images that lie in [0,1] with images that lie in [0, 255] will usually result in failure. Formatting images to have the same scale is the only kind of preprocessing that is strictly necessary. Many computer vision architectures require images of a standard size, so images must be cropped or scaled to fit that size. Even this rescaling is not always strictly necessary. Some convolutional models accept variably-sized inputs and dynamically adjust the size of their pooling regions to keep the output size constant (Waibel *et al.*, 1989). Other convolutional models have variable-sized output that automatically scales in size with the input, such as models that denoise or label each pixel in an image (Hadsell *et al.*, 2007).

Dataset augmentation may be seen as a way of preprocessing the training set only. Dataset augmentation is an excellent way to reduce the generalization error of most computer vision models. A related idea applicable at test time is to show the model many different versions of the same input (for example, the same image cropped at slightly different locations) and have the different instantiations of the model vote to determine the output. This latter idea can be interpreted as an ensemble approach, and helps to reduce generalization error.

Other kinds of preprocessing are applied to both the train and the test set with the goal of putting each example into a more canonical form in order to reduce the amount of variation that the model needs to account for. Reducing the amount of

variation in the data can both reduce generalization error and reduce the size of the model needed to fit the training set. Simpler tasks may be solved by smaller models, and simpler solutions are more likely to generalize well. Preprocessing of this kind is usually designed to remove some kind of variability in the input data that is easy for a human designer to describe and that the human designer is confident has no relevance to the task. When training with large datasets and large models, this kind of preprocessing is often unnecessary, and it is best to just let the model learn which kinds of variability it should become invariant to. For example, the AlexNet system for classifying ImageNet only has one preprocessing step: subtracting the mean across training examples of each pixel (Krizhevsky *et al.*, 2012).

12.2.1.1 Contrast Normalization

One of the most obvious sources of variation that can be safely removed for many tasks is the amount of contrast in the image. Contrast simply refers to the magnitude of the difference between the bright and the dark pixels in an image. There are many ways of quantifying the contrast of an image. In the context of deep learning, contrast usually refers to the standard deviation of the pixels in an image or region of an image. Suppose we have an image represented by a tensor $\mathbf{X} \in \mathbb{R}^{r \times c \times 3}$, with $X_{i,j,1}$ being the red intensity at row i and column j, $X_{i,j,2}$ giving the green intensity and $X_{i,j,3}$ giving the blue intensity. Then the contrast of the entire image is given by

$$\sqrt{\frac{1}{3rc}\sum_{i=1}^{r}\sum_{j=1}^{c}\sum_{k=1}^{3}\left(X_{i,j,k}-\bar{\mathbf{X}}\right)^2} \tag{12.1}$$

where $\bar{\mathbf{X}}$ is the mean intensity of the entire image:

$$\bar{\mathbf{X}} = \frac{1}{3rc}\sum_{i=1}^{r}\sum_{j=1}^{c}\sum_{k=1}^{3}X_{i,j,k}. \tag{12.2}$$

Global contrast normalization (GCN) aims to prevent images from having varying amounts of contrast by subtracting the mean from each image, then rescaling it so that the standard deviation across its pixels is equal to some constant s. This approach is complicated by the fact that no scaling factor can change the contrast of a zero-contrast image (one whose pixels all have equal intensity). Images with very low but non-zero contrast often have little information content. Dividing by the true standard deviation usually accomplishes nothing

more than amplifying sensor noise or compression artifacts in such cases. This motivates introducing a small, positive regularization parameter λ to bias the estimate of the standard deviation. Alternately, one can constrain the denominator to be at least ϵ. Given an input image $\mathbf{X}$, GCN produces an output image $\mathbf{X}'$, defined such that

$$X'_{i,j,k} = s \frac{X_{i,j,k} - \bar{X}}{\max\left\{\epsilon, \sqrt{\lambda + \frac{1}{3rc}\sum_{i=1}^{r}\sum_{j=1}^{c}\sum_{k=1}^{3}\left(X_{i,j,k} - \bar{X}\right)^2}\right\}}. \tag{12.3}$$

Datasets consisting of large images cropped to interesting objects are unlikely to contain any images with nearly constant intensity. In these cases, it is safe to practically ignore the small denominator problem by setting $\lambda = 0$ and avoid division by 0 in extremely rare cases by setting ϵ to an extremely low value like 10^{-8}. This is the approach used by Goodfellow *et al.* (2013a) on the CIFAR-10 dataset. Small images cropped randomly are more likely to have nearly constant intensity, making aggressive regularization more useful. Coates *et al.* (2011) used $\epsilon = 0$ and $\lambda = 10$ on small, randomly selected patches drawn from CIFAR-10.

The scale parameter s can usually be set to 1, as done by Coates *et al.* (2011), or chosen to make each individual pixel have standard deviation across examples close to 1, as done by Goodfellow *et al.* (2013a).

The standard deviation in equation 12.3 is just a rescaling of the L^2 norm of the image (assuming the mean of the image has already been removed). It is preferable to define GCN in terms of standard deviation rather than L^2 norm because the standard deviation includes division by the number of pixels, so GCN based on standard deviation allows the same s to be used regardless of image size. However, the observation that the L^2 norm is proportional to the standard deviation can help build a useful intuition. One can understand GCN as mapping examples to a spherical shell. See figure 12.1 for an illustration. This can be a useful property because neural networks are often better at responding to directions in space rather than exact locations. Responding to multiple distances in the same direction requires hidden units with collinear weight vectors but different biases. Such coordination can be difficult for the learning algorithm to discover. Additionally, many shallow graphical models have problems with representing multiple separated modes along the same line. GCN avoids these problems by reducing each example to a direction rather than a direction and a distance.

Counterintuitively, there is a preprocessing operation known as **sphering** and it is not the same operation as GCN. Sphering does not refer to making the data lie on a spherical shell, but rather to rescaling the principal components to have

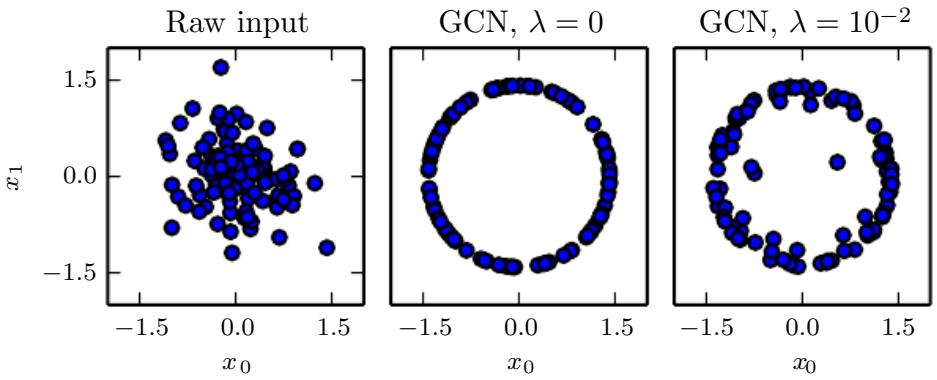

Figure 12.1: GCN maps examples onto a sphere. *(Left)*Raw input data may have any norm. *(Center)*GCN with $\lambda = 0$ maps all non-zero examples perfectly onto a sphere. Here we use $s = 1$ and $\epsilon = 10^{-8}$. Because we use GCN based on normalizing the standard deviation rather than the L^2 norm, the resulting sphere is not the unit sphere. *(Right)*Regularized GCN, with $\lambda > 0$, draws examples toward the sphere but does not completely discard the variation in their norm. We leave s and ϵ the same as before.

equal variance, so that the multivariate normal distribution used by PCA has spherical contours. Sphering is more commonly known as **whitening**.

Global contrast normalization will often fail to highlight image features we would like to stand out, such as edges and corners. If we have a scene with a large dark area and a large bright area (such as a city square with half the image in the shadow of a building) then global contrast normalization will ensure there is a large difference between the brightness of the dark area and the brightness of the light area. It will not, however, ensure that edges within the dark region stand out.

This motivates **local contrast normalization**. Local contrast normalization ensures that the contrast is normalized across each small window, rather than over the image as a whole. See figure 12.2 for a comparison of global and local contrast normalization.

Various definitions of local contrast normalization are possible. In all cases, one modifies each pixel by subtracting a mean of nearby pixels and dividing by a standard deviation of nearby pixels. In some cases, this is literally the mean and standard deviation of all pixels in a rectangular window centered on the pixel to be modified (Pinto *et al.*, 2008). In other cases, this is a weighted mean and weighted standard deviation using Gaussian weights centered on the pixel to be modified. In the case of color images, some strategies process different color

Figure 12.2: A comparison of global and local contrast normalization. Visually, the effects of global contrast normalization are subtle. It places all images on roughly the same scale, which reduces the burden on the learning algorithm to handle multiple scales. Local contrast normalization modifies the image much more, discarding all regions of constant intensity. This allows the model to focus on just the edges. Regions of fine texture, such as the houses in the second row, may lose some detail due to the bandwidth of the normalization kernel being too high.

channels separately while others combine information from different channels to normalize each pixel (Sermanet *et al.*, 2012).

Local contrast normalization can usually be implemented efficiently by using separable convolution (see section 9.8) to compute feature maps of local means and local standard deviations, then using element-wise subtraction and element-wise division on different feature maps.

Local contrast normalization is a differentiable operation and can also be used as a nonlinearity applied to the hidden layers of a network, as well as a preprocessing operation applied to the input.

As with global contrast normalization, we typically need to regularize local contrast normalization to avoid division by zero. In fact, because local contrast normalization typically acts on smaller windows, it is even more important to regularize. Smaller windows are more likely to contain values that are all nearly the same as each other, and thus more likely to have zero standard deviation.

12.2.1.2 Dataset Augmentation

As described in section 7.4, it is easy to improve the generalization of a classifier by increasing the size of the training set by adding extra copies of the training examples that have been modified with transformations that do not change the class. Object recognition is a classification task that is especially amenable to this form of dataset augmentation because the class is invariant to so many transformations and the input can be easily transformed with many geometric operations. As described before, classifiers can benefit from random translations, rotations, and in some cases, flips of the input to augment the dataset. In specialized computer vision applications, more advanced transformations are commonly used for dataset augmentation. These schemes include random perturbation of the colors in an image (Krizhevsky *et al.*, 2012) and nonlinear geometric distortions of the input (LeCun *et al.*, 1998b).

12.3 Speech Recognition

The task of speech recognition is to map an acoustic signal containing a spoken natural language utterance into the corresponding sequence of words intended by the speaker. Let $\boldsymbol{X} = (\boldsymbol{x}^{(1)}, \boldsymbol{x}^{(2)}, \ldots, \boldsymbol{x}^{(T)})$ denote the sequence of acoustic input vectors (traditionally produced by splitting the audio into 20ms frames). Most speech recognition systems preprocess the input using specialized hand-designed features, but some (Jaitly and Hinton, 2011) deep learning systems learn features from raw input. Let $\boldsymbol{y} = (y_1, y_2, \ldots, y_N)$ denote the target output sequence (usually a sequence of words or characters). The **automatic speech recognition** (ASR) task consists of creating a function f^*_{ASR} that computes the most probable linguistic sequence $\boldsymbol{y}$ given the acoustic sequence $\boldsymbol{X}$:

$$f^*_{\text{ASR}}(\boldsymbol{X}) = \arg\max_{\boldsymbol{y}} P^*(\mathbf{y} \mid \mathbf{X} = \boldsymbol{X}) \tag{12.4}$$

where P^* is the true conditional distribution relating the inputs $\boldsymbol{X}$ to the targets $\boldsymbol{y}$.

Since the 1980s and until about 2009–2012, state-of-the art speech recognition systems primarily combined hidden Markov models (HMMs) and Gaussian mixture models (GMMs). GMMs modeled the association between acoustic features and phonemes (Bahl *et al.*, 1987), while HMMs modeled the sequence of phonemes. The GMM-HMM model family treats acoustic waveforms as being generated by the following process: first an HMM generates a sequence of phonemes and discrete sub-phonemic states (such as the beginning, middle, and end of each

phoneme), then a GMM transforms each discrete symbol into a brief segment of audio waveform. Although GMM-HMM systems dominated ASR until recently, speech recognition was actually one of the first areas where neural networks were applied, and numerous ASR systems from the late 1980s and early 1990s used neural nets (Bourlard and Wellekens, 1989; Waibel *et al.*, 1989; Robinson and Fallside, 1991; Bengio *et al.*, 1991, 1992; Konig *et al.*, 1996). At the time, the performance of ASR based on neural nets approximately matched the performance of GMM-HMM systems. For example, Robinson and Fallside (1991) achieved 26% phoneme error rate on the TIMIT (Garofolo *et al.*, 1993) corpus (with 39 phonemes to discriminate between), which was better than or comparable to HMM-based systems. Since then, TIMIT has been a benchmark for phoneme recognition, playing a role similar to the role MNIST plays for object recognition. However, because of the complex engineering involved in software systems for speech recognition and the effort that had been invested in building these systems on the basis of GMM-HMMs, the industry did not see a compelling argument for switching to neural networks. As a consequence, until the late 2000s, both academic and industrial research in using neural nets for speech recognition mostly focused on using neural nets to learn extra features for GMM-HMM systems.

Later, with *much larger and deeper models* and much larger datasets, recognition accuracy was dramatically improved by using neural networks to replace GMMs for the task of associating acoustic features to phonemes (or sub-phonemic states). Starting in 2009, speech researchers applied a form of deep learning based on unsupervised learning to speech recognition. This approach to deep learning was based on training undirected probabilistic models called restricted Boltzmann machines (RBMs) to model the input data. RBMs will be described in part III. To solve speech recognition tasks, unsupervised pretraining was used to build deep feedforward networks whose layers were each initialized by training an RBM. These networks take spectral acoustic representations in a fixed-size input window (around a center frame) and predict the conditional probabilities of HMM states for that center frame. Training such deep networks helped to significantly improve the recognition rate on TIMIT (Mohamed *et al.*, 2009, 2012a), bringing down the phoneme error rate from about 26% to 20.7%. See Mohamed *et al.* (2012b) for an analysis of reasons for the success of these models. Extensions to the basic phone recognition pipeline included the addition of speaker-adaptive features (Mohamed *et al.*, 2011) that further reduced the error rate. This was quickly followed up by work to expand the architecture from phoneme recognition (which is what TIMIT is focused on) to large-vocabulary speech recognition (Dahl *et al.*, 2012), which involves not just recognizing phonemes but also recognizing sequences of words from a large vocabulary. Deep networks for speech recognition eventually

shifted from being based on pretraining and Boltzmann machines to being based on techniques such as rectified linear units and dropout (Zeiler *et al.*, 2013; Dahl *et al.*, 2013). By that time, several of the major speech groups in industry had started exploring deep learning in collaboration with academic researchers. Hinton *et al.* (2012a) describe the breakthroughs achieved by these collaborators, which are now deployed in products such as mobile phones.

Later, as these groups explored larger and larger labeled datasets and incorporated some of the methods for initializing, training, and setting up the architecture of deep nets, they realized that the unsupervised pretraining phase was either unnecessary or did not bring any significant improvement.

These breakthroughs in recognition performance for word error rate in speech recognition were unprecedented (around 30% improvement) and were following a long period of about ten years during which error rates did not improve much with the traditional GMM-HMM technology, in spite of the continuously growing size of training sets (see figure 2.4 of Deng and Yu (2014)). This created a rapid shift in the speech recognition community towards deep learning. In a matter of roughly two years, most of the industrial products for speech recognition incorporated deep neural networks and this success spurred a new wave of research into deep learning algorithms and architectures for ASR, which is still ongoing today.

One of these innovations was the use of convolutional networks (Sainath *et al.*, 2013) that replicate weights across time and frequency, improving over the earlier time-delay neural networks that replicated weights only across time. The new two-dimensional convolutional models regard the input spectrogram not as one long vector but as an image, with one axis corresponding to time and the other to frequency of spectral components.

Another important push, still ongoing, has been towards end-to-end deep learning speech recognition systems that completely remove the HMM. The first major breakthrough in this direction came from Graves *et al.* (2013) who trained a deep LSTM RNN (see section 10.10), using MAP inference over the frame-to-phoneme alignment, as in LeCun *et al.* (1998b) and in the CTC framework (Graves *et al.*, 2006; Graves, 2012). A deep RNN (Graves *et al.*, 2013) has state variables from several layers at each time step, giving the unfolded graph two kinds of depth: ordinary depth due to a stack of layers, and depth due to time unfolding. This work brought the phoneme error rate on TIMIT to a record low of 17.7%. See Pascanu *et al.* (2014a) and Chung *et al.* (2014) for other variants of deep RNNs, applied in other settings.

Another contemporary step toward end-to-end deep learning ASR is to let the system learn how to "align" the acoustic-level information with the phonetic-level

information (Chorowski *et al.*, 2014; Lu *et al.*, 2015).

12.4 Natural Language Processing

Natural language processing (NLP) is the use of human languages, such as English or French, by a computer. Computer programs typically read and emit specialized languages designed to allow efficient and unambiguous parsing by simple programs. More naturally occurring languages are often ambiguous and defy formal description. Natural language processing includes applications such as machine translation, in which the learner must read a sentence in one human language and emit an equivalent sentence in another human language. Many NLP applications are based on language models that define a probability distribution over sequences of words, characters or bytes in a natural language.

As with the other applications discussed in this chapter, very generic neural network techniques can be successfully applied to natural language processing. However, to achieve excellent performance and to scale well to large applications, some domain-specific strategies become important. To build an efficient model of natural language, we must usually use techniques that are specialized for processing sequential data. In many cases, we choose to regard natural language as a sequence of words, rather than a sequence of individual characters or bytes. Because the total number of possible words is so large, word-based language models must operate on an extremely high-dimensional and sparse discrete space. Several strategies have been developed to make models of such a space efficient, both in a computational and in a statistical sense.

12.4.1 n-grams

A **language model** defines a probability distribution over sequences of tokens in a natural language. Depending on how the model is designed, a token may be a word, a character, or even a byte. Tokens are always discrete entities. The earliest successful language models were based on models of fixed-length sequences of tokens called n-grams. An n-gram is a sequence of n tokens.

Models based on n-grams define the conditional probability of the n-th token given the preceding $n-1$ tokens. The model uses products of these conditional distributions to define the probability distribution over longer sequences:

$$P(x_1, \dots, x_\tau) = P(x_1, \dots, x_{n-1}) \prod_{t=n}^{\tau} P(x_t \mid x_{t-n+1}, \dots, x_{t-1}). \tag{12.5}$$

This decomposition is justified by the chain rule of probability. The probability distribution over the initial sequence $P(x_1, \ldots, x_{n-1})$ may be modeled by a different model with a smaller value of n.

Training n-gram models is straightforward because the maximum likelihood estimate can be computed simply by counting how many times each possible n gram occurs in the training set. Models based on n-grams have been the core building block of statistical language modeling for many decades (Jelinek and Mercer, 1980; Katz, 1987; Chen and Goodman, 1999).

For small values of n, models have particular names: **unigram** for n=1, **bigram** for n=2, and **trigram** for n=3. These names derive from the Latin prefixes for the corresponding numbers and the Greek suffix "-gram" denoting something that is written.

Usually we train both an n-gram model and an $n-1$ gram model simultaneously. This makes it easy to compute

$$P(x_t \mid x_{t-n+1}, \ldots, x_{t-1}) = \frac{P_n(x_{t-n+1}, \ldots, x_t)}{P_{n-1}(x_{t-n+1}, \ldots, x_{t-1})} \tag{12.6}$$

simply by looking up two stored probabilities. For this to exactly reproduce inference in P_n, we must omit the final character from each sequence when we train P_{n-1}.

As an example, we demonstrate how a trigram model computes the probability of the sentence "`THE DOG RAN AWAY`." The first words of the sentence cannot be handled by the default formula based on conditional probability because there is no context at the beginning of the sentence. Instead, we must use the marginal probability over words at the start of the sentence. We thus evaluate $P_3(\texttt{THE DOG RAN})$. Finally, the last word may be predicted using the typical case, of using the conditional distribution $P(\texttt{AWAY} \mid \texttt{DOG RAN})$. Putting this together with equation 12.6, we obtain:

$$P(\texttt{THE DOG RAN AWAY}) = P_3(\texttt{THE DOG RAN})P_3(\texttt{DOG RAN AWAY})/P_2(\texttt{DOG RAN}). \tag{12.7}$$

A fundamental limitation of maximum likelihood for n-gram models is that P_n as estimated from training set counts is very likely to be zero in many cases, even though the tuple $(x_{t-n+1}, \ldots, x_t)$ may appear in the test set. This can cause two different kinds of catastrophic outcomes. When P_{n-1} is zero, the ratio is undefined, so the model does not even produce a sensible output. When P_{n-1} is non-zero but P_n is zero, the test log-likelihood is $-\infty$. To avoid such catastrophic outcomes, most n-gram models employ some form of **smoothing**. Smoothing techniques

shift probability mass from the observed tuples to unobserved ones that are similar. See Chen and Goodman (1999) for a review and empirical comparisons. One basic technique consists of adding non-zero probability mass to all of the possible next symbol values. This method can be justified as Bayesian inference with a uniform or Dirichlet prior over the count parameters. Another very popular idea is to form a mixture model containing higher-order and lower-order n-gram models, with the higher-order models providing more capacity and the lower-order models being more likely to avoid counts of zero. **Back-off methods** look-up the lower-order n-grams if the frequency of the context $x_{t-1}, \ldots, x_{t-n+1}$ is too small to use the higher-order model. More formally, they estimate the distribution over x_t by using contexts $x_{t-n+k}, \ldots, x_{t-1}$, for increasing k, until a sufficiently reliable estimate is found.

Classical n-gram models are particularly vulnerable to the curse of dimensionality. There are $|\mathbb{V}|^n$ possible n-grams and $|\mathbb{V}|$ is often very large. Even with a massive training set and modest n, most n-grams will not occur in the training set. One way to view a classical n-gram model is that it is performing nearest-neighbor lookup. In other words, it can be viewed as a local non-parametric predictor, similar to k-nearest neighbors. The statistical problems facing these extremely local predictors are described in section 5.11.2. The problem for a language model is even more severe than usual, because any two different words have the same distance from each other in one-hot vector space. It is thus difficult to leverage much information from any "neighbors"—only training examples that repeat literally the same context are useful for local generalization. To overcome these problems, a language model must be able to share knowledge between one word and other semantically similar words.

To improve the statistical efficiency of n-gram models, **class-based language models** (Brown *et al.*, 1992; Ney and Kneser, 1993; Niesler *et al.*, 1998) introduce the notion of word categories and then share statistical strength between words that are in the same category. The idea is to use a clustering algorithm to partition the set of words into clusters or classes, based on their co-occurrence frequencies with other words. The model can then use word class IDs rather than individual word IDs to represent the context on the right side of the conditioning bar. Composite models combining word-based and class-based models via mixing or back-off are also possible. Although word classes provide a way to generalize between sequences in which some word is replaced by another of the same class, much information is lost in this representation.

12.4.2 Neural Language Models

Neural language models or NLMs are a class of language model designed to overcome the curse of dimensionality problem for modeling natural language sequences by using a distributed representation of words (Bengio *et al.*, 2001). Unlike class-based n-gram models, neural language models are able to recognize that two words are similar without losing the ability to encode each word as distinct from the other. Neural language models share statistical strength between one word (and its context) and other similar words and contexts. The distributed representation the model learns for each word enables this sharing by allowing the model to treat words that have features in common similarly. For example, if the word `dog` and the word `cat` map to representations that share many attributes, then sentences that contain the word `cat` can inform the predictions that will be made by the model for sentences that contain the word `dog`, and vice-versa. Because there are many such attributes, there are many ways in which generalization can happen, transferring information from each training sentence to an exponentially large number of semantically related sentences. The curse of dimensionality requires the model to generalize to a number of sentences that is exponential in the sentence length. The model counters this curse by relating each training sentence to an exponential number of similar sentences.

We sometimes call these word representations **word embeddings**. In this interpretation, we view the raw symbols as points in a space of dimension equal to the vocabulary size. The word representations embed those points in a feature space of lower dimension. In the original space, every word is represented by a one-hot vector, so every pair of words is at Euclidean distance $\sqrt{2}$ from each other. In the embedding space, words that frequently appear in similar contexts (or any pair of words sharing some "features" learned by the model) are close to each other. This often results in words with similar meanings being neighbors. Figure 12.3 zooms in on specific areas of a learned word embedding space to show how semantically similar words map to representations that are close to each other.

Neural networks in other domains also define embeddings. For example, a hidden layer of a convolutional network provides an "image embedding." Usually NLP practitioners are much more interested in this idea of embeddings because natural language does not originally lie in a real-valued vector space. The hidden layer has provided a more qualitatively dramatic change in the way the data is represented.

The basic idea of using distributed representations to improve models for natural language processing is not restricted to neural networks. It may also be used with graphical models that have distributed representations in the form of

multiple latent variables (Mnih and Hinton, 2007).

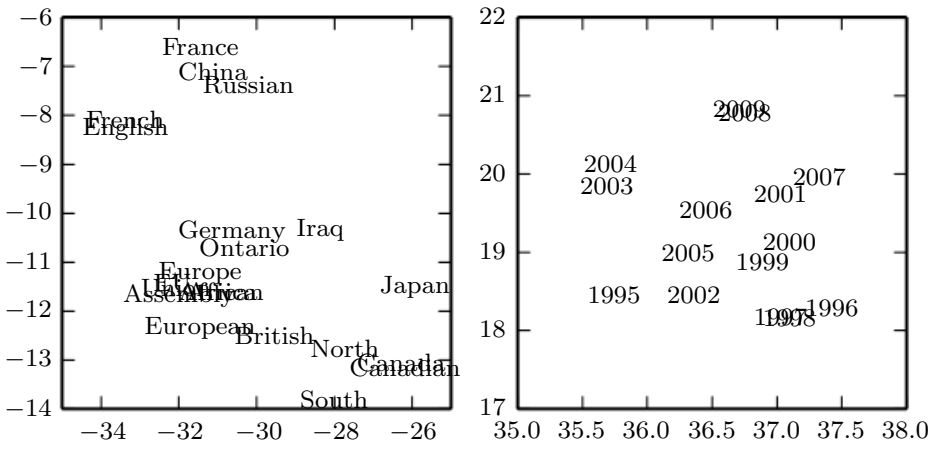

Figure 12.3: Two-dimensional visualizations of word embeddings obtained from a neural machine translation model (Bahdanau *et al.*, 2015), zooming in on specific areas where semantically related words have embedding vectors that are close to each other. Countries appear on the left and numbers on the right. Keep in mind that these embeddings are 2-D for the purpose of visualization. In real applications, embeddings typically have higher dimensionality and can simultaneously capture many kinds of similarity between words.

12.4.3 High-Dimensional Outputs

In many natural language applications, we often want our models to produce words (rather than characters) as the fundamental unit of the output. For large vocabularies, it can be very computationally expensive to represent an output distribution over the choice of a word, because the vocabulary size is large. In many applications, $\mathbb{V}$ contains hundreds of thousands of words. The naive approach to representing such a distribution is to apply an affine transformation from a hidden representation to the output space, then apply the softmax function. Suppose we have a vocabulary $\mathbb{V}$ with size $|\mathbb{V}|$. The weight matrix describing the linear component of this affine transformation is very large, because its output dimension is $|\mathbb{V}|$. This imposes a high memory cost to represent the matrix, and a high computational cost to multiply by it. Because the softmax is normalized across all $|\mathbb{V}|$ outputs, it is necessary to perform the full matrix multiplication at training time as well as test time—we cannot calculate only the dot product with the weight vector for the correct output. The high computational costs of the output layer thus arise both at training time (to compute the likelihood and its gradient) and at test time (to compute probabilities for all or selected words). For specialized

loss functions, the gradient can be computed efficiently (Vincent *et al.*, 2015), but the standard cross-entropy loss applied to a traditional softmax output layer poses many difficulties.

Suppose that $\boldsymbol{h}$ is the top hidden layer used to predict the output probabilities $\hat{\boldsymbol{y}}$. If we parametrize the transformation from $\boldsymbol{h}$ to $\hat{\boldsymbol{y}}$ with learned weights $\boldsymbol{W}$ and learned biases $\boldsymbol{b}$, then the affine-softmax output layer performs the following computations:

$$a_i = b_i + \sum_j W_{ij} h_j \quad \forall i \in \{1, \ldots, |\mathbb{V}|\}, \tag{12.8}$$

$$\hat{y}_i = \frac{e^{a_i}}{\sum_{i'=1}^{|\mathbb{V}|} e^{a_{i'}}}. \tag{12.9}$$

If $\boldsymbol{h}$ contains n_h elements then the above operation is $O(|\mathbb{V}| n_h)$. With n_h in the thousands and $|\mathbb{V}|$ in the hundreds of thousands, this operation dominates the computation of most neural language models.

12.4.3.1 Use of a Short List

The first neural language models (Bengio *et al.*, 2001, 2003) dealt with the high cost of using a softmax over a large number of output words by limiting the vocabulary size to 10,000 or 20,000 words. Schwenk and Gauvain (2002) and Schwenk (2007) built upon this approach by splitting the vocabulary $\mathbb{V}$ into a **shortlist** $\mathbb{L}$ of most frequent words (handled by the neural net) and a tail $\mathbb{T} = \mathbb{V} \backslash \mathbb{L}$ of more rare words (handled by an n-gram model). To be able to combine the two predictions, the neural net also has to predict the probability that a word appearing after context C belongs to the tail list. This may be achieved by adding an extra sigmoid output unit to provide an estimate of $P(i \in \mathbb{T} \mid C)$. The extra output can then be used to achieve an estimate of the probability distribution over all words in $\mathbb{V}$ as follows:

$$\begin{aligned} P(y = i \mid C) =& 1_{i \in \mathbb{L}} P(y = i \mid C, i \in \mathbb{L})(1 - P(i \in \mathbb{T} \mid C)) \\ &+ 1_{i \in \mathbb{T}} P(y = i \mid C, i \in \mathbb{T}) P(i \in \mathbb{T} \mid C) \end{aligned} \tag{12.10}$$

where $P(y = i \mid C, i \in \mathbb{L})$ is provided by the neural language model and $P(y = i \mid C, i \in \mathbb{T})$ is provided by the n-gram model. With slight modification, this approach can also work using an extra output value in the neural language model's softmax layer, rather than a separate sigmoid unit.

An obvious disadvantage of the short list approach is that the potential generalization advantage of the neural language models is limited to the most frequent

words, where, arguably, it is the least useful. This disadvantage has stimulated the exploration of alternative methods to deal with high-dimensional outputs, described below.

12.4.3.2 Hierarchical Softmax

A classical approach (Goodman, 2001) to reducing the computational burden of high-dimensional output layers over large vocabulary sets $\mathbb{V}$ is to decompose probabilities hierarchically. Instead of necessitating a number of computations proportional to $|\mathbb{V}|$ (and also proportional to the number of hidden units, n_h), the $|\mathbb{V}|$ factor can be reduced to as low as $\log |\mathbb{V}|$. Bengio (2002) and Morin and Bengio (2005) introduced this factorized approach to the context of neural language models.

One can think of this hierarchy as building categories of words, then categories of categories of words, then categories of categories of categories of words, etc. These nested categories form a tree, with words at the leaves. In a balanced tree, the tree has depth $O(\log |\mathbb{V}|)$. The probability of a choosing a word is given by the product of the probabilities of choosing the branch leading to that word at every node on a path from the root of the tree to the leaf containing the word. Figure 12.4 illustrates a simple example. Mnih and Hinton (2009) also describe how to use multiple paths to identify a single word in order to better model words that have multiple meanings. Computing the probability of a word then involves summation over all of the paths that lead to that word.

To predict the conditional probabilities required at each node of the tree, we typically use a logistic regression model at each node of the tree, and provide the same context C as input to all of these models. Because the correct output is encoded in the training set, we can use supervised learning to train the logistic regression models. This is typically done using a standard cross-entropy loss, corresponding to maximizing the log-likelihood of the correct sequence of decisions.

Because the output log-likelihood can be computed efficiently (as low as $\log |\mathbb{V}|$ rather than $|\mathbb{V}|$), its gradients may also be computed efficiently. This includes not only the gradient with respect to the output parameters but also the gradients with respect to the hidden layer activations.

It is possible but usually not practical to optimize the tree structure to minimize the expected number of computations. Tools from information theory specify how to choose the optimal binary code given the relative frequencies of the words. To do so, we could structure the tree so that the number of bits associated with a word is approximately equal to the logarithm of the frequency of that word. However, in

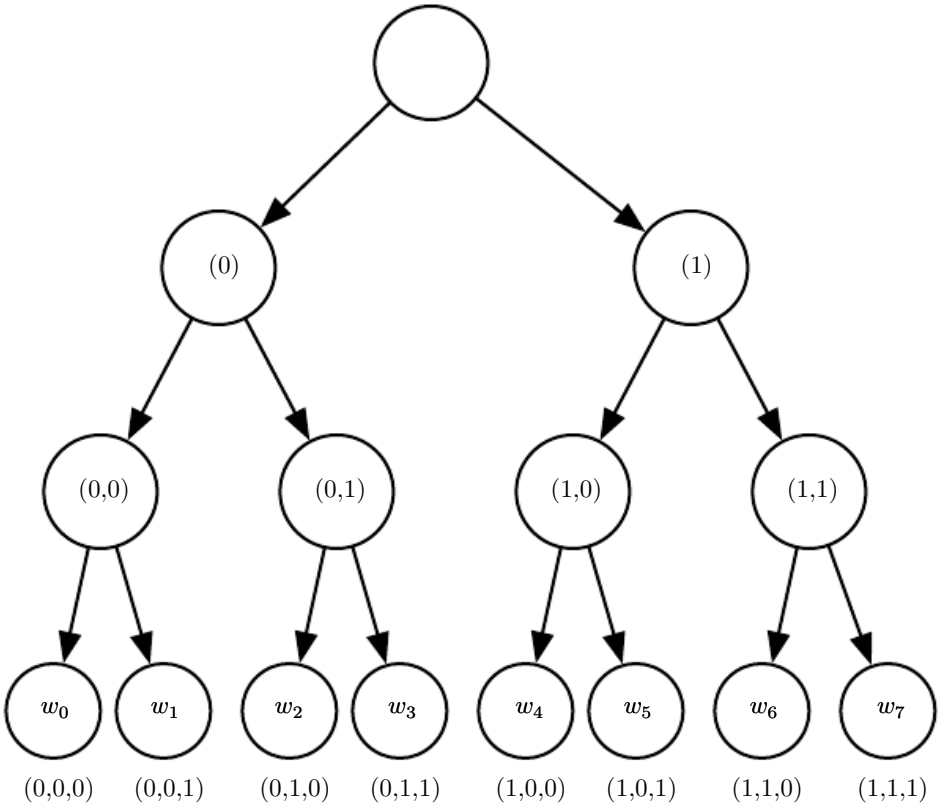

Figure 12.4: Illustration of a simple hierarchy of word categories, with 8 words $w_0, \ldots, w_7$ organized into a three level hierarchy. The leaves of the tree represent actual specific words. Internal nodes represent groups of words. Any node can be indexed by the sequence of binary decisions (0=left, 1=right) to reach the node from the root. Super-class (0) contains the classes (0, 0) and (0, 1), which respectively contain the sets of words $\{w_0, w_1\}$ and $\{w_2, w_3\}$, and similarly super-class (1) contains the classes (1,0) and (1, 1), which respectively contain the words (w_4, w_5) and (w_6, w_7). If the tree is sufficiently balanced, the maximum depth (number of binary decisions) is on the order of the logarithm of the number of words $|\mathbb{V}|$: the choice of one out of $|\mathbb{V}|$ words can be obtained by doing $O(\log |\mathbb{V}|)$ operations (one for each of the nodes on the path from the root). In this example, computing the probability of a word y can be done by multiplying three probabilities, associated with the binary decisions to move left or right at each node on the path from the root to a node y. Let $b_i(y)$ be the i-th binary decision when traversing the tree towards the value y. The probability of sampling an output y decomposes into a product of conditional probabilities, using the chain rule for conditional probabilities, with each node indexed by the prefix of these bits. For example, node $(1, 0)$ corresponds to the prefix $(b_0(w_4) = 1, b_1(w_4) = 0)$, and the probability of w_4 can be decomposed as follows:

$$P(\mathrm{y} = w_4) = P(\mathrm{b}_0 = 1, \mathrm{b}_1 = 0, \mathrm{b}_2 = 0) \tag{12.11}$$

$$= P(\mathrm{b}_0 = 1)P(\mathrm{b}_1 = 0 \mid \mathrm{b}_0 = 1)P(\mathrm{b}_2 = 0 \mid \mathrm{b}_0 = 1, \mathrm{b}_1 = 0). \tag{12.12}$$

practice, the computational savings are typically not worth the effort because the computation of the output probabilities is only one part of the total computation in the neural language model. For example, suppose there are l fully connected hidden layers of width n_h. Let n_b be the weighted average of the number of bits required to identify a word, with the weighting given by the frequency of these words. In this example, the number of operations needed to compute the hidden activations grows as as $O(ln_h^2)$ while the output computations grow as $O(n_h n_b)$. As long as $n_b \leq ln_h$, we can reduce computation more by shrinking n_h than by shrinking n_b. Indeed, n_b is often small. Because the size of the vocabulary rarely exceeds a million words and $\log_2(10^6) \approx 20$, it is possible to reduce n_b to about 20, but n_h is often much larger, around 10^3 or more. Rather than carefully optimizing a tree with a branching factor of 2, one can instead define a tree with depth two and a branching factor of $\sqrt{|\mathbb{V}|}$. Such a tree corresponds to simply defining a set of mutually exclusive word classes. The simple approach based on a tree of depth two captures most of the computational benefit of the hierarchical strategy.

One question that remains somewhat open is how to best define these word classes, or how to define the word hierarchy in general. Early work used existing hierarchies (Morin and Bengio, 2005) but the hierarchy can also be learned, ideally jointly with the neural language model. Learning the hierarchy is difficult. An exact optimization of the log-likelihood appears intractable because the choice of a word hierarchy is a discrete one, not amenable to gradient-based optimization. However, one could use discrete optimization to approximately optimize the partition of words into word classes.

An important advantage of the hierarchical softmax is that it brings computational benefits both at training time and at test time, if at test time we want to compute the probability of specific words.

Of course, computing the probability of all $|\mathbb{V}|$ words will remain expensive even with the hierarchical softmax. Another important operation is selecting the most likely word in a given context. Unfortunately the tree structure does not provide an efficient and exact solution to this problem.

A disadvantage is that in practice the hierarchical softmax tends to give worse test results than sampling-based methods we will describe next. This may be due to a poor choice of word classes.

12.4.3.3 Importance Sampling

One way to speed up the training of neural language models is to avoid explicitly computing the contribution of the gradient from all of the words that do not appear

in the next position. Every incorrect word should have low probability under the model. It can be computationally costly to enumerate all of these words. Instead, it is possible to sample only a subset of the words. Using the notation introduced in equation 12.8, the gradient can be written as follows:

$$\frac{\partial \log P(y \mid C)}{\partial \theta} = \frac{\partial \log \text{softmax}_y(\boldsymbol{a})}{\partial \theta} \tag{12.13}$$

$$= \frac{\partial}{\partial \theta} \log \frac{e^{a_y}}{\sum_i e^{a_i}} \tag{12.14}$$

$$= \frac{\partial}{\partial \theta}(a_y - \log \sum_i e^{a_i}) \tag{12.15}$$

$$= \frac{\partial a_y}{\partial \theta} - \sum_i P(y = i \mid C) \frac{\partial a_i}{\partial \theta} \tag{12.16}$$

where $\boldsymbol{a}$ is the vector of pre-softmax activations (or scores), with one element per word. The first term is the **positive phase** term (pushing a_y up) while the second term is the **negative phase** term (pushing a_i down for all i, with weight $P(i \mid C)$. Since the negative phase term is an expectation, we can estimate it with a Monte Carlo sample. However, that would require sampling from the model itself. Sampling from the model requires computing $P(i \mid C)$ for all i in the vocabulary, which is precisely what we are trying to avoid.

Instead of sampling from the model, one can sample from another distribution, called the proposal distribution (denoted q), and use appropriate weights to correct for the bias introduced by sampling from the wrong distribution (Bengio and Sénécal, 2003; Bengio and Sénécal, 2008). This is an application of a more general technique called **importance sampling**, which will be described in more detail in section 17.2. Unfortunately, even exact importance sampling is not efficient because it requires computing weights p_i/q_i, where $p_i = P(i \mid C)$, which can only be computed if all the scores a_i are computed. The solution adopted for this application is called **biased importance sampling**, where the importance weights are normalized to sum to 1. When negative word n_i is sampled, the associated gradient is weighted by

$$w_i = \frac{p_{n_i}/q_{n_i}}{\sum_{j=1}^{N} p_{n_j}/q_{n_j}}. \tag{12.17}$$

These weights are used to give the appropriate importance to the m negative samples from q used to form the estimated negative phase contribution to the

gradient:

$$\sum_{i=1}^{|\mathbb{V}|} P(i \mid C) \frac{\partial a_i}{\partial \theta} \approx \frac{1}{m} \sum_{i=1}^{m} w_i \frac{\partial a_{n_i}}{\partial \theta}. \tag{12.18}$$

A unigram or a bigram distribution works well as the proposal distribution q. It is easy to estimate the parameters of such a distribution from data. After estimating the parameters, it is also possible to sample from such a distribution very efficiently.

Importance sampling is not only useful for speeding up models with large softmax outputs. More generally, it is useful for accelerating training with large sparse output layers, where the output is a sparse vector rather than a 1-of-n choice. An example is a **bag of words**. A bag of words is a sparse vector $\boldsymbol{v}$ where v_i indicates the presence or absence of word i from the vocabulary in the document. Alternately, v_i can indicate the number of times that word i appears. Machine learning models that emit such sparse vectors can be expensive to train for a variety of reasons. Early in learning, the model may not actually choose to make the output truly sparse. Moreover, the loss function we use for training might most naturally be described in terms of comparing every element of the output to every element of the target. This means that it is not always clear that there is a computational benefit to using sparse outputs, because the model may choose to make the majority of the output non-zero and all of these non-zero values need to be compared to the corresponding training target, even if the training target is zero. Dauphin *et al.* (2011) demonstrated that such models can be accelerated using importance sampling. The efficient algorithm minimizes the loss reconstruction for the "positive words" (those that are non-zero in the target) and an equal number of "negative words." The negative words are chosen randomly, using a heuristic to sample words that are more likely to be mistaken. The bias introduced by this heuristic oversampling can then be corrected using importance weights.

In all of these cases, the computational complexity of gradient estimation for the output layer is reduced to be proportional to the number of negative samples rather than proportional to the size of the output vector.

12.4.3.4 Noise-Contrastive Estimation and Ranking Loss

Other approaches based on sampling have been proposed to reduce the computational cost of training neural language models with large vocabularies. An early example is the ranking loss proposed by Collobert and Weston (2008a), which views the output of the neural language model for each word as a score and tries to make the score of the correct word a_y be ranked high in comparison to the other

scores a_i. The ranking loss proposed then is

$$L = \sum_i \max(0, 1 - a_y + a_i). \tag{12.19}$$

The gradient is zero for the i-th term if the score of the observed word, a_y, is greater than the score of the negative word a_i by a margin of 1. One issue with this criterion is that it does not provide estimated conditional probabilities, which are useful in some applications, including speech recognition and text generation (including conditional text generation tasks such as translation).

A more recently used training objective for neural language model is noise-contrastive estimation, which is introduced in section 18.6. This approach has been successfully applied to neural language models (Mnih and Teh, 2012; Mnih and Kavukcuoglu, 2013).

12.4.4 Combining Neural Language Models with n-grams

A major advantage of n-gram models over neural networks is that n-gram models achieve high model capacity (by storing the frequencies of very many tuples) while requiring very little computation to process an example (by looking up only a few tuples that match the current context). If we use hash tables or trees to access the counts, the computation used for n-grams is almost independent of capacity. In comparison, doubling a neural network's number of parameters typically also roughly doubles its computation time. Exceptions include models that avoid using all parameters on each pass. Embedding layers index only a single embedding in each pass, so we can increase the vocabulary size without increasing the computation time per example. Some other models, such as tiled convolutional networks, can add parameters while reducing the degree of parameter sharing in order to maintain the same amount of computation. However, typical neural network layers based on matrix multiplication use an amount of computation proportional to the number of parameters.

One easy way to add capacity is thus to combine both approaches in an ensemble consisting of a neural language model and an n-gram language model (Bengio *et al.*, 2001, 2003). As with any ensemble, this technique can reduce test error if the ensemble members make independent mistakes. The field of ensemble learning provides many ways of combining the ensemble members' predictions, including uniform weighting and weights chosen on a validation set. Mikolov *et al.* (2011a) extended the ensemble to include not just two models but a large array of models. It is also possible to pair a neural network with a maximum entropy model and train both jointly (Mikolov *et al.*, 2011b). This approach can be viewed as training

a neural network with an extra set of inputs that are connected directly to the output, and not connected to any other part of the model. The extra inputs are indicators for the presence of particular n-grams in the input context, so these variables are very high-dimensional and very sparse. The increase in model capacity is huge—the new portion of the architecture contains up to $|sV|^n$ parameters—but the amount of added computation needed to process an input is minimal because the extra inputs are very sparse.

12.4.5 Neural Machine Translation

Machine translation is the task of reading a sentence in one natural language and emitting a sentence with the equivalent meaning in another language. Machine translation systems often involve many components. At a high level, there is often one component that proposes many candidate translations. Many of these translations will not be grammatical due to differences between the languages. For example, many languages put adjectives after nouns, so when translated to English directly they yield phrases such as "apple red." The proposal mechanism suggests many variants of the suggested translation, ideally including "red apple." A second component of the translation system, a language model, evaluates the proposed translations, and can score "red apple" as better than "apple red."

The earliest use of neural networks for machine translation was to upgrade the language model of a translation system by using a neural language model (Schwenk *et al.*, 2006; Schwenk, 2010). Previously, most machine translation systems had used an n-gram model for this component. The n-gram based models used for machine translation include not just traditional back-off n-gram models (Jelinek and Mercer, 1980; Katz, 1987; Chen and Goodman, 1999) but also **maximum entropy language models** (Berger *et al.*, 1996), in which an affine-softmax layer predicts the next word given the presence of frequent n-grams in the context.

Traditional language models simply report the probability of a natural language sentence. Because machine translation involves producing an output sentence given an input sentence, it makes sense to extend the natural language model to be conditional. As described in section 6.2.1.1, it is straightforward to extend a model that defines a marginal distribution over some variable to define a conditional distribution over that variable given a context C, where C might be a single variable or a list of variables. Devlin *et al.* (2014) beat the state-of-the-art in some statistical machine translation benchmarks by using an MLP to score a phrase $\mathrm{t}_1, \mathrm{t}_2, \ldots, \mathrm{t}_k$ in the target language given a phrase $\mathrm{s}_1, \mathrm{s}_2, \ldots, \mathrm{s}_n$ in the source language. The MLP estimates $P(\mathrm{t}_1, \mathrm{t}_2, \ldots, \mathrm{t}_k \mid \mathrm{s}_1, \mathrm{s}_2, \ldots, \mathrm{s}_n)$. The estimate formed by this MLP replaces the estimate provided by conditional n-gram models.

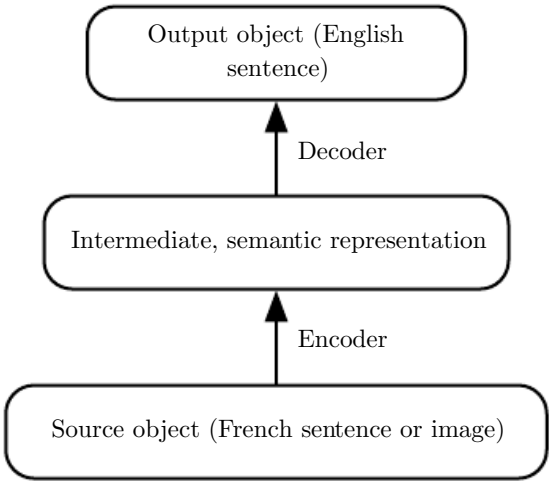

Figure 12.5: The encoder-decoder architecture to map back and forth between a surface representation (such as a sequence of words or an image) and a semantic representation. By using the output of an encoder of data from one modality (such as the encoder mapping from French sentences to hidden representations capturing the meaning of sentences) as the input to a decoder for another modality (such as the decoder mapping from hidden representations capturing the meaning of sentences to English), we can train systems that translate from one modality to another. This idea has been applied successfully not just to machine translation but also to caption generation from images.

A drawback of the MLP-based approach is that it requires the sequences to be preprocessed to be of fixed length. To make the translation more flexible, we would like to use a model that can accommodate variable length inputs and variable length outputs. An RNN provides this ability. Section 10.2.4 describes several ways of constructing an RNN that represents a conditional distribution over a sequence given some input, and section 10.4 describes how to accomplish this conditioning when the input is a sequence. In all cases, one model first reads the input sequence and emits a data structure that summarizes the input sequence. We call this summary the "context" C. The context C may be a list of vectors, or it may be a vector or tensor. The model that reads the input to produce C may be an RNN (Cho *et al.*, 2014a; Sutskever *et al.*, 2014; Jean *et al.*, 2014) or a convolutional network (Kalchbrenner and Blunsom, 2013). A second model, usually an RNN, then reads the context C and generates a sentence in the target language. This general idea of an encoder-decoder framework for machine translation is illustrated in figure 12.5.

In order to generate an entire sentence conditioned on the source sentence, the model must have a way to represent the entire source sentence. Earlier models were only able to represent individual words or phrases. From a representation

learning point of view, it can be useful to learn a representation in which sentences that have the same meaning have similar representations regardless of whether they were written in the source language or the target language. This strategy was explored first using a combination of convolutions and RNNs (Kalchbrenner and Blunsom, 2013). Later work introduced the use of an RNN for scoring proposed translations (Cho *et al.*, 2014a) and for generating translated sentences (Sutskever *et al.*, 2014). Jean *et al.* (2014) scaled these models to larger vocabularies.

12.4.5.1 Using an Attention Mechanism and Aligning Pieces of Data

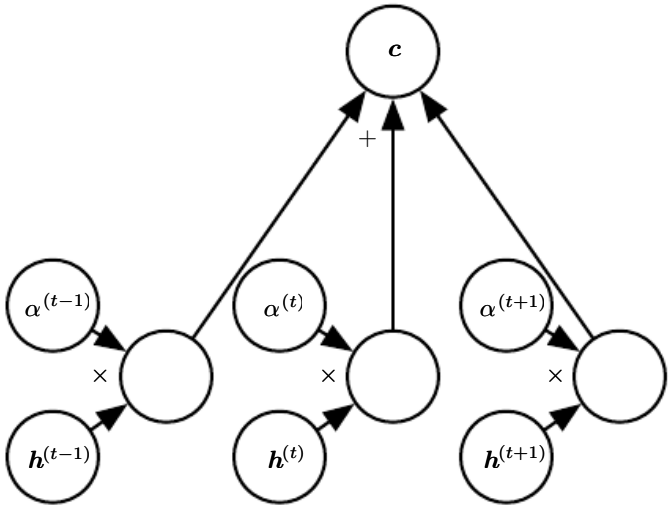

Figure 12.6: A modern attention mechanism, as introduced by Bahdanau *et al.* (2015), is essentially a weighted average. A context vector $\boldsymbol{c}$ is formed by taking a weighted average of feature vectors $\boldsymbol{h}^{(t)}$ with weights $\alpha^{(t)}$. In some applications, the feature vectors $\boldsymbol{h}$ are hidden units of a neural network, but they may also be raw input to the model. The weights $\alpha^{(t)}$ are produced by the model itself. They are usually values in the interval $[0, 1]$ and are intended to concentrate around just one $\boldsymbol{h}^{(t)}$ so that the weighted average approximates reading that one specific time step precisely. The weights $\alpha^{(t)}$ are usually produced by applying a softmax function to relevance scores emitted by another portion of the model. The attention mechanism is more expensive computationally than directly indexing the desired $\boldsymbol{h}^{(t)}$, but direct indexing cannot be trained with gradient descent. The attention mechanism based on weighted averages is a smooth, differentiable approximation that can be trained with existing optimization algorithms.

Using a fixed-size representation to capture all the semantic details of a very long sentence of say 60 words is very difficult. It can be achieved by training a sufficiently large RNN well enough and for long enough, as demonstrated by Cho *et al.* (2014a) and Sutskever *et al.* (2014). However, a more efficient approach is to read the whole sentence or paragraph (to get the context and the gist of what

is being expressed), then produce the translated words one at a time, each time focusing on a different part of the input sentence in order to gather the semantic details that are required to produce the next output word. That is exactly the idea that Bahdanau *et al.* (2015) first introduced. The attention mechanism used to focus on specific parts of the input sequence at each time step is illustrated in figure 12.6.

We can think of an attention-based system as having three components:

1. A process that "*reads*" raw data (such as source words in a source sentence), and converts them into distributed representations, with one feature vector associated with each word position.

2. A list of feature vectors storing the output of the reader. This can be understood as a "*memory*" containing a sequence of facts, which can be retrieved later, not necessarily in the same order, without having to visit all of them.

3. A process that "*exploits*" the content of the memory to sequentially perform a task, at each time step having the ability put attention on the content of one memory element (or a few, with a different weight).

The third component generates the translated sentence.

When words in a sentence written in one language are aligned with corresponding words in a translated sentence in another language, it becomes possible to relate the corresponding word embeddings. Earlier work showed that one could learn a kind of translation matrix relating the word embeddings in one language with the word embeddings in another (Kočiský *et al.*, 2014), yielding lower alignment error rates than traditional approaches based on the frequency counts in the phrase table. There is even earlier work on learning cross-lingual word vectors (Klementiev *et al.*, 2012). Many extensions to this approach are possible. For example, more efficient cross-lingual alignment (Gouws *et al.*, 2014) allows training on larger datasets.

12.4.6 Historical Perspective

The idea of distributed representations for symbols was introduced by Rumelhart *et al.* (1986a) in one of the first explorations of back-propagation, with symbols corresponding to the identity of family members and the neural network capturing the relationships between family members, with training examples forming triplets such as (Colin, Mother, Victoria). The first layer of the neural network learned a representation of each family member. For example, the features for Colin

might represent which family tree Colin was in, what branch of that tree he was in, what generation he was from, etc. One can think of the neural network as computing learned rules relating these attributes together in order to obtain the desired predictions. The model can then make predictions such as inferring who is the mother of Colin.

The idea of forming an embedding for a symbol was extended to the idea of an embedding for a word by Deerwester *et al.* (1990). These embeddings were learned using the SVD. Later, embeddings would be learned by neural networks.

The history of natural language processing is marked by transitions in the popularity of different ways of representing the input to the model. Following this early work on symbols or words, some of the earliest applications of neural networks to NLP (Miikkulainen and Dyer, 1991; Schmidhuber, 1996) represented the input as a sequence of characters.

Bengio *et al.* (2001) returned the focus to modeling words and introduced neural language models, which produce interpretable word embeddings. These neural models have scaled up from defining representations of a small set of symbols in the 1980s to millions of words (including proper nouns and misspellings) in modern applications. This computational scaling effort led to the invention of the techniques described above in section 12.4.3.

Initially, the use of words as the fundamental units of language models yielded improved language modeling performance (Bengio *et al.*, 2001). To this day, new techniques continually push both character-based models (Sutskever *et al.*, 2011) and word-based models forward, with recent work (Gillick *et al.*, 2015) even modeling individual bytes of Unicode characters.

The ideas behind neural language models have been extended into several natural language processing applications, such as parsing (Henderson, 2003, 2004; Collobert, 2011), part-of-speech tagging, semantic role labeling, chunking, etc, sometimes using a single multi-task learning architecture (Collobert and Weston, 2008a; Collobert *et al.*, 2011a) in which the word embeddings are shared across tasks.

Two-dimensional visualizations of embeddings became a popular tool for analyzing language models following the development of the t-SNE dimensionality reduction algorithm (van der Maaten and Hinton, 2008) and its high-profile application to visualization word embeddings by Joseph Turian in 2009.

12.5 Other Applications

In this section we cover a few other types of applications of deep learning that are different from the standard object recognition, speech recognition and natural language processing tasks discussed above. Part III of this book will expand that scope even further to tasks that remain primarily research areas.

12.5.1 Recommender Systems

One of the major families of applications of machine learning in the information technology sector is the ability to make recommendations of items to potential users or customers. Two major types of applications can be distinguished: online advertising and item recommendations (often these recommendations are still for the purpose of selling a product). Both rely on predicting the association between a user and an item, either to predict the probability of some action (the user buying the product, or some proxy for this action) or the expected gain (which may depend on the value of the product) if an ad is shown or a recommendation is made regarding that product to that user. The internet is currently financed in great part by various forms of online advertising. There are major parts of the economy that rely on online shopping. Companies including Amazon and eBay use machine learning, including deep learning, for their product recommendations. Sometimes, the items are not products that are actually for sale. Examples include selecting posts to display on social network news feeds, recommending movies to watch, recommending jokes, recommending advice from experts, matching players for video games, or matching people in dating services.

Often, this association problem is handled like a supervised learning problem: given some information about the item and about the user, predict the proxy of interest (user clicks on ad, user enters a rating, user clicks on a "like" button, user buys product, user spends some amount of money on the product, user spends time visiting a page for the product, etc). This often ends up being either a regression problem (predicting some conditional expected value) or a probabilistic classification problem (predicting the conditional probability of some discrete event).

The early work on recommender systems relied on minimal information as inputs for these predictions: the user ID and the item ID. In this context, the only way to generalize is to rely on the similarity between the patterns of values of the target variable for different users or for different items. Suppose that user 1 and user 2 both like items A, B and C. From this, we may infer that user 1 and

user 2 have similar tastes. If user 1 likes item D, then this should be a strong cue that user 2 will also like D. Algorithms based on this principle come under the name of **collaborative filtering**. Both non-parametric approaches (such as nearest-neighbor methods based on the estimated similarity between patterns of preferences) and parametric methods are possible. Parametric methods often rely on learning a distributed representation (also called an embedding) for each user and for each item. Bilinear prediction of the target variable (such as a rating) is a simple parametric method that is highly successful and often found as a component of state-of-the-art systems. The prediction is obtained by the dot product between the user embedding and the item embedding (possibly corrected by constants that depend only on either the user ID or the item ID). Let $\hat{\boldsymbol{R}}$ be the matrix containing our predictions, $\boldsymbol{A}$ a matrix with user embeddings in its rows and $\boldsymbol{B}$ a matrix with item embeddings in its columns. Let $\boldsymbol{b}$ and $\boldsymbol{c}$ be vectors that contain respectively a kind of bias for each user (representing how grumpy or positive that user is in general) and for each item (representing its general popularity). The bilinear prediction is thus obtained as follows:

$$\hat{R}_{u,i} = b_u + c_i + \sum_j A_{u,j} B_{j,i}. \tag{12.20}$$

Typically one wants to minimize the squared error between predicted ratings $\hat{R}_{u,i}$ and actual ratings $R_{u,i}$. User embeddings and item embeddings can then be conveniently visualized when they are first reduced to a low dimension (two or three), or they can be used to compare users or items against each other, just like word embeddings. One way to obtain these embeddings is by performing a singular value decomposition of the matrix $\boldsymbol{R}$ of actual targets (such as ratings). This corresponds to factorizing $\boldsymbol{R} = \boldsymbol{U}\boldsymbol{D}\boldsymbol{V}'$ (or a normalized variant) into the product of two factors, the lower rank matrices $\boldsymbol{A} = \boldsymbol{U}\boldsymbol{D}$ and $\boldsymbol{B} = \boldsymbol{V}'$. One problem with the SVD is that it treats the missing entries in an arbitrary way, as if they corresponded to a target value of 0. Instead we would like to avoid paying any cost for the predictions made on missing entries. Fortunately, the sum of squared errors on the observed ratings can also be easily minimized by gradient-based optimization. The SVD and the bilinear prediction of equation 12.20 both performed very well in the competition for the Netflix prize (Bennett and Lanning, 2007), aiming at predicting ratings for films, based only on previous ratings by a large set of anonymous users. Many machine learning experts participated in this competition, which took place between 2006 and 2009. It raised the level of research in recommender systems using advanced machine learning and yielded improvements in recommender systems. Even though it did not win by itself, the simple bilinear prediction or SVD was a component of the ensemble models

presented by most of the competitors, including the winners (Töscher *et al.*, 2009; Koren, 2009).

Beyond these bilinear models with distributed representations, one of the first uses of neural networks for collaborative filtering is based on the RBM undirected probabilistic model (Salakhutdinov *et al.*, 2007). RBMs were an important element of the ensemble of methods that won the Netflix competition (Töscher *et al.*, 2009; Koren, 2009). More advanced variants on the idea of factorizing the ratings matrix have also been explored in the neural networks community (Salakhutdinov and Mnih, 2008).

However, there is a basic limitation of collaborative filtering systems: when a new item or a new user is introduced, its lack of rating history means that there is no way to evaluate its similarity with other items or users (respectively), or the degree of association between, say, that new user and existing items. This is called the problem of cold-start recommendations. A general way of solving the cold-start recommendation problem is to introduce extra information about the individual users and items. For example, this extra information could be user profile information or features of each item. Systems that use such information are called **content-based recommender systems**. The mapping from a rich set of user features or item features to an embedding can be learned through a deep learning architecture (Huang *et al.*, 2013; Elkahky *et al.*, 2015).

Specialized deep learning architectures such as convolutional networks have also been applied to learn to extract features from rich content such as from musical audio tracks, for music recommendation (van den Oörd *et al.*, 2013). In that work, the convolutional net takes acoustic features as input and computes an embedding for the associated song. The dot product between this song embedding and the embedding for a user is then used to predict whether a user will listen to the song.

12.5.1.1 Exploration Versus Exploitation

When making recommendations to users, an issue arises that goes beyond ordinary supervised learning and into the realm of reinforcement learning. Many recommendation problems are most accurately described theoretically as **contextual bandits** (Langford and Zhang, 2008; Lu *et al.*, 2010). The issue is that when we use the recommendation system to collect data, we get a biased and incomplete view of the preferences of users: we only see the responses of users to the items they were recommended and not to the other items. In addition, in some cases we may not get any information on users for whom no recommendation has been made (for example, with ad auctions, it may be that the price proposed for an

ad was below a minimum price threshold, or does not win the auction, so the ad is not shown at all). More importantly, we get no information about what outcome would have resulted from recommending any of the other items. This would be like training a classifier by picking one class $\hat{y}$ for each training example $\boldsymbol{x}$ (typically the class with the highest probability according to the model) and then only getting as feedback whether this was the correct class or not. Clearly, each example conveys less information than in the supervised case where the true label y is directly accessible, so more examples are necessary. Worse, if we are not careful, we could end up with a system that continues picking the wrong decisions even as more and more data is collected, because the correct decision initially had a very low probability: until the learner picks that correct decision, it does not learn about the correct decision. This is similar to the situation in reinforcement learning where only the reward for the selected action is observed. In general, reinforcement learning can involve a sequence of many actions and many rewards. The bandits scenario is a special case of reinforcement learning, in which the learner takes only a single action and receives a single reward. The bandit problem is easier in the sense that the learner knows which reward is associated with which action. In the general reinforcement learning scenario, a high reward or a low reward might have been caused by a recent action or by an action in the distant past. The term **contextual** bandits refers to the case where the action is taken in the context of some input variable that can inform the decision. For example, we at least know the user identity, and we want to pick an item. The mapping from context to action is also called a **policy**. The feedback loop between the learner and the data distribution (which now depends on the actions of the learner) is a central research issue in the reinforcement learning and bandits literature.

Reinforcement learning requires choosing a tradeoff between **exploration** and **exploitation**. Exploitation refers to taking actions that come from the current, best version of the learned policy—actions that we know will achieve a high reward. Exploration refers to taking actions specifically in order to obtain more training data. If we know that given context $\boldsymbol{x}$, action a gives us a reward of 1, we do not know whether that is the best possible reward. We may want to exploit our current policy and continue taking action a in order to be relatively sure of obtaining a reward of 1. However, we may also want to explore by trying action a'. We do not know what will happen if we try action a'. We hope to get a reward of 2, but we run the risk of getting a reward of 0. Either way, we at least gain some knowledge.

Exploration can be implemented in many ways, ranging from occasionally taking random actions intended to cover the entire space of possible actions, to model-based approaches that compute a choice of action based on its expected reward and the model's amount of uncertainty about that reward.

Many factors determine the extent to which we prefer exploration or exploitation. One of the most prominent factors is the time scale we are interested in. If the agent has only a short amount of time to accrue reward, then we prefer more exploitation. If the agent has a long time to accrue reward, then we begin with more exploration so that future actions can be planned more effectively with more knowledge. As time progresses and our learned policy improves, we move toward more exploitation.

Supervised learning has no tradeoff between exploration and exploitation because the supervision signal always specifies which output is correct for each input. There is no need to try out different outputs to determine if one is better than the model's current output—we always know that the label is the best output.

Another difficulty arising in the context of reinforcement learning, besides the exploration-exploitation trade-off, is the difficulty of evaluating and comparing different policies. Reinforcement learning involves interaction between the learner and the environment. This feedback loop means that it is not straightforward to evaluate the learner's performance using a fixed set of test set input values. The policy itself determines which inputs will be seen. Dudik *et al.* (2011) present techniques for evaluating contextual bandits.

12.5.2 Knowledge Representation, Reasoning and Question Answering

Deep learning approaches have been very successful in language modeling, machine translation and natural language processing due to the use of embeddings for symbols (Rumelhart *et al.*, 1986a) and words (Deerwester *et al.*, 1990; Bengio *et al.*, 2001). These embeddings represent semantic knowledge about individual words and concepts. A research frontier is to develop embeddings for phrases and for relations between words and facts. Search engines already use machine learning for this purpose but much more remains to be done to improve these more advanced representations.

12.5.2.1 Knowledge, Relations and Question Answering

One interesting research direction is determining how distributed representations can be trained to capture the **relations** between two entities. These relations allow us to formalize facts about objects and how objects interact with each other.

In mathematics, a **binary relation** is a set of ordered pairs of objects. Pairs that are in the set are said to have the relation while those who are not in the set

do not. For example, we can define the relation "is less than" on the set of entities $\{1, 2, 3\}$ by defining the set of ordered pairs $\mathbb{S} = \{(1,2), (1,3), (2,3)\}$. Once this relation is defined, we can use it like a verb. Because $(1,2) \in \mathbb{S}$, we say that 1 is less than 2. Because $(2,1) \notin \mathbb{S}$, we can not say that 2 is less than 1. Of course, the entities that are related to one another need not be numbers. We could define a relation `is_a_type_of` containing tuples like (`dog`, `mammal`).

In the context of AI, we think of a relation as a sentence in a syntactically simple and highly structured language. The relation plays the role of a verb, while two arguments to the relation play the role of its subject and object. These sentences take the form of a triplet of tokens

$$(\text{subject}, \text{verb}, \text{object}) \tag{12.21}$$

with values

$$(\text{entity}_i, \text{relation}_j, \text{entity}_k). \tag{12.22}$$

We can also define an **attribute**, a concept analogous to a relation, but taking only one argument:

$$(\text{entity}_i, \text{attribute}_j). \tag{12.23}$$

For example, we could define the `has_fur` attribute, and apply it to entities like `dog`.

Many applications require representing relations and reasoning about them. How should we best do this within the context of neural networks?

Machine learning models of course require training data. We can infer relations between entities from training datasets consisting of unstructured natural language. There are also structured databases that identify relations explicitly. A common structure for these databases is the **relational database**, which stores this same kind of information, albeit not formatted as three token sentences. When a database is intended to convey commonsense knowledge about everyday life or expert knowledge about an application area to an artificial intelligence system, we call the database a **knowledge base**. Knowledge bases range from general ones like `Freebase`, `OpenCyc`, `WordNet`, or `Wikibase`,[1] etc. to more specialized knowledge bases, like `GeneOntology`.[2] Representations for entities and relations can be learned by considering each triplet in a knowledge base as a training example and maximizing a training objective that captures their joint distribution (Bordes *et al.*, 2013a).

[1] Respectively available from these web sites: `freebase.com`, `cyc.com/opencyc`, `wordnet.princeton.edu`, `wikiba.se`

[2] `geneontology.org`

In addition to training data, we also need to define a model family to train. A common approach is to extend neural language models to model entities and relations. Neural language models learn a vector that provides a distributed representation of each word. They also learn about interactions between words, such as which word is likely to come after a sequence of words, by learning functions of these vectors. We can extend this approach to entities and relations by learning an embedding vector for each relation. In fact, the parallel between modeling language and modeling knowledge encoded as relations is so close that researchers have trained representations of such entities by using *both* knowledge bases *and* natural language sentences (Bordes *et al.*, 2011, 2012; Wang *et al.*, 2014a) or combining data from multiple relational databases (Bordes *et al.*, 2013b). Many possibilities exist for the particular parametrization associated with such a model. Early work on learning about relations between entities (Paccanaro and Hinton, 2000) posited highly constrained parametric forms ("linear relational embeddings"), often using a different form of representation for the relation than for the entities. For example, Paccanaro and Hinton (2000) and Bordes *et al.* (2011) used vectors for entities and matrices for relations, with the idea that a relation acts like an operator on entities. Alternatively, relations can be considered as any other entity (Bordes *et al.*, 2012), allowing us to make statements about relations, but more flexibility is put in the machinery that combines them in order to model their joint distribution.

A practical short-term application of such models is **link prediction**: predicting missing arcs in the knowledge graph. This is a form of generalization to new facts, based on old facts. Most of the knowledge bases that currently exist have been constructed through manual labor, which tends to leave many and probably the majority of true relations absent from the knowledge base. See Wang *et al.* (2014b), Lin *et al.* (2015) and Garcia-Duran *et al.* (2015) for examples of such an application.

Evaluating the performance of a model on a link prediction task is difficult because we have only a dataset of positive examples (facts that are known to be true). If the model proposes a fact that is not in the dataset, we are unsure whether the model has made a mistake or discovered a new, previously unknown fact. The metrics are thus somewhat imprecise and are based on testing how the model ranks a held-out of set of known true positive facts compared to other facts that are less likely to be true. A common way to construct interesting examples that are probably negative (facts that are probably false) is to begin with a true fact and create corrupted versions of that fact, for example by replacing one entity in the relation with a different entity selected at random. The popular precision at 10% metric counts how many times the model ranks a "correct" fact among the top 10% of all corrupted versions of that fact.

Another application of knowledge bases and distributed representations for them is **word-sense disambiguation** (Navigli and Velardi, 2005; Bordes *et al.*, 2012), which is the task of deciding which of the senses of a word is the appropriate one, in some context.

Eventually, knowledge of relations combined with a reasoning process and understanding of natural language could allow us to build a general question answering system. A general question answering system must be able to process input information and remember important facts, organized in a way that enables it to retrieve and reason about them later. This remains a difficult open problem which can only be solved in restricted "toy" environments. Currently, the best approach to remembering and retrieving specific declarative facts is to use an explicit memory mechanism, as described in section 10.12. Memory networks were first proposed to solve a toy question answering task (Weston *et al.*, 2014). Kumar *et al.* (2015) have proposed an extension that uses GRU recurrent nets to read the input into the memory and to produce the answer given the contents of the memory.

Deep learning has been applied to many other applications besides the ones described here, and will surely be applied to even more after this writing. It would be impossible to describe anything remotely resembling a comprehensive coverage of such a topic. This survey provides a representative sample of what is possible as of this writing.

This concludes part II, which has described modern practices involving deep networks, comprising all of the most successful methods. Generally speaking, these methods involve using the gradient of a cost function to find the parameters of a model that approximates some desired function. With enough training data, this approach is extremely powerful. We now turn to part III, in which we step into the territory of research—methods that are designed to work with less training data or to perform a greater variety of tasks, where the challenges are more difficult and not as close to being solved as the situations we have described so far.